INVESTIGATING THE MECHANISMS OF p35-MEDIATED
NEURODEGENERATION AND ITS EFFECTS ON AGING

by
Joshua Spurrier

A dissertation submitted to Johns Hopkins University in conformity with the requirements for
the degree of Doctor of Philosophy

Baltimore, Maryland
August 2017

Abstract

Aging and adult-onset neurodegenerative diseases (NDDs) share multiple cellular phenotypes stemming from dysfunction of an overlapping set of molecular mechanisms; however, aging by itself fails to cause neurodegeneration in all individuals, indicating that NDDs are the result of more than brain aging alone. Thus, while aging is the greatest risk factor for NDDs, a complete understanding of NDD etiology and pathogenesis will require the full elucidation of the relationship between aging and degeneration. My thesis project investigates this relationship by probing the mechanisms underlying a model of adult-onset neurodegeneration in *Drosophila*. In humans, cyclin dependent kinase 5 (Cdk5) has been linked to multiple NDDs, such as Alzheimer's disease, Parkinson's disease, and amyotrophic lateral sclerosis. Cdk5 activity requires binding an activator subunit; in *Drosophila*, the sole activator is the neuron-specific p35. We develop a comprehensive metric for physiological age in *Drosophila* based on genome-wide expression profiling, and show that loss (mutant) or overexpression (OE) of p35 in young, presymptomatic flies accelerates the intrinsic rate of aging of brain and thorax tissue. Gene ontology analysis revealed that biological processes affected by altered p35 levels are also affected by aging. Further, modulation of p35 leads to degenerative phenotypes including impaired autophagy, loss of central brain neurons, motor defects, and shortened lifespan, all of which are observed in human ND diseases. These findings suggest that neuronal dysfunction can cause accelerated aging, which then acts as a driving mechanism to induce neurodegeneration.

In parallel work, we also investigated the regulatory role of p35 in regards to the axon initial segment (AIS) and its potential link to neurodegeneration. p35 activity modulates the size of the AIS of mushroom body (MB) neurons, and deletion of p35 results in swelling of the

ii

proximal axon in the vicinity of the AIS; furthermore, p35-mutant flies exhibited an accelerated loss of MB neurons. Thus, we sought to investigate whether perturbation of the AIS contributed to p35-mediated neurodegeneration. We identified a novel regulator that robustly modulates the AIS independently of p35, and showed that shortening of the AIS may be sufficient to induce MB neurodegeneration. Taken together, our results suggest p35-mediated neurodegeneration results from accelerated aging effects in combination with cell-autonomous neuronal insults. These data fundamentally recast our picture of the relationship between neurodegenerative processes and their most prominent risk factor, natural aging, and have profound implications for identifying which aspects of NDDs could be productive targets for therapy.

Thesis advisor/reader: Edward Giniger, PhD

Reader: Haiqing Zhao, PhD

Acknowledgements

First and foremost, I would like to thank my mentor, Dr. Ed Giniger, for his scientific mentorship and guidance. Over the years, Ed has continuously challenged me scientifically, and I am extremely grateful for his patience and support. I feel incredibly privileged to have had the opportunity to complete my PhD research in Ed's lab, and have benefited immensely from his experience and advice.

I sincerely thank Dr. Huaibin Cai, Dr. Susan Harbison, Dr. Ward Odenwald, and Dr. Haiqing Zhao, for serving as my thesis committee members and providing insightful feedback and guidance over the years. I'd also like to thank the support staff that enable us to do our science: in the lab, Dr. Joy Gu and Dr. Irina Kuzina, Stephen Wincovitch from the Microscopy Core, and Dr. Kory Johnson for his bioinformatics help. I am also grateful for scientific feedback from members of Dr. Chi-hon Lee's and Dr. Ela Serpe's labs, and from the *Drosophila* community at NIH.

Huge thanks to the past and present members of the Giniger lab, who have made my successes in the lab a possibility. It has been a pleasure learning from you all, and sharing and discussing ideas; you have all been wonderful colleagues and a joy to work with, even when the science wasn't cooperating.

To all of my friends, my utmost gratitude and thanks for providing me with a support network to share my successes and overcome my frustrations. In particular, I'd like to acknowledge Dr. Kristina McLinden, Becky Fallon, Akanni Clarke, Dr. Arvind Shukla, Dr. Darpan Medhi, Bill Keenan, and Jordan White for keeping me sane, or at least making me look sane by comparison.

To my family, I love you all very much. Mom, Dad, Kerri, Erin, Michael, and Paul: you have

never failed to be supportive, and have always challenged me to be my best. Thank you.

And lastly, I would like to thank Emma Taylor-Salmon for her love, motivation, and unwavering

support. I could never have asked for a better partner, and can't wait to spend the rest of my life

with you.

Table of Contents

List of Tables

List of Supplemental Tables
**supplemental tables can be found in the accompanying Excel file
"Spurrier_thesis_supplemental_tables"

List of Figures

Chapter 1

Introduction

Chapter 1. Introduction

Recent literature has estimated that the global population of people over 80 years old will triple in the next 30 years (Fontana et al, 2014). As populations are aging longer and longer, they are becoming more at risk for a variety of diseases. Detrimental changes occur with age, leading to an ever-increasing vulnerability and reduction in healthspan. The vast majority of elderly people over the age of 65 have multiple comorbidities, ranging from arthritis to cancer to neurodegenerative diseases (NDDs) (Hung, Ross et al. 2011). Indeed, aging has long been recognized as the greatest risk factor for multiple NDDs, including Alzheimer's disease (AD), Parkinson's disease (PD), and amyotrophic lateral sclerosis (ALS). Nearly half of people over the age of 85 have AD (Podtelezhnikov, Tanis et al. 2011), while the prevalence of PD, the second most common age-related NDD, quintuples in individuals older than 85, relative to the 60 years or older cohort (Reeve, Simcox et al. 2014). ALS rarely affects people under the age of 40, but its prevalence increases exponentially in older individuals, with 70-79 year olds having the highest incidence of the disease (Ingre, Roos et al. 2015). While aging very obviously plays a role in each of these diseases, the underlying age-related factors that predispose some individuals to disease remains unknown. It is therefore essential to elucidate the relationship between degeneration and aging to progress forward in the development of therapeutic strategies.

Although some cases of adult-onset NDDs are related to specific genetic risk factors, and thus proceed through hallmark mechanisms, most instances of NDD are a sporadic form. NDDs generally present with some combination of molecular and cellular phenotypes that are shared amongst multiple diseases; these phenotypes interconnect and modulate one another, eventually leading to cellular dysfunction and neurodegeneration. These pathologies will be discussed in detail below.

1.1 Pathologies of Neurodegeneration

Protein aggregation and proteostatic defects

Many protein aggregates contain misfolded protein. Proper protein folding is required for normal function, so misfolded proteins must either be re-folded in the appropriate conformation, or degraded and removed. Proteins can be highly dynamic, however, frequently changing conformation as they interact with other proteins, form complexes, or translocate across membranes. Thus, there is an ever-present risk for misfolding to occur. To combat this, cells utilize multiple mechanisms to ensure correct folding. Chaperone proteins assist folding at multiple steps. The most notable chaperones are the highly conserved heat-shock family of proteins. HSP60 and HSP70 are more promiscuous, interacting with a wide range of proteins, while other members exhibit more specialized localization and targeting. As polypeptides are translated in either the cytosol or the ER lumen, some chaperones assist in the initial folding (Koga, Kaushik et al. 2011). Other chaperones are located near organelle membranes to aid in protein refolding after translocation, and throughout the cytosol to help with refolding or disaggregation as needed. Notably, many proteins associated with NDDs are intrinsically disordered and therefore carry a higher risk of misfolding into a pathologic conformation (Uversky 2009). If the chaperone is unable to correct the misfolding or aggregation, it will target the dysfunctional protein for lysosomal or proteasomal degradation.

AD, PD, and ALS, among others, are all associated with improper protein aggregation (Ross and Poirier 2004). AD is characterized by the accumulation of amyloid beta peptide and hyperphosphorylated tau (Bloom 2014), PD is linked to α-synuclein (α-syn) deposits (Davie 2008), and ALS sometimes results in aggregates of superoxide dismutase 1 (SOD1) (Bruijn, Houseweart et al. 1998). The aggregates inhibit normal processing and function of the proteins

involved, and can further promote disease by sequestering additional interactors. Aggregates can also be deposited extracellularly, where they can cause neuronal injury (Zhao, Beers et al. 2010). Extracellular aggregates can induce aggregation in neighboring, unaffected cells, further propagating the detrimental effects (Desplats, Lee et al. 2009, Frost, Jacks et al. 2009, Luk, Song et al. 2009).

Proteasomal degradation occurs through chaperone-mediated autophagy (CMA) or via the ubiquitin proteasome system (UPS). A subset of heat shock proteins (Hsc70 and Hsp90) acquire post-translational modifications that are exclusively associated with CMA (Kaushik, Bandyopadhyay et al. 2011). Hsc70 recognizes and binds misfolded proteins exposing a KFERQ-like motif, and transports them to lysosomes expressing lysosome-associated membrane protein 2 (LAMP-2A). Intralumenal lys-Hsc70 facilitates the formation of a translocation complex and the transport of the protein into the lysosome, where it is degraded. Wild-type α-syn is typically degraded via CMA; certain mutated forms of α-syn, however, bind more strongly to LAMP-2A, but do not get translocated into the lysosome for degradation (Cuervo, Stefanis et al. 2004). Thus, mutant α-syn itself does not get degraded, and it prevents the degradation of wild-type α-syn, leading to toxic gain of function conditions.

While CMA is specific to mammals, the UPS is conserved among eukaryotes, with analogous mechanisms even found in archaea (Fu, Liu et al. 2016). The 26S proteasome comprises a catalytic core (20S core particle) sandwiched between two regulatory complexes (19S regulatory particle) (Koga, Kaushik et al. 2011). Polyubiquitinated proteins targeted for degradation are recognized by the regulatory subunits. The ubiquitin chains are removed by deubiquitinases and unfoldases straighten the substrate, which is then fed into the catalytic barrel. The substrate is proteolyzed into shorter polypeptides, which are released back into the

cytoplasm. Multiple types of NDD brain samples exhibit polyubiquitination of protein aggregates, as well as an accumulation of oxidized proteins, hinting at impaired ubiquitin-dependent proteolysis (Lim 2007, Oddo 2008, Lehman 2009). Further, treatment with a selective proteasome inhibitor is sufficient to induce neurodegeneration, and is accompanied by the formation of α-syn aggregates (McNaught, Björklund et al. 2002, Fornai, Lenzi et al. 2003, Miwa, Kubo et al. 2005). α-syn can also directly interact with proteasome subunits and potentially block polyubiquitin recognition (Ghee, Fournier et al. 2000, Paul 2008). Thus, impaired UPS function can contribute to protein aggregation, which can then further inhibit UPS function, leading to enhanced accumulation of aggregates. It remains to be seen if protein aggregation typically causes UPS dysfunction through direct interactions, through overloading the system, or through alternative mechanisms, or more likely, a context-dependent combination thereof.

Mitochondrial dysfunction

As the primary source of ATP, mitochondria are vital to cellular function. Notably, mitochondria are not static organelles, but are rather part of a dynamic network that rapidly divides and fuses. Through these processes, there is regular exchange of mitochondrial DNA (mtDNA), lipids, and proteins needed for normal function (Kowald and Kirkwood 2011). Additionally, fission allows for dysfunctional mitochondria to be separated from the network and selectively degraded through mitophagy, protecting the remaining mitochondria (Wang and Klionsky 2011).

The most susceptible mitochondrial components are mtDNA and the respiratory chain enzymes. mtDNA encodes thirteen peptide subunits of the electron transport chain complexes,

and includes tRNA and rRNA genes (Taanman 1999). Mitochondrial DNA is more vulnerable

to damage than nuclear DNA as mitochondria lack histones, which offer some protection, and

because mitochondria do not possess the complete repertoire of repair machinery found in the

nucleus. Given the high number of mitochondria within a cell, the detrimental consequences of

mutations can initially be suppressed by the abundance of non-mutated mtDNA. Over time,

however, clonal expansion of the mutated mtDNA can lead to dysfunctional mitochondria and

respiratory deficiency (Winklhofer and Haass 2010). Alzheimer's patients show significant

accumulation of mtDNA mutations, as well as reductions in mRNA levels (Coskun, Beal et al.

2004, Leuner, Hauptmann et al. 2007, Jellinger 2010). Substantia nigral neurons from PD

patients were found to have an increased number of mtDNA mutations relative to age-matched

controls (Bender, Krishnan et al. 2006), and maternally-inherited mtDNA mutations have been

associated with L-DOPA-responsive parkinsonism (Lin and Beal 2006). Mutations in the

control region can lead to altered expression of mtDNA genes, while mutations in coding

sequences can generate peptides that do not fold or complex properly and have altered activity.

The respiratory chain comprises Complexes I-V, located in the inner mitochondrial

membrane; as electrons are transferred from one complex to the next, protons are transported

across the membrane, generating a proton electrochemical gradient. This gradient drives energy

production via Complex V, which is an ATP synthase. As protons flow through the complex

back into the mitochondrial matrix, the free energy powers the oxidative phosphorylation of

ADP into ATP. Dysfunction of these complexes arises from stoichiometric imbalances and

changes in individual complex concentrations, as well as declines in specific complex efficiency

(Leuner, Hauptmann et al. 2007). AD brain tissue exhibits significant reductions in multiple

respiratory chain complexes, and Aβ was found to inhibit cytochrome oxidase (Complex IV), as

well as α-ketoglutarate dehydrogenase and pyruvate dehydrogenase (Casley, Canevari et al. 2002, Terni, Boada et al. 2010). PD is largely associated with deficiencies in Complex I activity, although the underlying causative mechanisms remain to be completely elucidated (Winklhofer and Haass 2010). Additionally, α-syn binds to Complex IV, which may interfere with respiratory complex activity in PD (Elkon, Don et al. 2002). In ALS, SOD1 mutants are associated with decreased respiratory efficiency (Borthwick, Johnson et al. 1999).

Additional causes of mitochondrial dysfunction include the formation of the mitochondrial permeability transition pore (mPTP) and perturbation of mitochondrial dynamics. Under certain pathological conditions, the mPTP forms in the mitochondrial membranes, creating a path from the mitochondrial matrix to the cytosol (Du and Yan 2010). Formation of the mPTP is associated with Aβ, as Aβ directly interacts with cyclophilin D (cypD), a major constituent of the mPTP (Du, Guo et al. 2008). Further, AD brains showed elevated levels of the Aβ-cypD complex, which was absent in control brains. Ultimately, the mPTP causes mitochondrial swelling, loss of membrane potential, and damage to the respiratory transport chain (Du and Yan 2010).

Mitochondrial fusion and fission are necessary for determining mitochondrial size, regulating mitochondrial degradation, and maintaining proper distribution (Itoh, Nakamura et al. 2013). Fusion proteins OPA1, Mfn1, and Mfn2 were found to be decreased in AD samples, while the fission protein Fis1 was upregulated (Wang, Su et al. 2009). PINK1 and Parkin, two proteins commonly dysregulated in PD, function in mitochondrial fission (Poole, Thomas et al. 2008) and degradation via mitophagy (Pickrell and Youle 2015). Additional PD-related proteins are also involved with impaired mitochondrial dynamics, as both α-syn and LRRK2 are

associated with mitochondrial fragmentation (Nakamura, Nemani et al. 2011, Wang, Yan et al. 2012).

Mitochondrial dysfunction results in a notable decline in energy metabolism as ATP production is significantly decreased. Lower ATP levels put an additional strain on cells, as many processes compete for available ATP. One such process is the UPS, which requires ATP at multiple steps. Thus, mitochondrial dysfunction can cause proteostatic defects, further perturbing cellular homeostasis. Mitochondrial dysfunction also results in impaired calcium homeostasis, and increased generation of reactive oxygen species (ROS) (Celsi, Pizzo et al. 2009). Notably, ~90% of cellular ROS is generated by the mitochondria (Balaban, Nemoto et al. 2005).

Oxidative Stress

Elevated production of ROS and other free radicals causes oxidative stress, leading to a host of detrimental consequences, including DNA mutations; damaged proteins, lipids, and nucleic acids; uncoupling of oxidative phosphorylation; induction of the mitochondrial permeability transition; and disrupted calcium homeostasis (Leuner, Hauptmann et al. 2007). Cells employ multiple antioxidant mechanisms to deal with oxidative stress. These mechanisms include enzymes such as superoxide dismutases, catalase, glutathione-S-transferases, glutathione peroxidase, and glutathione reductase, as well as a variety of non-enzymatic antioxidants like glutathione, vitamins, and β-carotene (Birben, Sahiner et al. 2012). Once the generation of free radicals exceeds the capabilities of the antioxidant defense mechanisms, oxidative stress occurs.

Neurons are notable for their extremely high energy and oxygen consumption (Raichle and Gusnard 2002). Indeed, neurons have a higher relative content of mitochondria to meet this

energy demand (Leuner, Hauptmann et al. 2007). Consequently, neurons generate a significant amount of ROS and are particularly vulnerable to oxidative stress. Further, neurons have a high concentration of unsaturated fatty acids that are more susceptible to lipid peroxidation (Coyle and Puttfarcken 1993), in combination with a relatively low concentration of antioxidant enzymes (Mattson, Chan et al. 2002). As with other cell types, neurons are also subject to genomic instability (Chow and Herrup 2015) and proteostatic defects (Powers, Morimoto et al. 2009), leading to an overall decline in neuronal function and decreased cognitive function.

Oxidative stress has been identified in many diseases, including AD, PD, and ALS (Uttara, Singh et al. 2009). Various markers of oxidative stress, such as lipid peroxidation products, oxidative modifications of proteins, and oxidized rRNA and mRNAs, have all been found to be elevated in multiple brain regions of AD patients (Kim, Kim et al. 2015). These increases are preceded by decreases in antioxidant enzyme activity and lower levels of non-enzymatic antioxidants, suggesting that an oxidative imbalance occurs at the earliest stages of AD (Wang, Wang et al. 2014). Similarly, there is elevated oxidative stress accompanied by a decrease in glutathione levels and glutathione peroxidase activity in PD (Martin and Teismann 2009). Of note, oxidative stress was found to be sufficient to induce α-syn aggregation (Hashimoto, Hsu et al. 1999). Evidence of oxidative stress, including elevated protein carbonyl levels, lipid oxidation, and oxidized DNA, has also been found in tissues from patients with either familial or spontaneous ALS (Barber and Shaw 2010).

The detrimental effects of oxidative stress are exacerbated by its feedback on multiple pathways regulating cellular homeostasis. mtDNA and mitochondrial proteins are all targets of oxidative stress, and their dysfunction can result in further generation of ROS, creating a cycle of increased stress accompanied by mitochondrial dysfunction (Winklhofer and Haass 2010,

Swerdlow 2011). Levels and activity of antioxidant enzymes can also suffer from oxidative stress, diminishing the cell's capacity of dealing with increased ROS levels. Accumulation of ROS leads to a higher number of damaged and misfolded proteins, which not only affects protein function but also puts an added strain on proteostasis. Further, oxidation of various potassium channels is suspected to alter channel activity, which could lead to perturbed electrophysiology (Sesti 2016).

Immune dysfunction

Multiple NDDs are associated with chronic activation of the immune system, which includes activation of microglia and astrocytes, increased pro-inflammatory signaling, and T-cell infiltration. Under normal conditions, microglia monitor the brain milieu to protect against invading pathogens or to identify and repair tissue damage. Microglia perform a host of functions to accomplish these tasks. Microglia will phagocytose foreign material, damaged or apoptotic cells, cellular debris, neurofibrillary tangles, and amyloid plaques. Microglia can also secrete cytokines to activate additional microglia, recruit other immune cells, promote B-cell maturation, and upregulate pro-inflammatory signaling (Graeber and Streit 2010). As a controlled response, these functions are neuroprotective; chronic microglial activation, however, can become detrimental to neurons and contribute to neurodegeneration.

Activated microglia have been found to localize around extracellular protein aggregates in post-mortem analysis of AD (Ishizuka, Kimura et al. 1997), PD (Yamada, McGeer et al. 1992), and ALS (Zhao, Beers et al. 2010) samples. Aβ has been shown to recruit and activate microglia by stimulating the release of CCL2 from astrocytes, neurons, oligodendrocytes, and microglial cells themselves (Guillot-Sestier and Town 2013); decreased levels of CCR2, the

receptor for CCL2, result in decreased microglia accumulation in response to elevated Aβ (El Khoury, Toft et al. 2007). Activated microglia also secrete a number of pro-inflammatory cytokines such as TNF-α, IL-6, IL-1α, and GM-CSF, as evidenced by elevated cytokine levels in transgenic mouse models and tissue samples from AD and PD patients (Patel, Paris et al. 2005, Long-Smith, Sullivan et al. 2009). Further, AD patients show elevated circulating levels of macrophage colony-stimulating factor (M-CSF), a chemokine that attracts monocytes and is produced by microglia (Laske, Stransky et al. 2010). The neurotoxic effects of extracellular SOD1 in ALS are suggested to be microglia-dependent, as blocking microglia activation failed to induce neurodegeneration in a cell-culture model (Zhao, Beers et al. 2010). Microglia are also known to secrete ROS, which can serve as an inflammatory signal by amplifying cytokine release (Giunta, Fernandez et al. 2008); chronic secretion of ROS can contribute to oxidative stress, as previously discussed.

Secreted cytokines and chemokines can disrupt the blood brain barrier (BBB) and attract other immune cells to the site of microglia activation. Both AD and PD patients exhibit increased BBB permeability, and an influx of activated T cells into the brain (Desai, Monahan et al. 2007, Amor, Puentes et al. 2010). T cell infiltration plays a significant role in dopaminergic neurodegeneration: in multiple mouse models, reducing levels of CD4+ T cells attenuates cell loss (Brochard, Combadiere et al. 2009). Reynolds et al demonstrated that T cells could recognize α-syn modified by oxidative stress and exacerbated the neurotoxic effects of microglia (Reynolds, Glanzer et al. 2008).

Defects in axonal transport and axonal swelling

Proper neuronal function requires an established microtubule network that connects each of the subcellular compartments and permits the transport of cargo between regions. Neurons are organized such that the stable, minus-end of microtubules is located in the cell body, while the more dynamic plus-end of microtubules extends into the axon. Motor proteins utilize this stereotypical organization to transport vesicles, organelles, and other cellular cargos throughout the neuron. Kinesins, the plus-end directed motor, transport cargo away from the soma in the anterograde direction. Dyneins, the minus-end directed motor, carry cargo from the synapse towards the cell body. Disruption of axonal trafficking can lead to mislocalization of proteins, lipids, and organelles, impaired clearance of cellular debris or protein aggregates, axonal swelling, and overall declines in neuronal function and neurotransmission.

Impaired axonal transport has been linked to a variety of NDDs, including AD, PD, and ALS. The two pathological hallmarks of AD, tau and Aβ aggregations, are both capable of impairing axonal transport. Aggregation of tau into filaments reveals an N-terminal amino acid sequence that is otherwise hidden; this sequence can activate protein phosphatase 1 (PP1), which leads to the subsequent activation of GSK3 and the eventual detachment of kinesin from its cargo, selectively inhibiting anterograde transport while not affecting retrograde transport (LaPointe, Morfini et al. 2009). Physiological concentrations of Aβ are sufficient to inhibit both anterograde and retrograde transport in squid axoplasm (Pigino, Morfini et al. 2009), and to attenuate synaptic transmission (Moreno, Yu et al. 2009). Further, multiple mouse models of AD have directly shown impaired transport of membrane bound organelles such as mitochondria, endosomes, and multivesicular bodies (Pigino, Morfini et al. 2003, Lazarov, Morfini et al. 2007), and mitochondria were redistributed and accumulate in the soma of AD

pyramidal neurons (Wang, Su et al. 2009). α-syn, associated with PD and numerous other NDDs, binds to synaptic vesicles and is thought to be involved in vesicular transport; mutant versions of α-syn associated with onset of PD are unable to bind vesicles (Jensen, Nielsen et al. 1998). Furthermore, injection of mutant α-syn into rats perturbs axonal transport by decreasing kinesin and dynein levels (Chung, Koprich et al. 2009). Lastly, a transgenic mouse model of ALS expressing G93A SOD1 exhibited impaired transport of radiolabeled cytoskeletal components (Zhang, Tu et al. 1997).

Another pathological hallmark common to many NDDs, axonal swelling, can result from and contribute to defects in axonal transport. Indeed, impairment of axonal transport can lead to accumulations of organelles and other cargos, forming a traffic jam that can cause swellings. These varicosities then further inhibit axonal trafficking in turn (Chevalier-Larsen and Holzbaur 2006). AD patients expressing amyloid precursor protein (APP) mutations, as well as animal models overexpressing APP, exhibit axonal aggregates and swellings (Gunawardena and Goldstein 2001, Stokin, Lillo et al. 2005). Further, Aβ accumulates in these swellings, and extracellular Aβ deposits are found in close proximity, suggesting the swellings may be a site of release (Christensen, Huettenrauch et al. 2014). In an experimental model of PD, expression of mutant α-syn impaired axonal transport and lead to axonal varicosities (Chung, Koprich et al. 2009, Chu, Morfini et al. 2012). Further, motor neurons from patients with ALS were found to have an elevated number of neurofibrillary swellings in the proximal axon which contained multiple types of cellular organelles (Delisle and Carpenter 1984, Sasaki, Maruyama et al. 1990).

Synaptic loss

The neuronal synapse permits interneuronal communication and communication between neurons and non-neural tissue. Briefly, this involves the regulated release of neurotransmitters

into the synaptic cleft. Interruption of this communication can lead to cognitive decline and other behavioral phenotypes. Each of the previously discussed mechanisms can lead to synaptic dysfunction and impaired signaling from the presynaptic neuron. Alternatively, neurons can also lose synapses in their dendritic arbor.

Synaptic loss often precedes neurodegeneration, and is considered the strongest correlate for cognitive decline (Koffie, Hyman et al. 2011). AD is associated with decreased expression of multiple synaptic proteins (Masliah, Mallory et al. 2001) and an overall decline in synaptic number. Notably, synaptic size appeared to increase as a compensatory mechanism to maintain the total synaptic contact area per volume (DeKosky and Scheff 1990). Dendritic regions in close proximity to amyloid plaques exhibited loss of dendritic spines and more robust loss of synapses than regions farther away (Tsai, Grutzendler et al. 2004). α-syn is capable of altering synaptic function at both the pre- and post-synaptic level. Aggregates of α-syn are commonly found in the presynaptic terminal, leading to a decrease in presynaptic markers (Kramer and Schulz-Schaeffer 2007). In parallel, postsynaptic markers were also decreased, and were accompanied by the loss of dendritic spines.

Mechanisms of cell-death

The terminal phenotype of neurodegeneration, neuronal death, is multi-faceted and complex. Cell-death may occur via programmed cell-death (PCD), which comprises apoptosis and autophagy, through necrosis, or through a handful of rarer modalities (Kroemer, Galluzzi et al. 2009). Apoptosis is primarily caspase-mediated, and can arise through cell-cycle reactivation, p53 activation, JNK signaling, or bcl-2 signaling, among other pathways; cell-cycle re-entry appears to be the most prominent apoptotic inducer in ND (Greene, Liu et al. 2007, Levy,

Malagelada et al. 2009). Autophagic cell death is characterized by cell death in the absence of the chromatin condensation that is typically observed with apoptosis; further, there is widespread vacuolization of the cytoplasm (Kroemer, Galluzzi et al. 2009). Morphologically, necrosis involves swelling of organelles and of the cell itself, plasma membrane rupture, and subsequent loss of intracellular contents.

For many NDDs, it is still unclear what the direct mechanism utilized is, and in many cases, it is highly likely that multiple pathways occur even within a single patient, sample, or cell. During AD, PD, and ALS, some post-mitotic neurons show evidence of re-entering the cell cycle, such as upregulation of mitotic markers and DNA replication (Ranganathan and Bowser 2003, Lee, Casadesus et al. 2009, Levy, Malagelada et al. 2009). Neurons cannot complete mitosis upon leaving G0, so initiation of the cell cycle leads to their death, usually via apoptosis. Indeed, there is evidence of transcriptional upregulation of caspases, as well as caspase activation, in AD samples (Spires-Jones, Stoothoff et al. 2009), and overexpressing the anti-apoptotic protein bcl-2 prevented degenerative phenotypes in a transgenic mouse model of AD (Rohn, Vyas et al. 2008). However, a separate study failed to find increases in activated caspases and other pro-apoptotic proteins, casting doubt on whether AD-related neurodegeneration occurs through apoptosis (Woodhouse, Dickson et al. 2006). Aβ has been shown to induce excitotoxicity, which can cause neuronal death with morphological changes observed with both apoptosis and necrosis, so multiple pathways are likely involved (Gorman 2008, Kroemer, Galluzzi et al. 2009). Similarly, there have been conflicting results regarding apoptosis in PD. Some studies have been able to show activation of caspases and an increase in apoptotic cells using TUNEL staining (Tompkins, Basgall et al. 1997, Tatton 2000), while others found no evidence of apoptosis (Kosel, Egensperger et al. 1997, Wullner, Kornhuber et al. 1999).

Drug models of PD have revealed that Parkinson mimetics can induce both apoptosis and necrosis (Levy, Malagelada et al. 2009). Of note, many of the cellular processes underlying apoptosis require ATP; thus, in cases of mitochondrial dysfunction where energy output is impaired, a neuron may be driven towards necrosis instead of apoptosis (Gorman 2008).

1.2 Investigating the relationship between aging and neurodegeneration

Hypotheses of aging

The scientific literature has detailed multiple molecular and cellular mechanisms that are associated with both aging and NDDs. In order to investigate aging, though, one must first define aging and gain a better understanding of its underlying causes. At its most basic, aging is merely the daily increase in chronological age; however, this view fails to account for the variety of physiological changes that occur with aging.

To date, there are more than 300 different hypotheses of aging that try to encapsulate the overwhelming abundance of experimental data regarding aging (Diaconeasa, Rachita et al. 2015). Earlier hypotheses viewed aging as a random, progressive decline in organismal fitness. Damage-accumulation theories posit that increased accumulation of toxic cellular byproducts, buildup of environmentally induced mutations, and/or decreased efficiencies of defense and repair mechanisms lead to physiological system failure and eventually death (Jin 2010). More prominent damage theories include the rate of living theory, the free radicals theory, and the somatic DNA damage theory (Jin 2010). The rate of living theory generally prescribes that organisms have a genetically predetermined metabolic capacity, and that lifespan is determined by the rate in which that energy is used; namely, the amount of metabolic energy expanded per gram of body weight (Sohal, Toy et al. 1986). The free radicals theory argues that aging is the

result of ROS and the resultant oxidative stress (Sohal and Weindruch 1996). The somatic DNA damage theory suggests that decline in fitness stems from the accumulation of DNA mutations in somatic cells, leading to gain or loss of function paradigms that impair cellular function (Kennedy, Loeb et al. 2012). Many aspects of these theories, however, fail to account for the wide range of lifespans among similar species, and furthermore, fail to explain more modern experimental observations (Goldsmith 2014).

Conversely, more recent theories point to the presence of an aging program, *per se*. Programmed aging hypotheses argue that aging is the result of a mechanism that intentionally permits organismal decline and death in order to achieve an evolutionary benefit by restricting lifespan beyond an optimum threshold (Goldsmith 2014). Theories of programmed aging include, among others, programmed longevity, the endocrine theory, and the immunological theory. Programmed longevity simply states that aging results from coordinated gene expression changes over time. The endocrine theory attributes these expression changes to altered hormonal levels. Alternatively, the immunological theory argues that the immune system is programmed to decline with aging in order to restrict lifespan by leaving organisms more susceptible to disease (Jin 2010).

Theories of programmed aging are supported by studies revealing that the rate of aging is malleable. Indeed, multiple studies have found that, even in humans, lifespan can be extended, suggesting a flexible rate of aging (Fontana, Kennedy et al. 2014). Furthermore, there is reproducible evidence of aging signatures on gene expression, as genome-wide profiling has identified hundreds of genes that exhibit consistent changes in expression with age. Studies have also detected an array of "longevity genes" that appear to regulate the lifespan, further supporting a programmed, genetic component of aging.

No current theory is sufficient to completely explain each of the facets of aging, so the reality is likely a complex combination of multiple theories. Indeed, a comprehensive theory of aging must encapsulate all known aging mechanisms and be applicable to every species. López-Otín et al recently summarized the cellular and molecular changes that arise with age (López-Otín, Blasco et al. 2013). These putative hallmarks include, among others, genomic instability, epigenetic changes, proteostatic dysfunction, defective mitochondria, and aberrant intercellular communication; each will be discussed in more detail in the subsequent section.

1.3 Mechanisms of Aging

Genomic instability

Cells are continuously exposed to a host of both endogenous and exogenous challenges to DNA integrity. Normal cellular processes, such as DNA replication, chemical reactions, and generation of reactive oxygen species, can compromise DNA. Exogenous factors, like radiation or biological or chemical agents, also put DNA at risk (Hoeijmakers 2009). The detrimental effects of such exposures can manifest as point mutations, insertions, translocations, and chromosomal duplication or deletion. To combat such events, cells typically employ multiple DNA repair mechanisms, although these too have been found to decline with age (Gorbunova, Seluanov et al. 2007, Lord and Ashworth 2012).

Telomere attrition is a unique form of genetic instability. Located at the distal end of chromosomes, telomeres are composed of repetitive nucleotide sequences and serve to protect genes from degradation stemming from end replication issues. It is well documented that telomeres of replicating cells deteriorate with age in both mice and humans (Blasco 2007). After a sufficient number of replicative cycles, telomere exhaustion occurs as cells reach the Hayflick

limit (Hayflick and Moorhead 1961), and cells enter replicative senescence. Notably, DNA repair is repressed at the telomere to prevent accidental fusion of chromosome ends; as such, telomeres are particularly susceptible to DNA damage (Fumagalli, Rossiello et al. 2012, Hewitt, Jurk et al. 2012).

Epigenetic changes

Epigenetic alterations include a vast array of modifications capable of adjusting gene expression without altering the DNA code itself. In order to maintain the proper epigenetic patterns, cells utilize multiple enzymes to add specific marks, including methyltransferases and acetylases, as well as the corresponding enzymes for removal. The function of these proteins, however, deteriorates with age. Global DNA methylation was found to decrease overall yet become more variable with age, with some loci actually showing hypermethylation (Maegawa, Hinkal et al. 2010, Talens, Christensen et al. 2012). Histone methylation is also implicated in aging, as H4K20 and H3K4 trimethylation increases with age, while H3K9 methylation and H3K27 trimethylation decrease. Further, blocking activity of histone demethylases actually extends lifespan in *C. elegans* (Jin, Li et al. 2011). Another epigenetic mark that changes with age is acetylation of H4K16. The accumulation of epigenetic changes can also drive chromatin remodeling by regulating heterochromatin assembly. Heterochromatin protein 1 α (HP1α) recognizes and binds methylated H3K9 (Grewal and Moazed 2003), serves as a link between chromatin and the nuclear lamina (Ye, Callebaut et al. 1997), and is associated with nucleating and maintaining heterochromatin (Nielsen, Oulad-Abdelghani et al. 2001, Yamada, Fischle et al. 2005). Other chromatin remodelers involved with heterochromatin maintenance include the Polycomb PRC2 complex and the nucleosome remodeling and deacetylase (NuRD) complex

(Pegoraro, Kubben et al. 2009). Markedly, there is downregulation of each of these heterochromatin regulators with age. Stemming from altered epigenetic modifications and chromatin remodeling, there are robust changes in gene expression with age. Indeed, multiple studies have characterized age-related transcriptional alterations (Lee, Klopp et al. 1999, Lee, Weindruch et al. 2000, Zou, Meadows et al. 2000, Pletcher, Macdonald et al. 2002, Golden and Melov 2004, McCarroll, Murphy et al. 2004, Lai, Parnell et al. 2007, de Magalhaes, Curado et al. 2009). Consistent among these analyses are perturbations to essential physiological pathways, including proteostasis and mitochondrial function.

Proteostatic dysfunction

Proteostasis has been strongly correlated with aging, as misfolded proteins accumulate and enzyme populations become less catalytically active (Taylor and Dillin 2011). Misfolded proteins can interact with other proteins, forming aggregates which are often cytotoxic (Chiti, Stefani et al. 2003, Stefani and Dobson 2003). Inappropriate interactions can also result in toxic gain or loss of function phenotypes. Aging is associated with decreased chaperone levels, leading to impaired ER stress-response and accumulation of protein aggregates. One mechanism underlying these declines is the downregulation of Hsp70, stemming from blockage of heat shock factor binding the heat shock element gene promoter (Heydari, Wu et al. 1993). Aging is also associated with a decreased ability to activate the unfolded protein response (Taylor 2016). Further, aging results in declines of both autophagy and the ubiquitin-proteasome system (Rubinsztein, Mariño et al. 2011, Tomaru, Takahashi et al. 2012). Modulation of proteostasis has been shown to directly regulate aging. Decreasing chaperone-mediated folding accelerates aging phenotypes (Min, Whaley et al. 2008) while upregulation increases longevity (Walker and

Lithgow 2003, Morrow, Samson et al. 2004). Proteostasis is also proposed to be downstream of

multiple genetically distinguishable pathways involved with enhanced longevity, providing

additional support for the role of proteome maintenance in aging (Taylor and Dillin 2011).

Defective mitochondria

Over time, mitochondrial function declines significantly, and is associated with

morphological changes, decreased ATP production, and oxidative stress (Shigenaga, Hagen et al.

1994). Complexes I and IV of the electron transport chain (ETC) are robustly affected by aging

and exhibit decreased enzymatic activity (Muller, Eckert et al. 2010); this is potentially due to

lower protein levels, as older mice have diminished mRNA expression of all ETC complex genes

(Manczak, Jung et al. 2005). Other enzymes involved in mitochondrial function, such as adenine

nucleotide translocase and acyl carnitine transferase, also exhibited declining activity with age

(Yan and Sohal 1998, Liu, Killilea et al. 2002).

Perturbations in normal mitochondrial function are associated with an increase in ROS

production. Elevated ROS can cause additional mitochondrial dysfunction, leading to a cyclical

increase in ROS generation. Aging is strongly correlated with an increase in ROS generation

and oxidative stress (Leutner, Eckert et al. 2001, Balaban, Nemoto et al. 2005). However, the

detrimental effects of elevated ROS and oxidative stress have been challenged in recent years.

Chronic reduction in SOD activity led to increased ROS and oxidative damage, but did not alter

longevity, although a higher incidence of cancer was observed (Zhang, Ikeno et al. 2009).

Further, increasing antioxidant defense can increase longevity in some cases, but is not sufficient

to extend lifespan (Leuner, Hauptmann et al. 2007, Perez, Van Remmen et al. 2009).

Interestingly, mtDNA mutator mice exhibit severe ETC deficiencies without an accompanying

increase in ROS production; these mice also exhibit premature aging phenotypes (Trifunovic, Hansson et al. 2005, Edgar, Shabalina et al. 2009). It has been proposed that ROS therefore initially acts as a stress-induced survival signal, although its chronic accumulation can eventually exacerbate age-related changes (López-Otín, Blasco et al. 2013). Surprisingly, there is also evidence that increasing ROS can actually extend the lifespan in yeast, worms, naked mole rates, and mice (Mesquita, Weinberger et al. 2010, Yang and Hekimi 2010, Ristow and Schmeisser 2011). Regardless, aging is associated with mitochondrial dysfunction that causes defective bioenergetics.

Aberrant intercellular communication

Aging results in defects in multiple communication paradigms, and there is accumulating evidence of non-cell autonomous effects. The immune system becomes less effective with advanced age, losing its ability to effectively remove pathogens and dysfunctional host cells (Jin 2010, López-Otín, Blasco et al. 2013). Activated microglia, which are normally neuroprotective, become neurotoxic with age (Sawada, Sawada et al. 2008). The persistence of pro-inflammatory signals leads to chronic inflammation with age, termed "inflammaging" (Salminen, Kaarniranta et al. 2012). Inflammaging is accompanied by upregulation of the NFkB pathway, which is a key regulator of inflammation (Tak and Firestein 2001). Overactivation of the NFkB pathway is consistently observed in genome-wide studies of aging (de Magalhaes, Curado et al. 2009), and has been linked with altered hypothalamic production of gonadotropin-releasing hormone (GnRH) (Zhang, Li et al. 2013). Notably, inhibiting NFkB signaling, either genetically or pharmacologically, or treating with exogenous GnRH can prevent aging phenotypes (Osorio, Barcena et al. 2012, Zhang, Li et al. 2013).

A separate modality of neuroendocrine signaling that is also affected in aging is the insulin/IGF-1 signaling (IIS) pathway. Insulin sensitivity can decline with age, leading to hyperinsulinemia (Muller, Elahi et al. 1996). Modulation of the IIS pathway has been found to control longevity and alter lifespan. In multiple invertebrate models, as well as some mouse models, genetic perturbations that reduce IIS signaling result in significant increases in longevity (van Heemst 2010). Caloric restriction, the most reproducible method of extending lifespan, is strongly linked to decreased IIS signaling, although additional mechanisms are also involved (Heilbronn and Ravussin 2003, Sinclair 2005). The FOXO family of transcription factors act downstream of IIS, and have been linked to multiple aspects of cellular homeostasis, including autophagy and resistance to oxidative stress (Martins, Lithgow et al. 2016). Modulation of IIS is not without controversy, however, as mammalian IIS signaling is more complex, and defects in this pathway have been associated with an increased risk of age-related disease, such as cardiovascular disease (van Heemst 2010).

How are neurodegeneration and aging related?

A side by side comparison of the described mechanisms for neurodegeneration and aging reveals tremendous overlap. Common characteristics of ND and aging include perturbation of proteostasis, mitochondrial dysfunction, enhanced oxidative stress, and aberrant immune function. Many neurodegenerative diseases are adult-onset, indicating that incidence of these diseases is age-related. Additional research is needed, however, to tease apart the relationship between ND and aging in order to completely reveal the causative mechanisms.

To investigate the relationship between degeneration and aging, we employed a *Drosophila* model of adult-onset neurodegeneration. Cyclin dependent kinase 5 (Cdk5) has been

implicated in a number of NDDs, including AD, PD, and ALS; in flies, Cdk5 loss of function

results in ND with degenerative phenotypes that resemble human pathologies. The physiological

role of Cdk5, and its role in ND, will be discussed in more detail in the upcoming sections.

1.4 Cdk5 is essential to nervous system development and function

Regulation of Cdk5

Since its discovery nearly 30 years ago, cyclin-dependent kinase 5 has been recognized as

a strong regulator of neuronal development and function, and as such, is of extreme interest for

its role in a wide variety of neuronal disorders. Cdk5 is ubiquitously expressed in mice, though

it exhibits higher expression throughout the nervous system (Hellmich, Pant et al. 1992, Tsai,

Takahashi et al. 1993, Ino, Ishizuka et al. 1994). Despite the systemic expression pattern, Cdk5

activity is largely restricted to postmitotic neurons due to the spatial expression of activator

subunits. Similar to other cdks, Cdk5 requires a direct interaction with a separate protein in

order to adopt a permissive conformation for activity. For cdks, the subunits are cyclins; for

Cdk5, the main activator subunits are p35 and p39. Indeed, deletion of p35 and p39 in mice

ablates Cdk5 activity and fully mimics loss of Cdk5 (Ko, Humbert et al. 2001). Both p35 and

p39 are expressed highest in neurons (Tsai, Delalle et al. 1994, Humbert, Dhavan et al. 2000),

although transient expression has also been detected in mouse testis, pancreatic β cells,

monocytes, and myoblasts (Sahlgren, Mikhailov et al. 2003, Chen, Wang et al. 2004, Rosales

and Lee 2006). p35 and p39 are partially redundant, as deletion of p39 has no apparent

phenotype and deletion of p35 results in lamination defects but does not affect viability and

fertility (Kwon and Tsai 1998, Ko, Humbert et al. 2001). Consistent with this redundancy, p35

and p39 share similar subcellular localization, although there are distinct microdomains where

only a single activator is present, such as growth cones and synapses (Humbert, Dhavan et al. 2000, Niethammer, Smith et al. 2000, Fu, Fu et al. 2001). Further, p35 and p39 are specific to Cdk5, as they do not bind or activate other cdks (Poon, Lew et al. 1997). While Cdk5 can bind other cyclins, most of these interactions do not result in Cdk5 activation. Cdk5 interacts with cyclins D1, D2, D3, and E, but does not show increased kinase activity (Xiong, Zhang et al. 1992, Miyajima, Nornes et al. 1995); rather, these interactions can serve to titrate cyclin availability or to modulate Cdk5 activity (Guidato, McLoughlin et al. 1998, Odajima, Wills et al. 2011). Conversely, cyclin I has been found to directly activate Cdk5 (Brinkkoetter, Olivier et al. 2009), although cyclin I is more prevalent in renal podocytes and expressed at a lower level in neurons. *Drosophila melanogaster* lack orthologs of p39 and Cyclin I, so the only known activator of Cdk5 in flies is p35. As with mice, p35 expression is largely restricted to the nervous system, although some expression is observed in testis, limiting Cdk5 activity mostly to neurons (Tsai, Delalle et al. 1994, Connell-Crowley, Le Gall et al. 2000, Chintapalli, Wang et al. 2007, Smith-Trunova, Prithviraj et al. 2015); deletion of p35 in flies abolishes Cdk5 activity and is indistinguishable from loss of Cdk5 (Connell-Crowley, Vo et al. 2007). Supporting the pronounced importance of the complex, Cdk5 and p35/p39 are evolutionarily conserved across multiple vertebrate and invertebrate species, including humans, mice, and flies, among others (Dhavan and Tsai 2001).

Structurally speaking, p35 adopts a three-dimensional topology similar to the characteristic cyclin-box fold of cyclins, but shares little sequence similarity (Tarricone, Dhavan et al. 2001). Upon binding between Cdk5 and p35, the activation loop (T-loop) of Cdk5 is stretched into an extended conformation, permitting Cdk5 kinase activity. Unlike other cdks, which require further phosphorylation to stabilize the T-loop, binding of Cdk5 to either p35 or

p39 is sufficient for normal activity (Tarricone, Dhavan et al. 2001). The list of Cdk5 substrates

includes the activator subunits themselves. While bound to Cdk5, both p35 and p39 are

phosphorylated. This phosphorylation leads to multi-ubiquitination of the subunits, targeting

them for degradation via the ubiquitin-proteasome system (UPS) (Figure 1.1). Ultimately, p35

has a short half-life of only 20-30 minutes, allowing for rigorous regulation of Cdk5 activity

(Patrick, Zhou et al. 1998). Further, p35 and p39 both contain an amino-terminal myristoylation

motif; this domain tethers the proteins to the plasma membrane, and serves to restrict the

subcellular localization of Cdk5 to the periphery of the cell. In mammals, the myristoylation

motif can be removed via calpain-mediated cleavage, generating p25 and p29 from p35 and p39,

respectively. Without a tether, the activated Cdk5 complex can then diffuse throughout the

cytoplasm and even enter the nucleus (Patrick, Zukerberg et al. 1999, Asada, Yamamoto et al.

2008). Along with the myristoylation motif, cleavage also removes the residue that targets

p35/p39 for degradation; thus, the truncated forms have a longer half-life and result in

hyperactivation of Cdk5 (Patrick, Zukerberg et al. 1999).
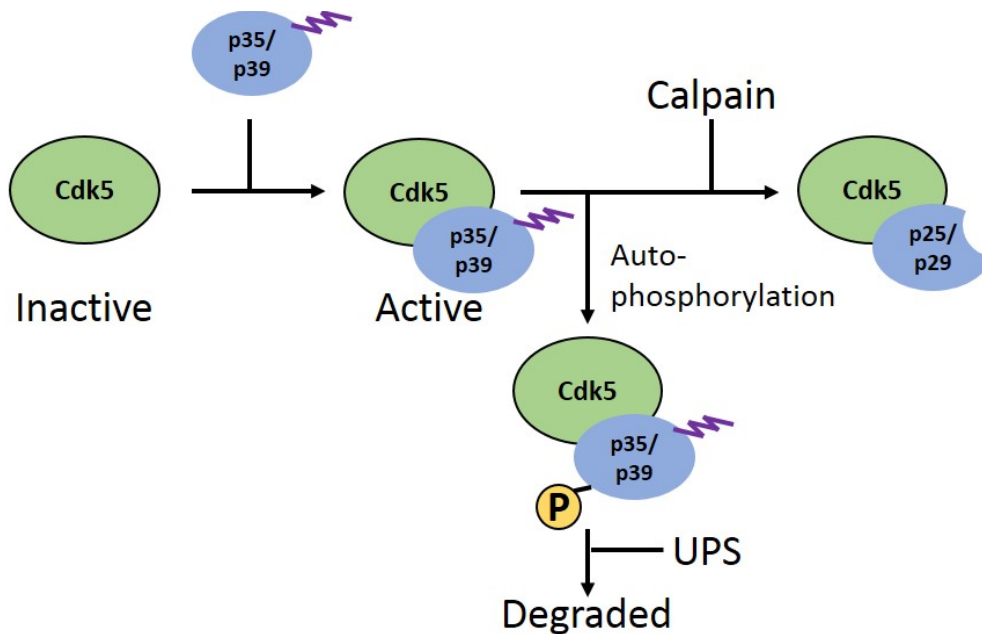
Figure 1.1. Cdk5 regulation by p35/p39.
Unbound Cdk5 is in an inactive confirmation. Upon binding to the myristoylated p35 or p39, Cdk5 undergoes a confirmation change, revealing its catalytic domain. The myristoylation domain (purple tail) tethers the complex to the plasma membrane, limiting Cdk5's access to local substrates only. One such substrate is the activator subunit itself. Phosphorylation of p35 or p39 by Cdk5 targets it for degradation via the ubiquitin-proteasome system (UPS). In mammals, certain contexts of increased cytosolic Ca2+ induce calpain-mediated cleavage, removing the myristoylation domain and allowing the complex to diffuse freely through the cytoplasm and interact with a different set of substrates. (Adapted from McLinden 2012).

Cdk5 is a member of the family of proline-directed protein kinases, and typically phosphorylates either serine or threonine in the consensus sequence (S/T)PX(K/H/R), although slight variations in the recognized sequence have been identified (Beaudette, Lew et al. 1993, Contreras-Vallejos, Utreras et al. 2012). Other members of the family include glycogen synthase kinase-3 beta (GSK3β) and mitogen activated protein kinases (MAPK). These kinases all interact with one another in various contexts, and are capable of cross-regulating one another. Cdk5 phosphorylates GSK3β at ser-9, inhibiting GSK3β activity (Morfini, Szebenyi et al. 2004). When Cdk5 activity is decreased, this inhibitory phosphorylation is reduced and GSK3β activity increases. Within the family of proline-directed kinases, there is also overlap in target-site

specificity, potentially indicating a compensatory mechanism and highlighting the importance of maintaining proper protein phosphorylation. Cdk5 can also be phosphorylated by a number of other kinases, including c-Abelson, Fyn, EphA4, and TrkB (Sasaki, Cheng et al. 2002, Lalioti, Pulido et al. 2010). Phosphorylation of Cdk5 at tyr-15 has been linked to enhanced Cdk5 activity while phosphorylation at thr-14 is actually inhibitory (Matsuura and Wang 1996, Zukerberg, Patrick et al. 2000). Furthermore, phosphorylation of the T-loop at ser-159 is thought to block Cdk5's interaction with p35 or p39, preventing activation (Tarricone, Dhavan et al. 2001). Alternative post-translation modifications, such as S-nitrosylation, have also been found to alter Cdk5 activity (Zhang, Yu et al. 2010).

Cdk5 is required for proper nervous system function

Given the increased expression of Cdk5 in nervous tissue, and the fact that its primary activators, p35 and p39, are expressed primarily in neurons, it follows that Cdk5's most important roles will be in the nervous system. Indeed, mice null for Cdk5 are perinatal lethal, but this lethality is completely rescued by selectively expressing Cdk5 in the nervous system (Ohshima, Ward et al. 1996, Tanaka, Veeranna et al. 2001), suggesting that non-neuronal Cdk5 is dispensable for survival. Consistent with this, Cdk5 plays no discernible role in cell cycle progression, unlike other cdks (Meyerson, Enders et al. 1992, van den Heuvel and Harlow 1993). Furthermore, podocytes from p35-null mice have a normal morphology and function, although they are more susceptible to stressors (Brinkkoetter, Wu et al. 2010). Transient p35-dependent Cdk5 activity has also been linked to monocyte differentiation (Chen, Wang et al. 2004) and the development of myogenic tissue (Sahlgren, Mikhailov et al. 2003). However, the most

significant roles of Cdk5 are its involvement in various aspects of neuronal development and homeostasis.

Role of Cdk5 in axonogenesis and neuronal migration

The first hints of Cdk5's role in neuronal development were gleaned from its expression pattern in developing mouse embryos. During early gestational stages, Cdk5 expression was relatively low; however, as development progressed, Cdk5 levels gradually increased until they reached their maximum in adult brains (Tsai, Takahashi et al. 1993). These trends correlated with an increase of post-mitotic neurons and a decreasing percentage of actively proliferating cells, suggesting that Cdk5 plays a role in neuronal differentiation and migration. Indeed, Cdk5-null mice exhibited disrupted stratification of neocortical and pyramidal neurons (Ohshima, Ward et al. 1996). The cortex is established by the "inside-out" generation of layers (Angevine and Sidman 1961, Luskin and Shatz 1985): migrating postmitotic neurons follow radial glial fibers, with later-born neurons moving superficially past earlier born neurons, generating discernible layers in a laminated structure (Chae, Kwon et al. 1997). Loss of Cdk5 activity results in a complete disorganization of the cortex, although cell density is initially the same (Gilmore, Ohshima et al. 1998). Cdk5-null mice also displayed layering defects in the cerebellum and other morphological defects throughout the central nervous system, although the peripheral nervous system appeared normal, as the dorsal root ganglia were not affected. Highlighting potential mechanisms for the observed defects, cultured embryonic cortical neurons showed colocalization of Cdk5 and p35 in neurites and axonal growth cones, and treatment with dominant negative Cdk5 mutants resulted in significant shortening of dendrites and axons (Nikolic, Dudek et al. 1996). Cdk5 activity is required for both nerve growth factor (NGF)-

induced neurite outgrowth (Harada, Morooka et al. 2001) and brain-derived neurotrophic factor (BDNF)-induced dendritic growth (Cheung, Chin et al. 2007).

Additional functions of Cdk5 in axonogenesis were elucidated in *Drosophila*, which are not susceptible to the neuronal migration defects observed in mice. When Cdk5 activity was either increased or decreased, guidance defects were observed in the transverse nerve, segmental nerve A, and the intersegmental nerve (Connell-Crowley, Le Gall et al. 2000); the observed phenotypes included overextension, stalling, and aberrant pathfinding, and suggest that Cdk5 activity, while not essential for axon guidance in *Drosophila*, could serve to coordinate multiple signaling paradigms. Cdk5 was also found to regulate *Drosophila* neuronal remodeling. Cdk5 controls the timing and rate of developmental mushroom body remodeling, specifically modulating neurite disassembly (Smith-Trunova, Prithviraj et al. 2015). Neurite remodeling, along with activity-dependent pruning, are observed in both vertebrates and invertebrates, and are required for establishing and refining neuronal circuitry (Chen and Regehr 2000, Kuo, Jan et al. 2005, Tessier and Broadie 2009, Schuldiner and Yaron 2015).

A plethora of studies have begun to elucidate the molecular mechanisms through which Cdk5 regulates axonogenesis and neuronal migration. Multiple Cdk5 substrates are involved in controlling the various levels of the cytoskeleton, including actin, microtubules, and neurofilaments. Rho GTPases are a family of signaling G proteins vital to intracellular actin dynamics and heavily regulated by Cdk5. Cdk5 co-localizes with Rac, Pak1, and F-actin, and Cdk5 phosphorylates Pak1 at multiple sites through a Rac-dependent mechanism (Nikolic, Chou et al. 1998). Cdk5-mediated phosphorylation of Pak1 inhibits its kinase activity, thereby temporarily regulating activity of Pak1's downstream effector proteins and their role in actin cytoskeleton reorganization. Further, Cdk5 can modulate Rac activity by targeting upstream

activators. Phosphorylation of ser-737 of Ras guanine nucleotide releasing factor 2 (RasGRF2) decreases its guanine exchange factor activity towards Rac, effectively inhibiting the Rac signaling cascade. Cdk5 also phosphorylates and inactivates WAVE1, which is responsible for activation of the actin polymerization complex Arp2/3 (Kim, Sung et al. 2006). During Semaphorin3A (Sema3A)-induced growth cone collapse, Sema3a induces phosphorylation of Cdk5 at tyr-15 via the Fyn/Plex-A2 receptor complex, hyperactivating Cdk5 to drive reorganization of the actin cytoskeleton (Sasaki, Cheng et al. 2002).

Cdk5 specifically targets multiple microtubule-associated proteins (MAPs), including tau and MAP1B. Cdk5-mediated hyperphosphorylation of tau causes dissociation of tau from microtubules, leading to tubulin depolymerization (Evans, Rank et al. 2000). In cerebellar neurons, Cdk5 phosphorylates MAP1B, increasing its affinity for and binding to microtubules (Pigino, Paglini et al. 1997). Cdk5-mediated phosphorylation of MAP1B is essential for netrin-1 dependent migration (Del Rio, Gonzalez-Billault et al. 2004). Another Cdk5 substrate capable of interacting with microtubules is doublecortin (DCX). DCX binds to microtubules and promotes stabilization and polymerization. Phosphorylation of DCX at ser-297 results in its displacement from microtubules (Tanaka, Serneo et al. 2004). In mouse cerebral cortex, Cdk5 contributes to axon outgrowth by phosphorylating Axin. This phosphorylation facilitates Axin's interaction with GSK-3β, inhibiting GSK-3β activity (Fang et al, 2011). With decreased GSK-3β activity, collapsin response mediator protein-2 (CRMP2) gets dephosphorylated and binds microtubules, stabilizing them and promoting axon outgrowth. Conversely, Uchida *et al* demonstrated that Cdk5 directly phosphorylates CRMP2, leading to secondary phosphorylation by GSK-3β (Uchida et al, 2005). The dual-phosphorylated CRMP2 dissociates from microtubules, leading to MT destabilization, and contributing to Sema3A-induced growth cone collapse. Furthermore,

the Cdk5-p35 complex can itself bind to tubulin, contributing to the stability and polymerization of microtubules. This interaction can be outcompeted by Calmodulin (CaM) in the presence of calcium, suggesting there is an intrinsic balance required to maintain the proper microtubule cytoskeleton (He et al, 2008).

Lastly, Cdk5 directly targets neurofilament proteins. Neurofilaments comprise three subunits of varying molecular mass: NF-high (NF-H), NF-medium (NF-M), and NF-low (NF-L). These subunits combine to form 10 nanometer filaments that stabilize axons and control axon caliber (Shea, Zheng et al. 2004). Cdk5 phosphorylates both NF-H and NF-M (Lew, Qi et al. 1995) to effectively regulate spacing between filaments; hyperphosphorylation of NF-H led to perikaryal bundling of NFs (Shea, Zheng et al. 2004). Furthermore, phosphorylated NF-H has a decreased affinity for microtubules, indicating that phosphorylation status also regulates interactions between different aspects of the cytoskeleton (Hisanaga, Ishiguro et al. 1993).

Cdk5 control of neuronal migration could also occur through cadherin-mediated adhesion. Cdk5 has been shown to directly phosphorylate β-catenin, regulating the interaction between β-catenin and N-cadherin (Kesavapany, Lau et al. 2001). Dissociation of β-catenin from N-cadherin leads to decreased adhesion; thus, loss of Cdk5 activity could decrease phosphorylation of β-catenin, stabilizing the β-catenin/N-cadherin complex, permitting stronger adhesion and preventing neuronal migration. Cdk5 also regulates neuronal response to extracellular matrix proteins, as laminin induced p35 expression in cultured cerebellar neurons, accompanied by axonal elongation and phosphorylation of the microtubule-associated protein MAP1B (Paglini, Pigino et al. 1998).

Role of Cdk5 in neuronal function and homeostasis

Trafficking

Aside from its role in establishing the nervous system, Cdk5 is also essential to the normal physiological functioning of mature neurons. Cdk5 activity is responsible for regulating multiple aspects of intracellular transport essential for proper neuronal function. At the molecular level, Cdk5 interacts with NUDEL and LIS1, mediating dynein-dependent neuronal transport (Niethammer, Smith et al. 2000, Sasaki, Shionoya et al. 2000). Cdk5 directly phosphorylates NUDEL, which disrupts its binding to the dynein/dynactin complex, thus permitting axonal conveyance by removing a brake. Inhibition of Cdk5 blocks axonal transport, resulting in axonal swelling. Cdk5 is also involved in kinesin-mediated anterograde transport. Cdk5 inhibits GSK3β by phosphorylating it, preventing GSK3β-dependent phosphorylation of kinesin light chains and the release of cargo proteins (Morfini, Szebenyi et al. 2002, Morfini, Szebenyi et al. 2004). In addition to the motor proteins, Cdk5 influences axonal transport through cytoskeletal regulation. Cdk5 phosphorylation of NFs alters NF caliber and spacing, and Cdk5 hyperactivation was found to inhibit NF-dependent axonal transport (Shea, Zheng et al. 2004).

Proper neuronal trafficking is dependent on the establishment and maintenance of neuronal polarity, as specific proteins are targeted to certain cellular regions, such as the dendrites or axon. This polarity is achieved in part through the axon initial segment (AIS), a subcellular domain segregating the somatodendritic and axonal regions of the neuron. The AIS is also responsible for action potential initiation. Cdk5's role in regulating the AIS will be expanded on in Chapter 4.

Proteostasis

Cdk5 has been linked to proteostasis through both protein translation and degradation. Cdk5 phosphorylates S6K1, blocking its autoinhibition and permitting its activation by mTOR (Hou, He et al. 2007). S6K1 targets ribosomal proteins, among other substrates, mediating protein synthesis. Additionally, Cdk5 mediates Sema3A-induced activation of eukaryotic translation initiation factor 4E (eIF-4E) in the growth cone of dorsal root ganglia neurons (Li, Sasaki et al. 2004). In the absence of Cdk5 activity, Sema3A fails to activate eIF-4E, and local translation is impaired. On the other hand, Cdk5 plays a role in protein degradation and has been linked to autophagy. A number of Cdk5 substrates are targeted for degradation upon phosphorylation, including p35/ p39 (Minegishi, Asada et al. 2010) and GKAP (Roselli, Livrea et al. 2011), among others. Alternatively, Cdk5 can regulate the activity of E3 ubiquitin ligase complexes, such as Cdh1/APC, suppressing their ubiquitination activity and subsequently preventing substrate targeting for degradation via the UPS (Maestre, Delgado-Esteban et al. 2008). Cdk5 is also significantly involved in regulation of autophagy. Cdk5 phosphorylates endophilin B1 and VPS34, two proteins that interact with beclin 1 to regulate autophagosome formation in opposite directions (Takahashi, Coppola et al. 2007, Furuya, Kim et al. 2010, Wong, Lee et al. 2011). The role of Cdk5 in autophagy is an evolutionarily conserved function. In *Drosophila* lacking Cdk5 activity, exposure to starvation, which is used to indicate impaired autophagy, led to significantly decreased survival times (Trunova and Giniger 2012). This behavioral phenotype was accompanied by an accumulation of autophagic organelles in the brain, further supporting that autophagy is perturbed in the absence of normal Cdk5 activity.

Synaptic homeostasis

Presynaptically, Cdk5 functions in vesicle trafficking, release and recycling. Subcellular fractionation has revealed that Cdk5 and its activators are present in synaptic membranes (Dhavan and Tsai 2001). Cdk5 helps regulate the reserve and recycling pools of synaptic vesicles (SVs) at the synapse by phosphorylating synapsin I (synI) (Matsubara, Kusubata et al. 1996, Verstegen, Tagliatti et al. 2014). Phosphorylated synI exhibits enhanced binding to the actin cytoskeleton, driving its trafficking of SVs to the recycling pool, situated proximal to the readily releasable pool. Cdk5 modulates SV exocytosis indirectly by phosphorylating Munc18. Munc18 binds the SNARE protein syntaxin 1 (Hata, Slaughter et al. 1993), preventing interactions of the SNARE complex with SVs. Upon phosphorylation, Munc18 dissociates, allowing syntaxin 1 to bind vesicles and promote membrane fusion and neurotransmitter release (Fletcher, Shuang et al. 1999, Lilja, Johansson et al. 2004). Further, Cdk5 is involved in SNARE protein recycling. Upon activation from Cdk5-mediated phosphorylation, PCTAIRE1 activates N-ethylmaleimide-sensitive fusion protein (NSF), which disassembles and recovers SNARE monomers from the presynaptic membrane (Liu, Cheng et al. 2006).

Cdk5 contributes to clathrin-mediated endocytosis by phosphorylating amphiphysin I (Floyd, Porro et al. 2001), dynamin I (Tan, Valova et al. 2003), and synaptojanin I (Lee, Wenk et al. 2004). In all three cases, Cdk5-mediated phosphorylation disrupts protein interaction: Cdk5 activity induces dissociation of amphiphysin I from β-adaptin, of dynamin I from amphiphysin I (Tomizawa, Sunada et al. 2003), and of synaptojanin I from endophilin (Lee, Wenk et al. 2004). The ultimate effects of Cdk5 activity on endocytosis remain murky, and are likely context dependent. In cultured hippocampal neurons, disruption of these interactions is thought to inhibit vesicular endocytosis, as blocking Cdk5 activity enhanced endocytosis. Conversely, *in*

vitro experiments utilizing synaptosomes revealed that Cdk5 activity is required for endocytosis (Tan, Valova et al. 2003). Endocytosis is further regulated by the phosphatase calcineurin; interplay regulating protein phosphorylation status likely contributes to the plasticity required for proper neuronal function.

Neurotransmission is regulated by Cdk5 at both the transmitter and receptor levels. Cdk5 phosphorylates tyrosine hydroxylase (TH), the rate-limiting enzyme involved in dopamine (DA) synthesis, stabilizing the protein and increasing its activity (Kansy, Daubner et al. 2004, Moy and Tsai 2004). Consistent with this function, Cdk5-null mice exhibited decreased levels of TH (Moy and Tsai 2004). Dopamine- and cAMP-regulated phosphoprotein of *Mr* 32 kDa (DARPP-32) serves as an additional link between Cdk5 and DA signaling. DARPP-32 is a central modulator of a pathway receiving input from Cdk5, protein phosphatase 1, and protein kinase A (Bibb, Snyder et al. 1999). Cdk5-phosphorylation of DARPP-32 leads to PKA inhibition and ultimately suppressed DA signaling. Cdk5 itself is subject to DA signaling, as stimulation of the dopamine D1 receptor results in elevated calcium influx, calpain-mediated generation of p25, and hyperactivation of Cdk5 (Lebel and Cyr 2011).

In postsynaptic neurons and muscle tissue, Cdk5 modulates the synaptic response of multiple neurotransmitter receptors. In hippocampal neurons, Cdk5 phosphorylates ser-1232 of the NR2A subunit of NMDA receptors, leading to enhanced channel activity (Li, Sun et al. 2001). Conversely, NMDA activity was enhanced in striatal neurons by Cdk5 loss of function, although this occurred indirectly via dysregulated DA signaling (Chergui, Svenningsson et al. 2004). Levels of NMDA receptor are affected by Cdk5 interactions with Src. Phosphorylation of Src modulates its binding to post-synaptic density protein 95 (PSD-95), which regulates NMDA receptor endocytosis (Zhang, Edelmann et al. 2008). Through an alternative pathway,

Cdk5 activity induces ubiquitination of PSD-95, targeting the protein for proteasomal degradation (Colledge, Snyder et al. 2003). Loss of PSD-95 is accompanied by loss of NMDA and AMPA from the synaptic terminal. Receptor clustering is further regulated by interactions of PSD-95 with guanylate kinase-associated protein (GKAP). GKAP colocalizes with PSD-95 and NMDA receptors and potassium channels at the synapse (Kim, Naisbitt et al. 1997), and links them to the underlying cytoskeleton (Roselli, Livrea et al. 2011). Phosphorylation of GKAP by Cdk5 targets it for ubiquitin-mediated proteasomal degradation, severing the tether to the actin cytoskeleton, and resulting in disassembly of the synaptic cluster. Lastly, Cdk5 phosphorylates the BDNF receptor TrkB, initiating a signaling cascade culminating in phosphorylation of S6 ribosomal protein, enhanced localized protein translation, and dendritic spine remodeling (Lai, Wong et al. 2012).

Cdk5 activity also plays a postsynaptic role at the junction between neuron and muscle. p35 is transiently upregulated in embryonic muscle tissue, providing temporary Cdk5 activity, which is required for the formation of neuromuscular junctions (Fu, Fu et al. 2001). At the NMJ, Cdk5 and p35 colocalize with acetylcholine (ACh) receptor (Fu, Ip et al. 2005, Lin, Dominguez et al. 2005). Notably, neuregulin-1 (NRG-1) binds to and activates its receptor ErbB, inducing Cdk5-dependent upregulation of ACh receptor expression (Fu, Fu et al. 2001).

Role of Cdk5 in memory and cognition

Cdk5-mediated regulation of neuronal function overall, and specifically of neurotransmission, are an essential component of the neuronal plasticity vital to cognition and memory. Plasticity largely arises from a neuron's ability to alter synaptic strength. Long-term potentiation (LTP) and depression (LTD) describe activity-dependent strengthening or reduction

in synaptic efficacy, respectively. Given the wide range of Cdk5-mediated regulation of neuronal plasticity, the exact role of Cdk5 regarding LTP remains contradictory. Under different paradigms, pharmacological inhibition of Cdk5 has been found to either block LTP (Wang, Walsh et al. 2004) or be permissive (Li, Sun et al. 2001, Wei, Tomizawa et al. 2005). Similarly, loss of Cdk5 function has been linked to both impaired (Guan, Su et al. 2011) and enhanced (Hawasli, Benavides et al. 2007) memory formation and retrieval. These contrasting results are further complicated by the fact that Cdk5 effects can be time dependent. Conditional upregulation of Cdk5 activity in the hippocampus initially enhanced LTP, but sustained Cdk5 hyperactivity eventually impaired LTP (Fischer, Sananbenesi et al. 2005). Accordingly, transient upregulation of Cdk5 enhanced learning and memory, while prolonged expression of p25 severely impaired cognition. Although the specific role of Cdk5 in learning and memory remains clouded, Cdk5 is without question an essential regulator of neuronal plasticity. Furthermore, these findings hint at a putative role for Cdk5 in the cognitive impairment that is a hallmark of neurodegenerative disease.

Role of Cdk5 in neurodegenerative diseases

Given the essential role that Cdk5 plays in nervous system function, it is not surprising that disruption of normal Cdk5 function is detrimental. Multiple studies have linked Cdk5 to a variety of NDDs in humans. Alzheimer's disease is a neurodegenerative disease resulting in progressive memory loss that culminates in dementia. The hallmark pathologies of AD include neurofibrillary tangles (NFTs) and amyloid plaques, although how these relate to the causative mechanisms underlying AD is not completely understood. Remarkably, Cdk5 has been linked to the formation of both NFTs and plaques. As such, Cdk5 is considered one of the primary

candidates for therapeutic targeting in the treatment of AD, making the elucidation of Cdk5's

physiologically relevant contributions to AD essential.

NFTs are formed by aggregation of the microtubule-associated protein (MAP) tau, which

amasses more readily when the protein is hyperphosphorylated. Under normal circumstances,

tau regulates microtubule stability within axons. Tau has two primary functional domains: a C-

terminal microtubule-binding domain and an N-terminal projection domain. The C-terminal

domain of tau binds the interface between tubulin heterodimers, stabilizing the microtubule and

facilitating polymerization (Kadavath, Hofele et al. 2015). Independent of its role in microtubule

stability, tau is also capable of regulating axonal transport. The N-terminal domain of tau

contains a phosphatase-activating domain (PAD); this domain, spanning amino acids 2-18 of tau,

is capable of activating protein phosphatase 1 (PP1) (Kanaan, Morfini et al. 2012). This

activation initiates a cascade resulting in the dephosphorylation and resultant activation of

GSK3β (LaPointe, Morfini et al. 2009, Kanaan, Morfini et al. 2012), followed by the eventual

dissociation of the motor protein from its cargo (Morfini, Szebenyi et al. 2002, Morfini, Szebenyi

et al. 2004). Ultimately, tau functions in stabilizing the microtubule cytoskeleton and regulating

kinesin-mediated anterograde fast axonal transport.

Hyperphosphorylated tau dissociates from microtubules. This leads to destabilization of

the microtubule cytoskeleton, as well as perturbation of trafficking. Further, the dissociated tau

aggregates into NFTs. These aggregates can also sequester normal tau, exacerbating the

detrimental effects of hyperphosphorylated tau. When Cdk5 was first discovered, it was found to

be a kinase that could phosphorylate tau at the specific sites that are hyperphosphorylated in

NFTs (Paudel, Lew et al. 1993). Initially referred to as 'brain proline-directed protein kinase,'

Cdk5 phosphorylates multiple sites of bovine tau *in vitro*, including ser-202, ser-209, thr-212,

thr-238, ser-242, ser-403, and ser-411. The corresponding residues of human tau are all phosphorylated in tau isoforms associated with NFTs (Lund, McKenna et al. 2001, Liu, Iqbal et al. 2002). While these experiments were conducted *in vitro*, similar results have been demonstrated in cell-based assays (Michel, Mercken et al. 1998, Patrick, Zukerberg et al. 1999), and transgenic mice overexpressing the Cdk5 activator p25 exhibited tau hyperphosphorylation, increased tau aggregation, and an increased number of NFTs (Noble, Olm et al. 2003). Furthermore, Cdk5 activity was found to be elevated in tissue from patients with AD (Lee, Clark et al. 1999, Patrick, Zukerberg et al. 1999, Shelton and Johnson 2004).

Cdk5 hyperactivity also led to increases in amyloid beta (Aβ) levels in the forebrains of mice. Aβ is a cleavage product of amyloid precursor protein (APP) and is the main component of amyloid plaques that are found in the brains of AD patients. Since Cdk5-induced elevations of Aβ levels are detected prior to any observable neuropathology, it is thought that multiple Cdk5-mediated pathways contribute to AD (Cruz et al 2006). Cdk5 directly regulates Aβ at multiple steps. Cdk5 phosphorylates both APP and presenilin-1 (PSEN-1); PSEN-1 is the catalytic subunit of gamma secretase, which is involved in the processing and cleavage of APP to generate Aβ. Phosphorylation of PSEN-1 by Cdk5 stabilizes it, allowing the complex to persist longer and therefore cleave more APP, generating more Aβ peptides (Lau and Ahlijanian 2003). Phosphorylated APP is also associated with increased generation of Aβ fragments (Wen, Planel et al. 2008, Sadleir and Vassar 2012). Elevated levels of Aβ42 lead to the formation of the amyloid plaques associated with AD.

Aside from AD, Cdk5 has also been linked to Parkinson's disease (PD), a degenerative disorder that primarily affects the dopaminergic system and its regulation of motor function. The pathological hallmark of PD is the formation of Lewy bodies (abnormal aggregates of α-

synuclein) that are associated with neurodegeneration of dopamine-secreting cells in the substantia nigra. α-syn is primarily restricted to the nervous system, and further localizes specifically to the presynaptic terminal (Bendor, Logan et al. 2013). The function of α-syn at the synapse is contradictory, as studies have found evidence that α-syn both promotes neurotransmitter release (Cabin, Shimazu et al. 2002) and is a negative regulator of neurotransmission (Abeliovich, Schmitz et al. 2000). Likely, the role of α-syn is different in various cell types and is context-dependent.

While the normal function of α-syn remains unclear, it is well established that α-syn deposits are associated with PD. Immunohistochemical staining of post-mortem brain tissue from PD patients revealed that some of these deposits also contained both Cdk5 and p35 (Brion and Couck 1995, Nakamura, Kawamoto et al. 1997, Takahashi, Iseki et al. 2000). α-syn can induce a calcium influx, leading to calpain-mediated cleavage of p35 and eventual Cdk5 hyperactivity (Czapski, Gassowska et al. 2013). Once Cdk5 is activated, one of its targets is peroxiredoxin 2 (Prx2), an anti-oxidant enzyme. Phosphorylation of Prx2 reduces its peroxidase activity, limiting its ability to help against oxidative stress; hyperphosphorylated Prx2 was found in substantia nigra neurons in tissue from Parkinson's disease patients (Qu, Rashidian et al. 2007).

Cdk5 also phosphorylates parkin, an E3 ubiquitin ligase that is commonly mutated in inherited forms of PD (Kitada, Asakawa et al. 1998) and is also found in Lewy bodies of sporadic PD (Schlossmacher, Frosch et al. 2002). Cdk5-mediated phosphorylation of parkin at ser-131 decreases parkin auto-ubiquitination and parkin-dependent ubiquitination of synphilin-1 and p38 (Avraham, Rott et al. 2007). Expression of a Cdk5-phosphorylation-deficient parkin

mutant lead to increased ubiquitination of both synphilin-1 and p38 and formation of toxic aggregates.

Amyotrophic lateral sclerosis is an axonopathy that affects motor neurons of the central nervous system, leading to muscle weakness, paralysis, and ultimately death (Williamson and Cleveland 1999). Further, motor neurons from patients with ALS were found to have an elevated number of neurofibrillary swellings in the proximal axon (Delisle and Carpenter 1984). Mutations in the gene for copper-zinc superoxide dismutase 1 (SOD1) account for approximately 20% of familial ALS cases (Deng, Hentati et al. 1993, Rosen, Siddique et al. 1993). SOD1 catalyzes the conversion of superoxide anion into hydrogen peroxide and oxygen, protecting cells against damage caused by oxidative stress (Fridovich 1986). More recently, SOD1 has also been found to function in regulating cellular respiration (Reddi and Culotta 2013).

In a mouse model of ALS, mutations of SOD1 correlating with those seen in humans resulted in elevated Cdk5 activity (Nguyen, Larivière et al. 2001). Mutant mice exhibited an increase of p25 and resultant mislocalization of Cdk5 to the cytoplasm and nucleus, and the degree of Cdk5 hyperactivation strongly correlated with a shortened lifespan. The authors proposed that SOD1 dysfunction leads to oxidative stress and elevated intracellular calcium levels, inducing calpain-mediated cleavage of p35 into p25 and upregulating Cdk5. Cdk5 hyperactivity caused hyperphosphorylation of tau and neurofilament proteins, which are known to be involved in axonal transport. Indeed, one of the earliest observed events in motor neurons expressing mutant SOD1 is the reduced transport of specific cargos such as tubulin (Williamson and Cleveland 1999).

Using altered p35 levels as a model of Cdk5 dysfunction

In *Drosophila*, Cdk5 activity requires direct interaction with the activator subunit p35. To investigate the physiological roles of Cdk5, it is possible to target Cdk5 directly or to modulate p35. We have shown previously, however, that Cdk5 has an extremely long half-life (>24 hours; LCC and EG, unpublished data), making disruption of the Cdk5 gene an ineffective way to produce loss-of-function phenotypes in many experimental paradigms. Moreover, high-level overexpression of Cdk5 does not reliably produce a gain-of-function phenotype (Connell-Crowley, Le Gall et al. 2000). In contrast, altering expression of the activator, p35, has predictable and nearly immediate effects on Cdk5 activity. p35 has a half-life of 20-30 minutes (Patrick, Zukerberg et al. 1999), and is a limiting factor of Cdk5 activity in neurons as Cdk5 is present at excess levels (Takasugi, Minegishi et al. 2016).

Modulation of Cdk5 activator levels have previously been shown to regulate Cdk5 activity. Overexpression of p35 enhances Cdk5 activity in *Drosophila* (Connell-Crowley, Le Gall et al. 2000), and the deletion of p35 or of p35 and p39 abolishes Cdk5 activity in flies and mice, respectively (Ko, Humbert et al. 2001, Connell-Crowley, Vo et al. 2007). It should be noted that we cannot formally rule out the existence of Cdk5-independent functions of p35; additional experiments are required to discern roles of p35 outside of Cdk5 activation. However, it has been shown that p35 is unable to bind and activate other Cdks with similar structure to Cdk5 (Poon, Lew et al. 1997, Connell-Crowley, Le Gall et al. 2000). Furthermore, deletion of p35 in *Drosophila* mimics Cdk5-null phenotypes (Connell-Crowley, Vo et al. 2007, Kissler, Pettersson et al. 2009), and is non-additive when combined with a dominant negative Cdk5 (Connell-Crowley, Vo et al. 2007). Additionally, *Drosophila* lack orthologs to either of the two known non-p35 activators of Cdk5, p39 or Cyclin I, making it unlikely that Cdk5 has non-p35

activators in this organism. As such, experiments described in the following chapters will use

perturbation of p35 levels as a proxy for altering Cdk5 activity.

1.5 Aims of this thesis

To date, there has been little success with treating neurodegenerative disorders, and no cure exists for any of the major age-related degenerative diseases affecting humans. Work in this thesis is aimed towards identifying new mechanisms of degeneration through the study of *Drosophila* models of adult-onset neurodegeneration. Our lab has previously shown that Cdk5-mediated phenotypes in fly overlap with pathologies associated with degeneration in humans, and that these phenotypes are also consistent with aging-induced phenotypes. Thus, we hypothesized that Cdk5-mediated ND stems from both aging-dependent and aging-independent mechanisms. The work presented here challenges the current view of the relationship between neurodegeneration and aging, and provides a foundation for the development of a variety of new therapeutic strategies.

In chapter 2, I present work towards the improvement of assays for quantifying neurodegeneration. I demonstrate a method for the fully automatic quantification of mushroom body neurons within adult *Drosophila* brains. I also describe progress in adapting a silver-staining technique for the selective labeling of degenerating neurons to the *Drosophila* model, in addition to techniques for assessing neuronal physiology during degeneration.

In chapter 3, I show that altered Cdk5 activity induces multiple degenerative phenotypes and causes robust neurodegeneration. I then develop a genome-wide expression-based metric for quantifying the physiological age of a tissue, and show that Cdk5 dysfunction accelerates the intrinsic rate of aging. These results suggest that accelerated aging is actually a driving force underlying Cdk5-mediated ND.

In chapter 4, I investigate the role of the axon initial segment in neurodegeneration. Although previous research has linked the AIS to ND, it has never been demonstrated in

Drosophila before. Here, I characterize a novel mechanism for modulating the AIS that is independent of Cdk5. I then show that perturbation of the AIS is sufficient to induce ND. This data suggests that regulation of the AIS likely contributes to Cdk5-mediated ND, and is yet another therapeutic target.

Chapter 2

Development of assays for improved assessment of neurodegeneration

Chapter 2: Development of assays for improved assessment of neurodegeneration

2.1 Introduction

The ever-increasing portion of the human population afflicted with neurodegenerative diseases (NDDs), combined with the fact that many of the underlying mechanisms of these diseases have yet to be elucidated, highlights a growing issue that needs to be solved. In order to investigate these mechanisms, and to gauge efficacy of therapies designed to treat NDDs, it is essential that techniques continue to be developed for enhanced quantification of neurodegeneration (ND). ND involves significantly more than just the terminal result of neuronal death; indeed, multiple physiological processes are disrupted prior to cellular demise. To fully understand the underlying causes of ND, it is necessary to assess neuronal dysfunction throughout the course of the entire degenerative process.

Many of today's current neurodegenerative assays are hindered by a variety of limitations. Organismal level degenerative assays, such as lifespan and motor function, are good for approximating an overall level of fitness, but they fail to address the underlying mechanisms contributing to loss of fitness. Further, ND can occur in neuronal populations whose functional output might not be obvious at the organismal level, leading to detrimental defects that are overlooked. At the cellular level, the primary tools for analyzing ND are end-point assays that measure levels of cell death, such as terminal deoxynucleotidyl transferase dUTP nick end labeling (TUNEL) staining for apoptosis or propidium iodide staining for necrosis. While useful, these tools are not ideal for detecting degeneration at earlier stages or in situations that do not result in cell death. Other assays, such as histological sectioning, show 'vacuoles' that are consistent with ND, but that do not directly illustrate neuronal death. Such tissue loss could be

the result of degeneration of the dendritic arborization without accompanying neuronal death, or

even happen because tissue is merely more sensitive to processing. Another limitation of these

assays is the failure to assess the earliest stages of ND, and to distinguish the different

mechanisms through which ND occurs. These limitations underline the vast need for improved

assays. Further, the pitfalls of current techniques clearly demonstrate that no single assay on its

own will suffice; rather, a panel of assays testing the entire degenerative process is necessary for

assessing the underlying mechanisms.

Here, we present multiple methods for directly quantifying neuronal loss, including a

method for fully automatic counting of mushroom body neurons from a confocal z-stack. We

also describe techniques for examining earlier stages of ND, including one method to selectively

label degenerating neurons and other methods measuring different aspects of neuronal

physiology. Ultimately, utilizing a panel of such assays, which probe the physiological state of

the neuron throughout the course of degenerative processes, is vital to uncovering the key

features of disease etiology.

2.2 Materials and Methods

Fly stocks

Control flies were from either an Oregon Red wild-type background (w+) or a w^{1118}

white-eyed mutant background (w-), as described. Cdk5 loss of function conditions ($p35^{20C}$ and

DfC2) have been previously described (Connell-Crowley, Le Gall et al. 2000, Connell-Crowley,

Vo et al. 2007, Trunova, Baek et al. 2011, Trunova and Giniger 2012, Smith-Trunova, Prithviraj

et al. 2015). The p35-null alleles were crossed into the wild-type background (w+; $p35^{20C}$).

Overexpression of p35 was achieved by adding four copies of a transgene encoding the p35

genomic locus (Connell-Crowley, Le Gall et al. 2000) in the same background (w+; P[w+,Tn p35] ^{R244}/P[w+,Tn p35] ^{R244}; P[w+,Tn p35]^{R157}/P[w+,Tn p35] ^{R157}). For MB cell counting, the UAS-nls-GFP and UAS-nls-mCherry fly stocks were obtained from the Bloomington *Drosophila* Stock Center (BDSC). The gamma-neuron specific Gal4 driver 201Y-Gal4 was used to express UAS-nls-GFP in control (w+; 201Y-Gal4/+; UAS-nls-GFP/+), p35-null (w+; DfC2,201Y-Gal4/p35^{20C}; UAS-nls-GFP/+), or p35-OE (w+; 201Y-Gal4,P[w+,Tn p35] ^{R244}/P[w+,Tn p35] ^{R244}; UAS-nls-GFP, P[w+,Tn p35] ^{R157}/P[w+,Tn p35] ^{R157}) backgrounds. hs-Gal4, UAS-hid was procured from the BDSC, and ELAV-Gal4/+; UAS-Aβ42 was provided by Dr. Koichi Iijima. The UAS-mito-GFP stock was a gift of Dr. Ramakrishnan Kannan.

Immunohistochemistry

Adult brains were dissected in ice-cold phosphate buffered saline (PBS) (pH 7.4) (Invitrogen), fixed in 4% paraformaldehyde (PFA) in PBS for 30 min, and then transferred to 4% PFA in PBS with 0.5% Triton X-100 (PBST) for an additional 30 min. Brains were then rinsed once in PBST, followed by three five-minute washes in PBST. Brains were incubated in blocking buffer (PBST, 4% bovine serum albumin (BSA), 4% goat serum, 4% donkey serum) for 1 h, then incubated with primary antibodies in blocking buffer for 48 hours at 4°C. Primary antibodies included: 1:200 mouse anti-Fasciclin 2 (Fas2) and 1:100 mouse anti-dachshund (Dac) from Developmental Studies Hybridoma Bank. Samples were then rinsed and washed thrice in PBST, before being incubated with secondary antibodies overnight at 4°C. Secondary antibodies were diluted 1:500 in blocking buffer, and included goat anti-mouse conjugated with either A488, A568, or A633 fluorochromes (Invitrogen). Lastly, brains were rinsed and washed thrice in PBST before being mounted in VectaShield antifade medium. In order to prevent samples

from being squished, coverslips were set on number 1 glass chips. Prepared samples were imaged under 40X-oil on a Zeiss NLO510 confocal microscope and analyzed using Imaris.

Silver staining

Whole adult brains were microdissected in ice-cold PBS, and then transferred into fixative (4% PFA in 0.1M cacodylate buffer, pH 7.4). Brains were placed on a nutator for 1 hour at room temperature (RT), and then transferred to a nutator at 4°C for 24 hours. After five five-minute washes in water, the brains were transferred into a cupric-silver solution (6ml deionized water, 0.0525g AgNO3, 50μl 1% CuNO3, 500μl 0.1% allantoin, 300μl pyridine, 600μl absolute ethanol, and 300μl borate buffer) and incubated at 40°C for 1 hour. The samples were then removed from heat and left at RT overnight. Samples were washed in 100% acetone for 90 seconds, then immediately transferred to a silver diamine incubation solution (6ml deionized water, 1.2g AgNO3, 3ml 0.4% NaOH, 1.5ml NH4OH, 6ml deionized water). After a 35-minute incubation in the dark, the samples are transferred to a reducing agent solution (13.5ml deionized water, 1.5ml absolute ethanol, 18μl 37% w/w formaldehyde, 1.05mg anhydrous citric acid) for 5 minutes. Samples were then incubated in ferricyanide bleaching solution (0.3% K3Fe(CN)6) for no more than 10 minutes with gentle agitation, until the brains achieved a dark straw color. Once the brains were the appropriate color, they were washed thrice in distilled water, then transferred to 0.1% sodium thiosulfate for 1 minutes. Following three more washes, the brains were then mounted and imaged on a Nikon Optiphot-2 microscope.

Thioflavin S staining

Whole adult brains were microdissected in ice-cold PBS, then fixed in 4% PFA for 1 hour. After three five-minute washes, brains were permeabilized in 2% Triton X-100 for 4 hours. Brains were then washed twice in PBS, washed once in 50% ethanol/PBS, and then incubated in 0.2% thioflavin-S for 11-13 hours. Following this overnight incubation, samples were washed once in 50% ethanol/PBS, washed twice in PBS, and then mounted. Microscopy was performed on a Zeiss NLO510 confocal microscope using a Chameleon 750nm laser to excite the thioflavin S. Images were acquired using either a 20-X dry or 40-X oil objective.

Mushroom Body Neuron Counting

Whole adult brains were microdissected in ice-cold PBS and fixed in 4% PFA for 1 hour, washed, and then mounted on slides with VectaShield (Vector Laboratories, Burlingame, CA). Microscopy was performed on a Zeiss NLO510 confocal microscope or with the Zeiss Yokogawa Spinning Disk (SD) system mounted on an inverted Zeiss Axio Observer Z1 microscope; images were acquired using a 40-X oil objective. Z-stacks were collected from individual brain hemispheres, and were analyzed using Bitplane's IMARIS (version 7.5.2) and its 'Add spots' function to semi-automatically count the labeled neurons; false positives were manually removed, and false negative nuclei were manually added.

For automatic quantification of MB neurons using UAS-nls-mCherry, the spot counting diameter was set to "2" and the threshold value was set to "2.12." These values were determined through manual testing to yield the most accurate results.

2.3 Results

Nuclear reporters can assay neurodegeneration by directly counting neuron number

Prior to assessing specific stages of neurodegeneration, it is necessary to first establish that neurodegeneration is even occurring. In a *Drosophila* model of adult-onset neurodegeneration, histological sectioning of p35-null brains revealed the formation of 'vacuoles' in the brain; these holes in the tissue were largely localized to the mushroom bodies (MB), responsible for olfactory learning and memory (Trunova and Giniger 2012). While such vacuole formation is consistent with neurodegeneration, it falls short of directly showing neuronal loss. As such, we sought to directly count the number of MB neurons. First, we used antibody staining to selectively label MB neurons. The protein Dachshund is expressed in a large set of neurons, including MB neurons. To restrict our analysis to MB neurons only, we analyzed flies carrying a MB-specific Gal4 driver and a fluorescent-tagged membrane marker (OK107-Gal4>UAS-mCD8-GFP), and focused our analysis on double positive neurons. Co-labeling with anti-Dac antibody staining and with UAS-mCD8-GFP revealed individual MB neurons (Figure 2.3.1a-c); however, quantifying neurons from the entire MB by counting each Z-slice in a stack proved problematic due to issues with tallying the same neuron multiple times from adjacent slices. To solve this, we used mCD8-GFP to outline a MB volume, and only counted Dac-positive neurons contained within it (Figure 2.3.1d). However, Dac-staining could not sufficiently distinguish between adjacent neurons for automatic counting, as the cell bodies are in close proximity with one another.
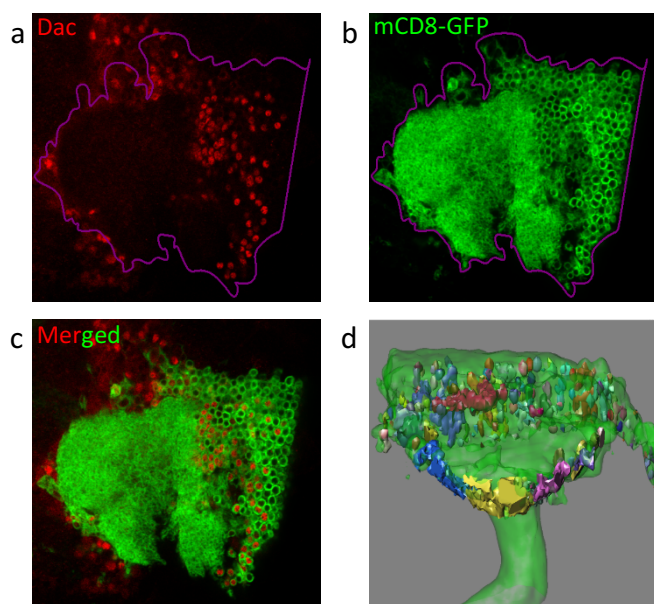
Figure 2.3.1. Antibody staining and mCD8-GFP expression labels MB neurons for direct quantification.
Flies with OK107-Gal4-driven MB-specific expression of mCD8-GFP were stained with anti-Dac to co-label the MB neurons. **(A)** anti-Dac staining labels the nuclei of a large set of neurons including MB neurons, while **(B)** expression of mCD8-GFP specifically labels MB neurons. **(C)** Neurons that are positive for both Dac and mCD8-GFP are selected for quantification. **(D)** A 3D volume was generated from composite confocal images of the mCD8-GFP label; only Dac staining that was encompassed by the volume was quantified.

Given the lack of sensitivity and insufficient signal:noise ratio from antibody staining and the membrane marker, we next tested a nuclear-targeted fluorescent protein to quantify MB neurons. We combined UAS-nls-GFP with 201Y-Gal4, which expresses in a subset of MB neurons. This combination permitted quantification of most gamma neurons, as well as some alpha and beta neurons (Figure 2.3.2A; (Aso, Grübel et al. 2009)). Out of multiple platforms tested, Imaris proved the most successful at automatically counting labeled neurons. However, it was observed that the nls-GFP signal was not entirely restricted to nuclei and also labeled the calyx (Figure 2.3.2A – side view), which added to the background noise and ultimately prevented fully automatic quantification. Nevertheless, the signal was sufficient for precise counting of individual neurons. The tallied number of labeled MB neurons was consistent

regardless of the microscope used to collect the images (Figure 2.3.2C-D), and regardless of the orientation of the brain when mounted on a slide (Figure 2.3.2E). We also tested a separate construct, UAS-nls-mCherry, which revealed better restriction of the fluorescent probe to the nuclei (Figure 2.3.2B). With the enhanced signal:noise ratio, fully automatic quantification could reliably count ~90% of the labeled neurons (Figure 2.3.2F).
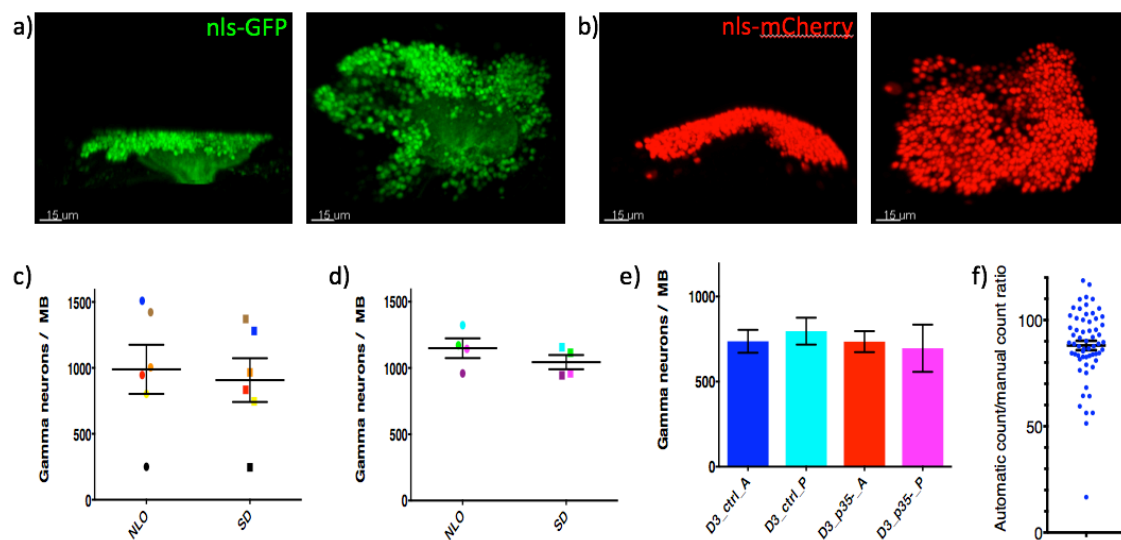
Figure 2.3.2. Expression of nuclear-localized fluorescent protein permits automatic quantification of MB neurons.
201Y-Gal4-driven MB-specific expression of (**A**) UAS-nls-GFP or (**B**) UAS-nls-mCherry is used to quantify MB neurons (side and top views are presented). (**C-D**) Quantification with a nuclear label is robust enough that samples imaged on different microscopes yield essentially identical counts, regardless of whether imaging was first completed on the NLO microscope (**C**) or initially done on the spinning disk (**D**). Brain hemispheres are color-coded to identify which counts come from the same sample. (**E**) MB neuron quantification is not affected by the orientation of the brains on the slide when imaged. 3-day old control and p35-null samples were dissected and mounted with either the anterior (A) side of the brain adjacent to the coverslip, or the posterior (P) side of the brain. Subsequent quantification revealed no significant difference between orientations, regardless of genotype. (**F**) Labeling with nls-mCherry is precise enough that completely automated counting can quantify 88.03$\pm$2.21 (mean$\pm$SEM) of the labeled MB neurons (n=61 hemispheres).

As this method of labeling relies on expression from a Gal4 driver, we next verified that that expression remains constant with age. Specifically, we wanted to be sure that any observed decrease in cell numbers was due to neurodegeneration and not the result of decreased Gal4 expression. We addressed this by two methods: co-labeling MB neurons of young and old flies with both nls-GFP and anti-Dac antibody, and by co-labeling MB neurons with both ROBO2-GFP and anti-FasII antibody. In either case, a significant increase in the number of antibody-positive/GFP-negative neurons in old flies would indicate that some neurons are still present but are not expressing Gal4. Co-labeling MB neurons of 3- and 30-day old control flies (201Y-Ga4/+; UAS-nls-GFP/+) with anti-Dac revealed robust GFP expression even at old age (Figure 2.3.3A, C). Both FasII and ROBO2-GFP are restricted to the axonal lobes of MB neurons. In adult flies, FasII is expressed to varying degrees in different subsets of MB neurons; in the gamma neurons where 201Y-Gal4 is primarily expressed, FasII has low but still detectable expression (Figure 2.3.3B'). Similar to nls-GFP, ROBO2-GFP expression does not diminish with age (Figure 2.3.3B,D). These trends hold true regardless of p35 expression, as p35-null flies also exhibited robust 201Y-Gal4 expression at 30 days (Figure 2.3.3E-H). Taken together, these data demonstrate that 201Y-Gal4-driven expression of a nuclei reporter is a viable option for quantifying neuronal loss in the MB.
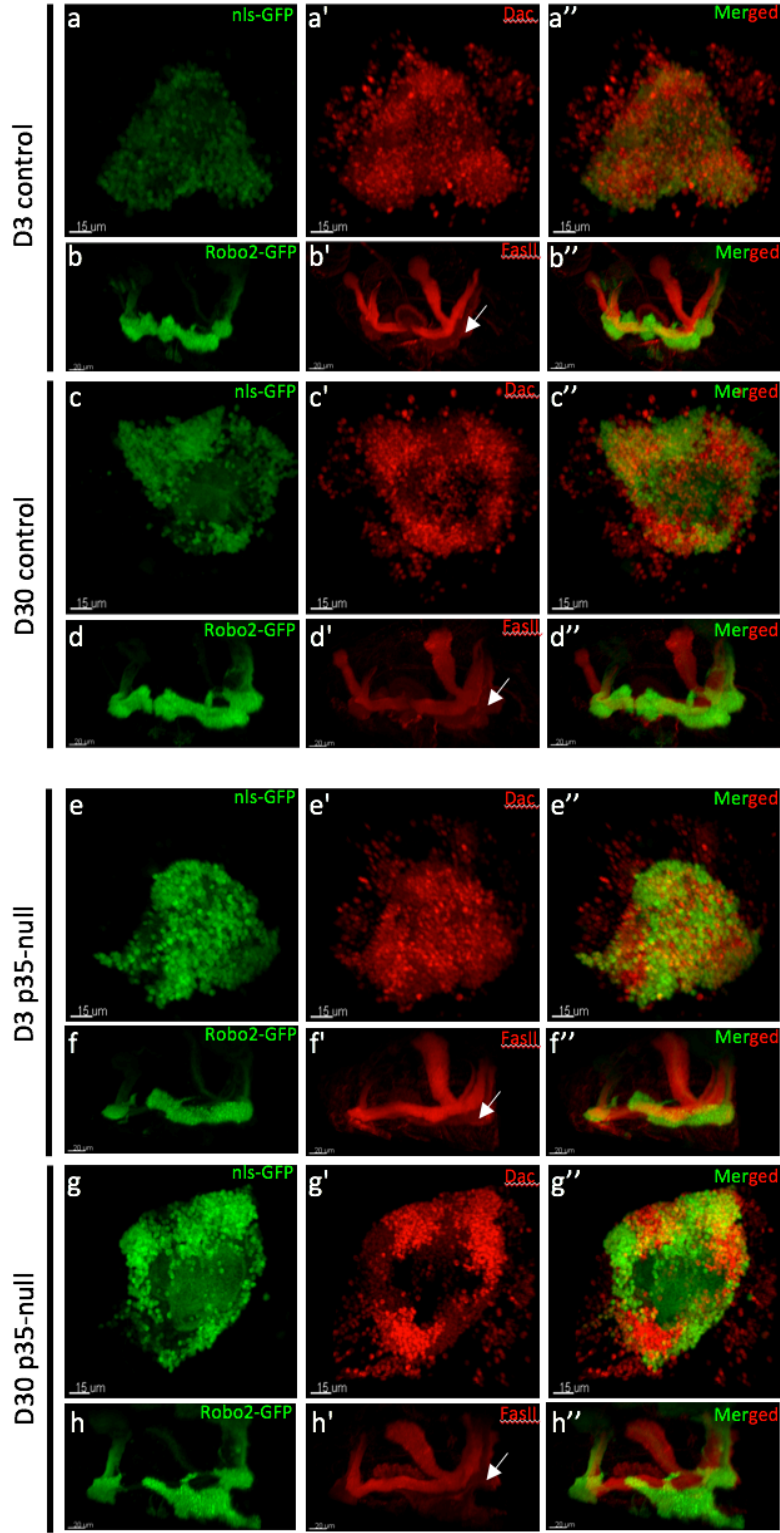
Figure 2.3.3: 201Y-Gal4-driven expression does not decrease with age. Composite confocal images of MB cell bodies and axonal lobes from control and p35-null flies aged to 3- or 30-days old. Specific loss of the fluorescently-labeled marker without concordant loss of antibody staining would reveal decreased Gal4 expression with age. **(A,C,E,G)** Flies expressing UAS-nls-GFP driven by 201Y-Gal4 were stained with anti-Dac. **(B,D,F,H)** Flies expressing UAS-Robo2-GFP driven by 201Y-Gal4 were stained with anti-FasII. White arrows highlight the subset of gamma neurons where 201Y expression is the highest.

A modified silver-strain protocol labels degenerating neurons

As an alternative to quantifying the number of remaining MB neurons, which fails to distinguish between healthy and dying neurons, we sought to selectively label degenerating neurons. Over the past few decades, significant progress has been made towards such a goal in mammalian samples. de Olmos first developed a modified cupric-silver technique for the selective impregnation of degenerating neurons in 1969 (De Olmos 1969). Since then, others have continued to develop techniques that can label neuronal cell bodies, axons, dendritic processes, and synaptic terminals of degenerating neurons, while healthy neurons are left unlabeled (Switzer 2000, Tenkova and Goldberg 2007). Starting with these mammalian-specific protocols, we combined aspects of multiple methods to generate a new protocol for use in *Drosophila*, as no such technique has been developed for insects. To be certain that we were detecting neurodegeneration, we employed several methods to induce neuronal death. Neuronal apoptosis was triggered by heat-shock induced expression of the *head involution defective* gene (HS-Gal4>UAS-hid), which has been shown to cause programmed cell death (Grether, Abrams et al. 1995). Second, expression of amyloid beta 42 (Aβ42) was driven pan-neuronally using ELAV-Gal4. In humans, Aβ42 aggregates into plaques and is linked to Alzheimer's disease; in *Drosophila*, expression of Aβ42 has been found to induce age-dependent memory defects, locomotor dysfunction, and neurodegeneration (Iijima, Chiang et al. 2008). Lastly, we examined p35-null flies, which exhibited age-dependent formation of 'vacuoles' in the MB (Trunova and Giniger 2012). In each case, there were instances of successful silver staining and evidence of neurodegeneration (Figure 2.3.4). However, staining results were largely inconsistent; indeed, only 1/30 p35-null brains exhibited evidence of selectively-labeled degenerating neurons within the MB. Furthermore, there was extreme variation in the staining of samples within genotypes,

even among controls; this observation pointed to the prerequisite for additional troubleshooting

before any meaningful conclusions could be drawn. Ultimately, this labor-intensive procedure,

which would require even further optimization, was removed from the panel of

neurodegenerative assays.
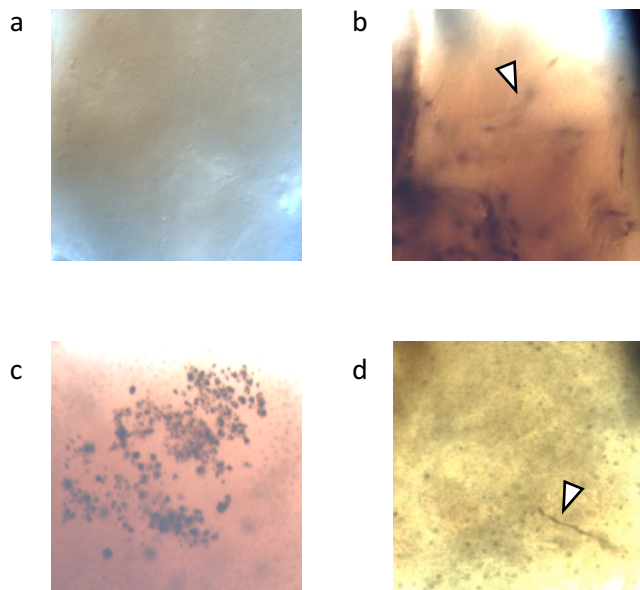
Figure 2.3.4. Modified silver staining can selectively label degenerating neurons.
Silver staining of **(A)** heat-shock control samples reveals minimal neuronal labeling. Staining of
(B) hs-hid, **(C)** 45 day old p35-null, and **(D)** ELAV-Gal4>UAS-AB42 samples reveals selective
labeling of cell bodies and neuronal processes (white arrowheads).

Development of assays to evaluate defects in neuronal physiology

Proper mitochondrial function is essential for neuronal maintenance and homeostasis.

Certainly, damaged and non-functional mitochondria have been associated with

neurodegeneration in many paradigms across multiple species (Leuner, Hauptmann et al. 2007).

Here, we sought to analyze the ratio of healthy, functional mitochondria to total mitochondria,

positing that an increase in non-functional mitochondria could be an underlying mechanism of

Cdk5-mediated neurodegeneration. To accomplish this, we stained unfixed whole brains with

tetramethylrhodamine, methyl ester (TMRM), a fluorescent dye that permeates into cells and is readily sequestered by healthy, active mitochondria; mitochondria with a perturbed membrane potential fail to take up the dye (Perry, Norman et al. 2011). Additionally, we co-labeled mitochondria by staining with MitoTracker-Green, which stains all mitochondria regardless of membrane potential (Cottet-Rousselle, Ronot et al. 2011). Thus, all mitochondria will be labeled with MitoTracker-Green, while only healthy mitochondria will also be labeled with TMRM. As our previous findings identified the MB as a susceptible population in the p35-null background, we focused our analyses on this neuronal subpopulation. As a positive control, we treated intact brains with the mitochondrial uncoupler carbonyl cyanide p-trifluoromethoxyphenylhydrazone (FCCP) to disrupt mitochondrial membrane potential (Perry, Norman et al. 2011). The addition of FCCP resulted in a drastic decrease of TMRM-positive puncta, indicating loss of healthy mitochondrial with intact membrane potential (Figure 2.3.5E). In the end, we failed to get adequate depth of penetration of the TMRM dye into the intact brain samples to stain the MB neurons (Figure 2.3.5B), so we could not quantify the ratio of healthy versus unhealthy mitochondria. As such, TMRM staining is not a viable option for analyses in whole brain; however, future experiments can utilize UAS-mito-GFP constructs to visualize mitochondrial number and defects in fission or fusion.
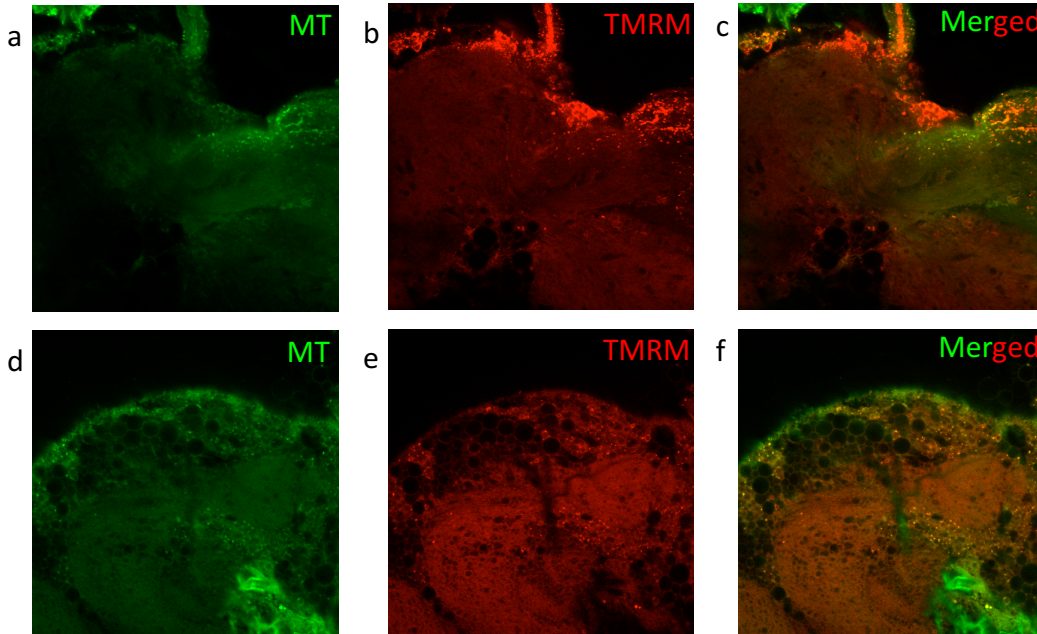
Figure 2.3.5: Labeling of mitochondria with multiple reagents distinguishes healthy versus damaged mitochondria.
Wild-type brains were dissected and stained with **(A,D)** MitoTracker-Green (MT) and **(B,E)** TMRM in the presence or absence of the decoupler FCCP. **(D-F)** Treatment with FCCP significantly reduced TMRM staining, indicating effective disruption of the mitochondrial membrane potential.

In addition to mitochondrial dysfunction, disrupted autophagy has been associated with multiple neurodegenerative diseases (NDDs) (Hara, Nakamura et al. 2006, Komatsu, Waguri et al. 2006, Spencer, Potkar et al. 2009, Inagaki, Kamikouchi et al. 2010, Winslow, Chen et al. 2010). Indeed, it was demonstrated that p35-null mutants are more sensitive to autophagic stress as they exhibit enhanced sensitivity to starvation (Trunova and Giniger 2012). Furthermore, utilizing electron microscopy, it was found that p35-null mutants also exhibited enhanced accumulation of autophagic organelles both at young and old ages. To assess if autophagy was being compromised by the aberrant formation of protein aggregates, which has been observed in several NDDs (Menzies, Fleming et al. 2015), whole brains were stained with thioflavin S (TS). TS recognizes beta-sheet rich protein aggregates and intercalates within the beta-sheet folds; this

interaction induces a conformational shift of the TS molecule and leads to a detectable shift in

fluorescence (Greenfield 2008). TS has previously been used as a diagnostic marker for some

NDDs, and has even been used in *Drosophila* (Iijima, Chiang et al. 2008). As a positive control,

flies with pan-neuronal overexpression of Aβ42 were first stained with TS. 97.3% (36/37) of

ELAV-Gal4/+, UAS- Aβ42/+ brains showed elevated levels of TS staining, relative to age-

matched controls. (Figure 2.3.6A-B).
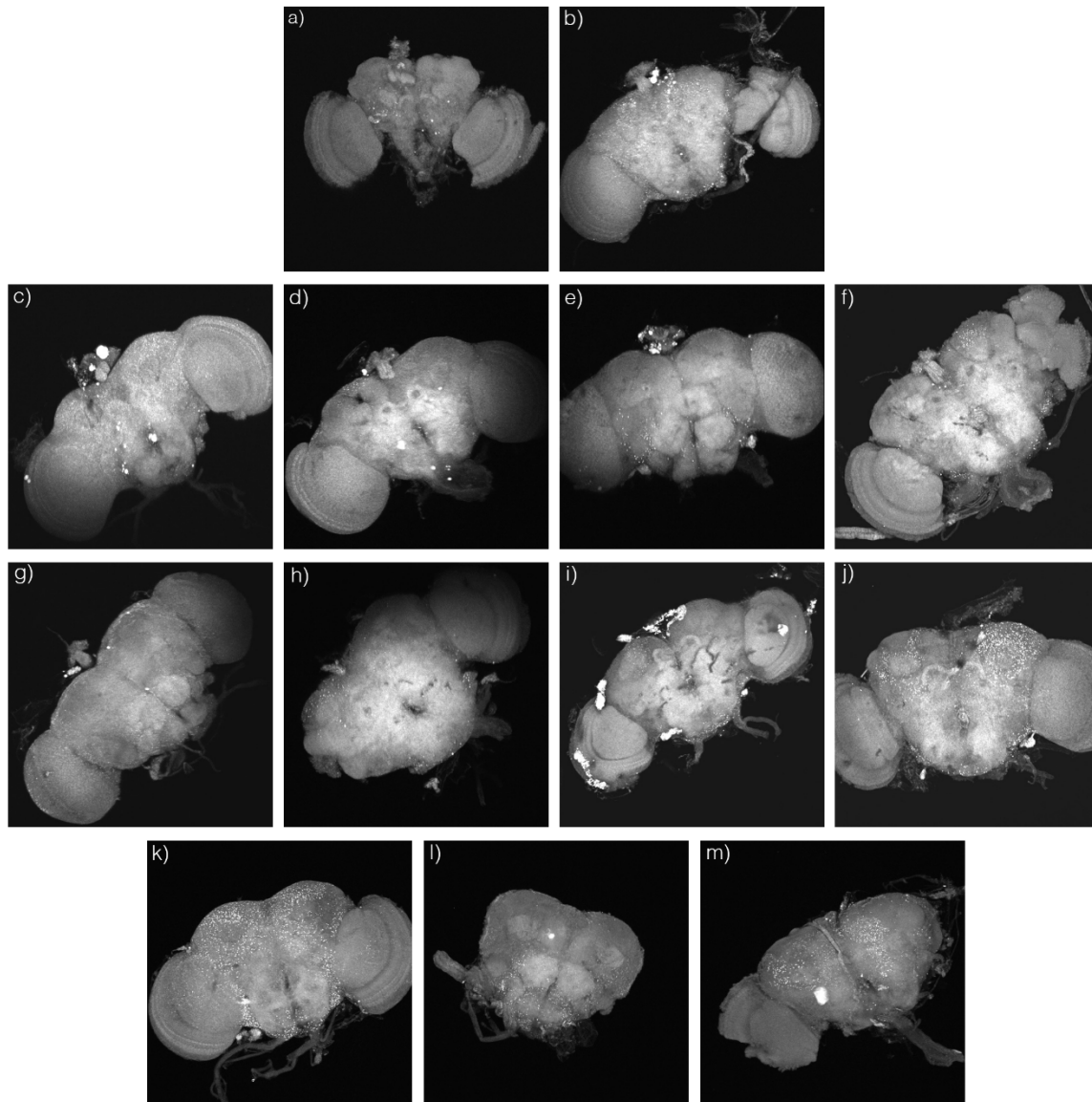
Figure 2.3.6. Thioflavin-S staining labels protein aggregates.
Adult brains of various age and genotype are stained with Thioflavin-S to label protein aggregates. 20-day old w[1118] **(A)** control flies and **(B)** flies overexpressing Aβ42 (ELAV-Gal4> UAS-Aβ42) were used to test the TS-staining protocol; Aβ42-expressing samples exhibited significantly higher numbers of TS-positive puncta. **(C-J)** w[1118] control and p35-null samples show age-dependent accumulation of aggregates, although the phenotype is accelerated by loss of Cdk5 activity. **(C-F)** Control and **(G-J)** p35-null samples were aged to **(C,G)** Day 3, **(D,H)** Day 10, **(E,I)** Day 30, or **(F,J)** Day 45. 3-day old red-eyed w[+] **(K)** control, **(L)** p35-null, and **(M)** p35-OE samples all show elevated levels of TS staining, relative to age-matched w[1118] samples.

After confirming that the protocol worked in our hands, we next stained control (w[1118])

and p35-null (w[1118]; p3520C) flies at various ages (Figure 2.3.6C-J). Controls and p35-null

samples both exhibited a trend of increasing TS-positive puncta with age, with this trend being

accelerated in p35-null brains, consistent with evidence that p35 deficiency accelerates the age-

dependent disruption of autophagy seen in controls. Additionally, p35-null mutant brains show a

shift from a high number of small aggregates to a smaller number of larger aggregates with age.

In some cases, p35-null brains showed TS-positive puncta localized within the MB calyx (Figure

2.3.6J), consistent with previously described ND (Trunova and Giniger 2012).

We next looked for protein aggregation in control, p35-null, and p35-OE flies of a wild-

type genetic background (w+). Surprisingly, staining revealed a large number of TS-positive

puncta regardless of genotype. Relative to the w[1118] samples, which exhibited minimal staining

at Day 3, the w+ samples all showed an increase in TS-positive puncta, with w+ control samples

actually displaying the greatest number of spots (Figure 2.3.6K-M). As the young, 3-day old

control samples, which are essentially a negative control, exhibited a significant number of

puncta, we were forced to question the specificity of the stain. Thus, while TS reactivity is

modified by neurodegeneration, that effect is obscured by an effect of the wild-type white

protein, a transporter of small molecules. Consequently, this assay was not practical and was

replaced with other established markers of autophagy. Specifically, we analyzed Atg8-II and

Ref(2)P levels, two proteins which are known to accumulate when autophagy is impaired

(Ichimura, Kirisako et al. 2000, Li, Zhang et al. 2008, Nezis, Simonsen et al. 2008).

Accumulation of these proteins will be described in more detail in Chapter 3. Additionally, the

lab has tested a fluorescent probe capable of discerning between autophagic induction and

autophagic flux (Arvind Shukla, personal communications). Atg8a tagged with both mCherry

and GFP labels all autophagosomes, thereby tracking levels of autophagic induction. In the non-acidic autophagosome, both mCherry and GFP express, resulting in yellow fluorescence. Once the autophagosome fuses with a lysosome, the GFP fluorescence is quenched by the increased acidity, leaving only red fluorescence to label the autolysosome (DeVorkin and Gorski 2014).

2.4 Discussion

One pitfall of current assays for labeling degenerating neurons is that they can be selective to the mechanism of induced neuronal death and be excluded from neurons dying through separate pathways. To counter this, we used direct neuron counting, which has the benefit of revealing neurodegeneration regardless of how neuronal death was induced. In some cases, antibody staining is sufficient for quantification. However, this is not a viable option when dealing with dense populations of neurons such as the mushroom bodies. Further, antibody staining can be dependent on the functional state of the neuron: if the neuron is no longer producing the targeted protein, it will not be labeled. Using Gal4 expression, which we demonstrated was not age- or genotype-dependent, we were able to robustly label and quantify neurons, thus revealing neurodegeneration. Notably, this method can be applied to any other cell type by using specific Gal4 constructs to drive expression of the nuclear labels, although controlling for the reliability of Gal4 expression will be essential.

In addition to directly measuring neuron loss, flies will be evaluated for various degenerative phenotypes. While overall lifespan can be subject to non-biological confounding factors, it is generally accepted as a method for demonstrating degeneration and loss of fitness. Another behavioral technique for testing degeneration is to assess motor function. To do so in *Drosophila*, flies are tested for their ability to climb up the wall of a vial in response to being

startled and knocked down to the bottom. Typically, simple wall-climbing assays generate a binary score of either pass or fail. Conversely, the counter-current apparatus permits a more quantitative assessment through the calculation of a partition coefficient. Lifespan and motor function assays will be described in more detail in Chapter 3.

Although cell counting, motor defects, and shortened lifespan can all measure degeneration, these phenotypes can sometimes take weeks to manifest. To fully understand the underlying mechanisms leading to neurodegeneration, it is necessary to assess the degenerative processes at their earliest stages. Unfortunately, technical difficulties prevented silver staining and mitochondrial staining from being viable options for quantifying neurodegeneration. Using thioflavin-S staining to detect protein aggregation appeared to be successful in white-eyed w^{1118} mutants, but not in wild-type red-eyed w^+ flies. In *Drosophila*, the white gene encodes a subunit of an ATP-binding cassette transporter (O'Hare, Murphy et al. 1984, Hazelrigg 1987). This complex transports a variety of substrates, and plays a role in pigment synthesis from precursor granules, vesicular accumulation of cyclic guanosine monophosphate, and neurotransmission (Xiao and Robertson 2016). Thus, the increased TS staining observed in w^+ flies likely reflects physiologically relevant aggregates generated through normal neuronal activity, although additional studies would be necessary to confirm this. In place of TS staining, we will measure Atg8-II and Ref(2)P levels to assess proteostasis and autophagy. Atg8 (LC3 homolog) is cleaved and lipidated before it binds to autophagosomes and gets degraded (Ichimura, Kirisako et al. 2000); impaired autophagy results in an accumulation of the cleaved form, assayed as an increase of Atg8-II levels. Ref(2)P, a p62 homolog, accumulates on autophagosomes and then gets degraded upon fusion of the autophagosome with a lysosome. However, if autophagy is impaired, an increase in Ref(2)P levels is observed (Li, Zhang et al. 2008, Nezis, Simonsen et al.

2008). Furthermore, we will assess autophagic induction and flux using the double-tagged Atg8a construct (DeVorkin and Gorski 2014).

Staining earlier stages of degeneration alone is not a sufficient marker of neurodegeneration, as perturbation of physiological processes does not always result in neuronal death. Thus, a panel of assays that probes both the initial dysfunction and the terminal phenotypes is needed. Here, we have established a method for fully automated quantification of mushroom body neurons in adult flies. For experiments presented in following chapters, we will also utilize techniques to assess a range of organismal and cellular phenotypes. As an overall measure of organismal health and fitness, we will track the lifespan of flies, while negative-geotaxis will be used to measure motor function. At the cellular level, autophagy will be assessed by measuring levels of autophagic proteins. Assays developed here, in combination with previously existing assays, will allow the effective analysis of multiple points of the degenerative process, permitting the elucidation of the core mechanisms of neurodegeneration.

Chapter 3

Altered activity of Cdk5/p35 kinase causes neurodegeneration

in part by accelerating the rate of aging

Chapter 3: Altered activity of Cdk5/p35 kinase causes neurodegeneration in part by accelerating the rate of aging

3.1 Introduction

Age is the most prominent risk factor for neurodegenerative disease (NDD), but the relationship between neurodegeneration and aging is complex and controversial. While each NDD has its own unique hallmarks, most degenerative diseases share a variety of cellular phenotypes with aging, including disrupted proteostasis, impaired cellular trafficking, and increased generation of oxidative stress. Despite this, NDD goes beyond being merely brain aging; indeed, not every individual that grows old develops a NDD, so aging alone is insufficient to cause neurodegeneration. Gaining a productive understanding of the pathogenesis of neurodegenerative disease will require that we untangle the relationship of degeneration to aging.

Cyclin-dependent kinase 5 (Cdk5) has previously been linked to multiple NDDs, including Alzheimer's disease (AD), amyotrophic lateral sclerosis (ALS), and Parkinson's disease (PD) (Patrick, Zukerberg et al. 1999, Nguyen, Larivière et al. 2001, Qu, Rashidian et al. 2007). Cdk5 is an atypical cdk that has no role in cell cycle progression, but rather has only been found to act in postmitotic cells. Cdk5 also does not depend on a canonical cyclin for activation; instead, its kinase activity requires binding to an activator that has a three-dimensional fold similar to cyclins, but little sequence similarity. In mammals, there are two Cdk5 activators, p35 and p39, while *Drosophila* has only a single activator, p35 (Tsai, Delalle et al. 1994, Connell-Crowley, Le Gall et al. 2000). Expression of these activators is largely restricted to neurons, localizing Cdk5 activity to the nervous system (Tsai, Delalle et al. 1994, Tang, Yeung et al. 1995, Connell-Crowley, Le Gall et al. 2000). In addition to the spatial regulation by activator

availability, the activity of Cdk5 is further regulated by the phosphorylation status of the kinase and its activator subunits. Upon binding to p35, Cdk5 autophosphorylates its activator, targeting it for proteasomal degradation. There is also cross-regulation of activity with other kinases that share a similar target sequence preference ("proline-directed" protein kinases) (Anderton, Betts et al. 2001, Morfini, Szebenyi et al. 2004, Zheng, Li et al. 2007). Proper regulation of Cdk5 activity is essential to maintaining normal neuronal function and homeostasis.

Deregulation of Cdk5 activity contributes to a variety of NDDs. Altered Cdk5 activity has been found to lead to hyperphosphorylation of tau, inducing formation of neurofibrillary tangles associated with AD (Patrick, Zukerberg et al. 1999), and of neurofilament, as in ALS (Nguyen, Larivière et al. 2001). Cdk5 also hyperphosphorylates and inhibits peroxiredoxin 2 (Prx2), an antioxidant enzyme; elevated levels of phosphorylated Prx2 were found in brain tissue of PD patients (Qu, Rashidian et al. 2007). Aside from links to multiple NDDs, both gain and loss of Cdk5 function have been shown to cause neuronal death in culture, and to cause neurodegeneration in mouse models (Patrick, Zukerberg et al. 1999, Cruz, Tseng et al. 2003, Zheng, Li et al. 2007, Takahashi, Ohshima et al. 2010). We have shown previously that p35 loss of function in the fly produces degeneration-like phenotypes that mimic cellular phenotypes observed in human disease (Trunova and Giniger 2012). This is consistent with a large and growing literature documenting that the fly is a valid and valuable model for dissecting the molecular mechanisms underlying the cascade of events in human NDDs (Feany and Bender 2000, Iijima, Liu et al. 2004, Watson, Lagow et al. 2008). While investigating p35-associated neurodegeneration in the fly, we noted that many of its central phenotypes resemble early onset of normal aging phenotypes (Trunova and Giniger 2012). As in human disease, this underscored the need to distinguish degeneration from aging, both analytically and mechanistically.

Here, we first demonstrate that either gain or loss of p35 causes death of neurons in the learning and memory center of the *Drosophila* brain (the mushroom body), and is associated with characteristic phenotypes of degeneration and aging, including impaired autophagy, progressive loss of motor function, and shortening of the lifespan. We then used gene expression profiling to develop an unbiased and quantitative metric for physiological age. Applying this metric reveals that gain or loss of p35 accelerates the intrinsic rate of aging of the fly. Finally, we further test this hypothesis and show that an age-dependent phenotype identified by the expression profiling, sensitivity to oxidative stress, also shows aging-like changes in flies with altered p35 levels. Taken together, our data suggest that neurodegeneration in response to altered p35 arises from a combination of the direct effects of accelerated aging, in concert with non-aging pathologies induced by the altered pattern of cytoplasmic protein phosphorylation.

3.2 Materials and methods

Fly stocks

Control flies were from an Oregon Red wild-type background (w+). Loss of p35 conditions (p35^{20C} and DfC2) have been previously described (Connell-Crowley, Le Gall et al. 2000, Connell-Crowley, Vo et al. 2007, Trunova, Baek et al. 2011, Trunova and Giniger 2012, Smith-Trunova, Prithviraj et al. 2015). The p35-null alleles were crossed into the control background (w+; p35^{20C}). Overexpression of p35 was achieved by adding four copies of a transgene encoding the p35 genomic locus (Connell-Crowley, Le Gall et al. 2000) in the same background (w+; P[w+,Tn p35]^{R244}/P[w+,Tn p35]^{R244}; P[w+,Tn p35]^{R157}/P[w+,Tn p35]^{R157}). The 'rescue' line was generated by putting a single copy of the transgene into the p35-null background (w+; p35^{20C}/p35^{20C}; P[w+,Tn p35]^{R157}/+). For MB cell counting, the original UAS-

nls-GFP fly stock was obtained from the Bloomington *Drosophila* Stock Center. The gamma-neuron specific Gal4 driver 201Y-Gal4 was used to express UAS-nls-GFP in control (w+; 201Y-Gal4/+; UAS-nls-GFP/+), p35-null (w+; DfC2,201Y-Gal4/p35^{20C}; UAS-nls-GFP/+), or p35-OE (w+; 201Y-Gal4,P[w+,Tn p35]^{R244}/P[w+,Tn p35]^{R244}; UAS-nls-GFP, P[w+,Tn p35]^{R157}/P[w+,Tn p35]^{R157}) backgrounds.

Mushroom Body Neuron Counting

Control, mutant, and p35-OE male flies carrying single copies of 201Y-Gal4 and UAS-nls-GFP were aged to 3-, 10-, 30-, or 45-days old. MB cell counting was done as described in Chapter 2.

Lifespan Assay

To assay lifespan, 10-14 male and 10 female newly-eclosed flies were aliquoted into a vial containing standard KD food and a strip of tegocept paper. Flies were maintained at 25°C with a 12 hr:12 hr light:dark cycle. Flies were transferred to fresh vials every three days; dead male flies were counted at each transfer until all flies had died. At least three sets of seven to 10 vials were collected for each genotype (control = 485, p35-null = 378, rescue = 410, p35-OE = 472 total flies).

Motor Function Assay

Motor function was assayed using a modified version of the negative geotaxis assay originally developed by Benzer (Benzer 1967); our version of the apparatus had six tubes on the lower frame and five tubes on the upper frame. We completed five replicates for each genotype

at each of the four time points, and assayed each replicate twice; a single replicate contained 20 male flies. For the assay, the flies were slightly anesthetized under CO_2, divided into replicates, and transferred to fresh vials. After waiting for three hours to let the anesthesia wear off, flies were transferred to the first tube of the lower frame, and then given three minutes to acclimate to the apparatus. Once acclimated, the apparatus was gently tapped down on the table five times to pool the flies at the bottom of the tube. The top frame is then slid to the left, such that the flies can climb from their current tube in the bottom into the first tube on the top. After 20 seconds, the upper frame is slid to the right. The apparatus is gently tapped down on the table again, depositing all of the flies that climbed up into the top tube down into the second tube on the bottom frame. This process is then repeated four more times, ultimately resulting in the flies being distributed throughout the six bottom tubes based on their climbing ability.

A partition coefficient (PC) was calculated using a weighted average as described by the formula below (Inagaki, Kamikouchi et al. 2010):

$$PC = [(\#F_6 \times 5)+(\#F_5 \times 4)+(\#F_4 \times 3)+(\#F_3 \times 2)+(\#F_2 \times 1)]/[\#F_T]$$

where $\#F_n$ is the number of flies in tube 'n,' and $\#F_T$ is the total number of flies. Percent change was calculated relative to the Day 3 control ($100-100*(PC_{Sample}/PC_{D3ctrl})$). Percent rescue was calculated as "$100*(PC_{Rescue} - PC_{p35-null})/(PC_{Control} - PC_{p35-null})$" at each time point.

Western Analysis

Twenty male flies of each genotype were collected at the defined age (3, 10, 30 and 45 days), then flash frozen with liquid nitrogen and stored at $-80°C$. Six independent biological samples were collected to analyze Atg8-II levels; for Ref(2)P, three independent biological

samples were collected. Heads were separated from the rest of the body and homogenized in

lysis buffer (2% SDS, 150 mM NaCl, 50 mM Tris, pH 7.5) containing protease inhibitors

(Thermo Scientific, Pierce, Rockford, IL, USA). Supernatant protein concentrations were

determined using the Coomassie Protein assay reagent (Thermo Scientific). Protein samples

(25μg) were resolved on a 4-12% Bis-Tris plus gel (Invitrogen/Thermo Fisher Scientific,

Carlsbad, CA, USA) and transferred onto iBlot2 NC membranes using the iBlot 2 system

(Invitrogen/Thermo Fisher Scientific). Membranes were cut to separate bands based on

molecular weight, and then probed with primary antibodies overnight at 4°C. Primary antibodies

used included anti-Ref(2)P (1:1000; gift from Sheng Zhang, University of Texas, TX, USA)

(Rui, Xu et al. 2015), anti-dATG8 (1:500; gift from Sara Cherry, University of Pennsylvania,

PA, USA; (Shelly, Lukinova et al. 2009)) and anti-β-Tubulin (Catalog #E7,1:500,

Developmental Studies Hybridoma Bank (E7 was deposited to the DSHB by Klymkowsky,

Michael)). Infrared fluorescence IRDye secondary antibodies, including goat anti-rabbit IgG

(H+L) 800 CW, goat anti-rabbit (680 RD) and/or goat anti-mouse (H+L), were applied for 20

minutes at room temperature (1∶5000, LI-COR Biosciences, USA) followed by washing with

PBS. Visualization and quantification was carried out with the LI-COR Odyssey scanner and

software (LI-COR), with tubulin serving as a loading control.

Microarray and mRNA expression analysis

For microarray analysis, five biological replicates for each genotype and time point were

collected. Each replicate consisted of 140 male flies, aged as described for the lifespan assay;

following aging, collected totals ranged from 90-140 flies. We did not use any formal *a priori*

statistical methods to predetermine sample sizes; rather, sample sizes were selected based on

recommendations from the microarray literature to account for variability. Replicates consisted

of pooled tissue samples to provide sufficient material for microarray and qPCR analysis. Upon

collection, flies were transferred to a 1.5ml Eppendorf tube and flash frozen in liquid nitrogen,

then stored at -80°C. All time points were collected and stored prior to processing. Eppendorf

tubes containing frozen flies were transferred into liquid nitrogen to further chill them, then

vortexed to separate the heads, wings, and legs from the rest of the bodies. Keeping the samples

cold on dry ice, the heads were manually transferred to a fresh 1.5ml Eppendorf tube. Thoraces

were separated from the abdomen using a surgical blade, and then transferred to their own tube.

Total RNA was extracted for both head and thorax samples using TRIzol (Invitrogen), then

processed and labeled according to the manufacturer's guidelines for use with the DroGene 1.0

ST GeneChip (Affymetrix, GeneChip Whole Transcript Sense Target Labeling). The Scanner

3000 (Affymetrix) was used in conjunction with GeneChip Operation Software (Affymetrix) to

generate one .CEL file per hybridized cRNA. Two separate batch runs were required due to

logistical reasons, with a common technical replicate sample included in both batches. The first

batch run included control samples from four time points (Day 3, Day 10, Day 30, and Day 45)

plus 10-day-old p35-null and p35-OE samples; the second batch run included Day 10 control and

Day 10 rescue samples. The Expression Console (Affymetrix) was used to summarize the data

contained across all .CEL files and generate 16,322 RMA normalized gene probe expression

values. Subsequent analysis of these values was then performed for head and separately for

thorax. Specifically, quality of expression was challenged and assured via Tukey box plot,

covariance-based PCA scatter plot, and correlation-based heat map using functions supported in

"R" (www.cran.r-project.org, data not shown). Following this initial inspection, a single Day 3

control head sample present itself as a cohort-level outlier; this sample was removed and not

included in any downstream analysis. To remove batch effects between the two runs, baseline subtraction was performed using expression for a common technical replicate present across batches followed by use of quantile normalization to correct for differences in spread. To remove noise-biased expression values, we used lowess modeling to look for a relationship between mean gene expression and the corresponding coefficient of variation (CV). Lowess fits were then over-plotted to identify the common low-end expression value where the relationship between mean expression (signal) and CV (noise) deviated from linearity (mean expression value = 7.5). Expression values less than this value were set to equal 7.5, while gene probes not having at least one sample greater than 7.5 were discarded as non-informative. Annotations for genes observed to have differential expression and/or modeled were obtained from NetAffx (Affymetrix) and FlyBase (www.flybase.org). Full probe lists are available in Supplemental Tables ST4.3.1-ST4.3.4.

Polyserial correlation (library = polycor) was used to generate estimates of how expression observed per gene linearly relates to age in control samples. These estimates were in turn compared to those obtained when true age is randomized, with estimates greater than or less than two standard deviations of the mean of random generated estimates considered as significant ($p<0.05$); genes passing these conditions were deemed aging-related. To identify p35-related genes, ANOVA testing was applied using sample class as the factor under Benjamini-Hochberg false discovery rate multiple comparison condition. Gene probes observed to have a corrected p-value < 0.05 by this test were further post hoc challenged via TukeyHSD test. Gene probes observed to have a post hoc p-value < 0.05 and an absolute difference of means >1.5X for a class comparison were considered to have differential expression between the two classes. Chi-square with Yates' continuity correction was used to determine the significance

of the overlap between gene lists. The linear relationship between overlapping probes was tested with Pearson's correlation analysis.

To test similarities in the expression profiles, the mean expression value of the set of genes affected by both aging and altered p35 was calculated. Each individual Day 10 p35-null or p35-OE sample was compared to each Day 3-, Day 10-, Day 30-, and Day 45-control sample, generating a set of Pearson correlation coefficients. Comparing each of five p35-null replicates to four Day 3 control head and five of every other control sample yielded 95 total comparisons for head tissue, and 100 comparisons for thorax tissue. The same number of comparisons was used for p35-OE. Significance was determined using one-way ANOVA with Tukey's MTC.

To identify aging classifiers, leave-one-out (LOO) testing was employed using the same methods described, but on gene expression not discarded for Day 3-, Day 10-, Day 30-, and Day 45-control samples only. For each LOO round, gene probes deemed to have differential expression for at least one class comparison were used to construct a k-Nearest Neighbor (k-NN) model and predict the class of the left out sample (Dudoit, Fridlyand et al. 2002). Gene probes selected 100% of the time over all LOO rounds were deemed control aging classifiers. These genes were then used to construct a principal component seeded AIC-optimized linear model using expression for Day 3-, Day 10-, Day 30-, and Day 45-control samples only. This model was used to predict the physiological age of each biological replicate (four Day 3 control head samples, and five of every other sample and time point). Statistical differences in the predictions produced by the linear model were determined by performing one-way ANOVA with Tukey's MTC on the predictions themselves.

To test whether expression changes observed in the p35-null samples were specific to p35, a transgene carrying the p35 genomic locus was added to the p35-null background. Genes

77

were considered fully rescued if they showed $\geq$1.5-fold change (based on microarray data) relative to D10 controls in the p35-null samples, but not the rescue samples. Partially rescued genes were those with expression values that trended towards the control values but still exhibited $\geq$1.5-fold change relative to D10 controls.

Gene Ontology Analysis

Gene ontology analysis was performed using annotated probes identified as aging-related or p35-related (see Statistical Analysis section below), using version 6.7 of Database for Annotation, Visualization, and Integrated Discovery (DAVID; http://david.abcc.ncifcrf.gov; Huang, Sherman et al. 2009a, Huang, Sherman et al. 2009b). The background was set to "Drosophila_2 Array," and then "Functional Annotation Clustering" with medium classification stringency was used to identify groups that were significantly enriched. An Enrichment Score greater than 1.3, correlating to a non-log scale p-value less than 0.05, was considered statistically significant. The resulting annotated clusters were grouped together based on similarity of biological modules; only the highest enrichment score for each ontology group is presented here. Full DAVID results are available in Supplemental Tables 4.3.5-4.3.6 and 4.3.9-4.3.12.

qPCR validation

Excess RNA from the microarray samples was converted into cDNA using the Applied Biosystems High Capacity cDNA Reverse Transcription kit; three biological replicates were run in triplicate for every gene probe. qPCR reactions were prepared using the Affymetrix VeriQuest Probe qPCR Master Mix with specific TaqMan gene primers (Supplemental Table

4.3.7); reactions were carried out on the BioRad iQ5 Multicolor Real-time PCR Detection System. Threshold cycle numbers were determined automatically by the BioRad software.

The set of probes included four reference genes (eIF-1a, Rap2L, Rpl32, and Sdha), which were used to compute a geometric mean for normalization. Fold changes were determined using $\Delta\Delta Ct$ (Livak and Schmittgen 2001), relative to Day 3 controls (for aging-specific changes) or Day 10 controls (for mutant-specific changes). qPCR probe information is provided in Supplemental Table 4.3.7.

Oxidative stress sensitivity assay

Sensitivity to oxidative stress was assayed by survival following challenge with paraquat (PQ; 15mM), which catalyzes the production of superoxide and induces oxidative stress (Farrington, Ebert et al. 1973), or hydrogen peroxide (H_2O_2; 5%), which induces oxidative stress through the generation of reactive hydroxyl radicals (Halliwell and Gutteridge 1984). Male flies were mated for three days, and then females were removed. Males were then aged to 3-, 10-, 30-, or 45-days old, starved for four hours on filter paper damp with water, and then transferred to vials containing filter paper moistened with 5% sucrose solution and PQ or H_2O_2. A separate set of flies received only 5% sucrose as control (data not shown). Survival was scored every 12 hours, and median survival time calculated. Three biological replicates were analyzed for each genotype and time point. Each replicate consisted of 2-5 vials of 7-20 males each (Day 3 control = 189, Day 10 control = 175, Day 30 control = 196, Day 45 control = 256, Day 3 p35-null = 190, Day 10 p35-null = 150, Day 30 p35-null = 199, Day 45 p35-null = 259, Day 3 rescue = 199, Day 10 rescue = 147, Day 30 rescue = 209, Day 45 rescue = 240, Day 3 p35-OE = 200, Day 10 p35-

OE = 179, Day 30 p35-OE = 223, Day 45 p35-OE = 239 total flies); individual replicate sizes are presented in Supplemental Table 4.3.14.

Statistical Analysis

All data were analyzed with GraphPad Prism 7.0b and R. Differences between groups were assessed by either one-way or two-way ANOVA with post-hoc Tukey multiple comparison testing, as described. Statistical differences in survival curves (lifespan and oxidative stress response) were measured by log rank (Mantel-Cox). All statistical tests were two-tailed, and statistical significance was considered at $p < 0.05$. Experimental groups were determined based on genotype, so no randomization was used; data collect and analysis was not performed blind to the conditions of the experiments. Sample sizes were not predetermined using statistical methods. Data distribution was assumed to be normal with equal variance, although this was not formally tested.

Data Availability

Microarray data are available from NCBI GEO under accession number GSE7483.

Code Availability

R sessions, R code, and R input files used in the analysis of the microarray data will be available through https://data.ninds.nih.gov/ upon manuscript publication.

3.3 Results

Loss or gain of p35 causes accelerated neuron loss with age

Histology of p35-null flies has previously demonstrated age-dependent formation of 'vacuoles' in the brain, particularly in the mushroom bodies (MB) (Trunova and Giniger 2012). While these vacuoles are suggestive of neurodegeneration, this assay was not definitive as it did not directly demonstrate neuron loss, as opposed to alternative explanations, such as expansion of inter-neuronal spaces or reduced dendritic arborization. We therefore counted a specific class of MB neurons directly. Flies expressing a nuclear-localized GFP (UAS-nls-GFP) under the control of a MB-specific Gal4 driver (201Y-Gal4, which labels gamma neurons and a small subset of alpha and beta neurons (Aso, Grübel et al. 2009)) were grown to various ages and then dissected. Control flies showed steady numbers of 201Y-positive neurons through early and middle age, before showing a decline at Day 45 (mean±SEM: D3 control = 763.2±50.3, D30 control = 731.3±37.0, D45 control = 532.4±72.3 neurons/MB; Figure 3.3.1B). At Day 3 and Day 10, p35-null flies exhibited a similar number of MB neurons as controls. At Day 30, however, p35-null flies showed a sharp decline in neuron number (D30 p35-null 515.0±35.2 neurons/MB, p=0.0012 (two-way ANOVA with Tukey's multiple comparison test (MTC)); Figure 3.3.1B).
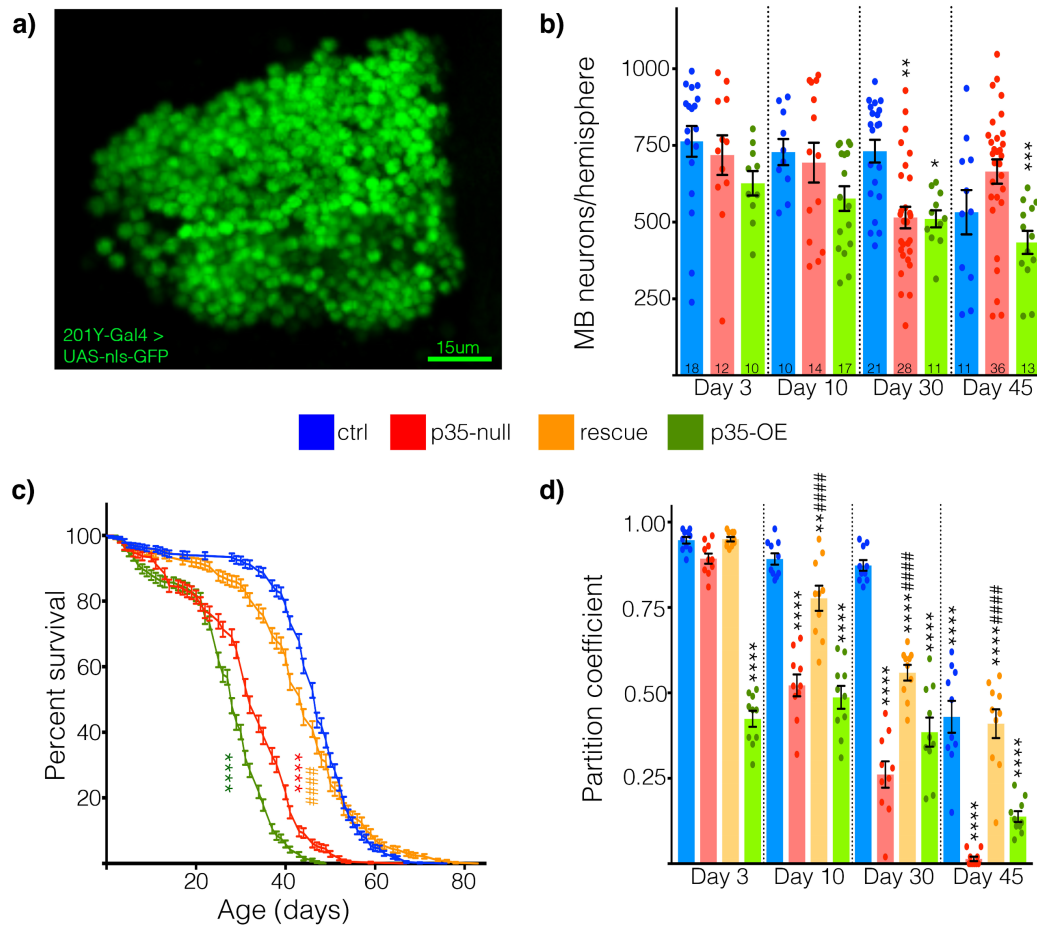
Figure 3.3.1. Gain and loss of p35 induces overt neurodegeneration and degenerative phenotypes.
(A) Projected confocal image of MB neuron nuclei labeled with nls-GFP. **(B)** Altered p35 levels lead to progressive loss of MB neurons. The number of 201Y>nls-GFP positive MB neurons per hemisphere is presented as mean±SEM, along with individual counts. For each genotype and time point, the number of hemispheres analyzed is presented at the bottom of the bar. Significant differences are determined using two-way ANOVA with Tukey's MTC; presented p-values are from MTC, and are relative to the Day 3 control. **(C)** Altered p35 leads to a shortened lifespan. Sample size for control, p35-null, p35-OE, and rescue samples were as follows: 485 male flies, 518, 472, and 410, respectively. Significant differences in lifespan were determined using the Mantel-Cox log-rank test. **(D)** Loss or overexpression of p35 leads to progressive loss of motor function. A partition coefficient (PC) was calculated from the flies' ability to complete a series of negative geotactic tasks (see Materials and methods). PC is presented as mean±SEM; individual replicate PCs are also shown. Five replicates of 20 flies were analyzed twice for each genotype and time point. Significant differences are determined using two-way ANOVA with Tukey's MTC; presented p-values are from MTC, and are relative to the Day 3 control. In all panels, *p<0.05; **p<0.01; ***p<0.001; ****p<0.0001. For the rescue samples, significant differences between rescue and age-matched p35-null samples are indicated as follows: ####p<0.0001.

82

We noted that the average number of MB neurons at Day 45 was actually higher in p35-null flies than at Day 30 (D45 p35-null = 668.3±33.9 neurons/MB), though still less than the number measured at Day 3. Based on staining for phosphorylated histone H3, which stains mitotic cells, and EdU, which labels newly synthesized DNA, we found no evidence of neurogenesis (data not shown). Since no new neurons are being born, the simplest hypothesis is that the small fraction of p35-null flies still surviving at Day 45 (8.3%) are those that had sustained the least amount of neuron loss with age. Consistent with this, MB neuron number in individual brain hemispheres of the mutant shows large variance at middle age, including a population with relatively little cell loss, and experiments suggest that the flies retaining the most motor function at middle age (15 days), as assayed by counter-current, tend to have more remaining MB neurons than the feeblest flies (data not shown).

In mammals, increased activity of Cdk5 causes neuronal death, as does the loss of function (Patrick, Zukerberg et al. 1999). We therefore modestly overexpressed p35 and assayed MB neuron survival. We introduced four copies of a transgene bearing the p35 genomic locus (Connell-Crowley, Le Gall et al. 2000), which results in an increase of p35 levels by 3.5-fold in head tissue, and 2.2-fold in thorax tissue, as measured by qPCR (Supplemental Table 4.3.8C). Overexpression of p35 is sufficient to increase Cdk5 activity (Connell-Crowley et al, 2000). At three- and 10-days-old, the number of 201Y-positive MB neurons in flies overexpressing p35 was lower than controls, albeit not significantly so (D3 p35-OE = 626.8±39.8, D10 p35-OE = 576.9±40.2 neurons/MB). By Day 30, however, p35-OE flies exhibited a significant decrease in MB neuron number, with a further reduction by Day 45 (D30 p35-OE = 510.8±27.7, p=0.0271; D45 p35-OE = 433.9±37.6 neurons/MB, p=0.0002). Thus, in the fly, as in mammals, both p35

deletion and overexpression lead to progressive age-dependent neurodegeneration, demonstrated by loss of MB neurons.

Altered p35 expression induces degeneration-associated phenotypes

We have shown previously that a p35 mutation causes a variety of degeneration-associated phenotypes, consistent with the cell loss we observed here in the brain (Connell-Crowley, Vo et al. 2007, Trunova and Giniger 2012). We now show organismal- and cellular-level degenerative phenotypes in animals with increased p35 similar to what was observed in flies lacking p35. In a wild-type (w+) genetic background, deletion of p35 results in a 31.9% reduction in lifespan relative to control flies (control median survival = 47 days; p35-null = 32 days, $p<1.0E-15$ (Mantel-Cox log rank test); Figure 3.3.1C). To confirm that the shortened lifespan was a result of p35 levels, we expressed a single copy of the p35 genomic transgene in the p35-null flies, and found that one copy of the transgene substantially rescues lifespan, resulting in a median survival nearly equivalent to the control (rescue median survival = -6.4% change relative to control, p=0.19; rescue vs. null: $p<1.0E-15$ (Mantel-Cox log rank test)). Therefore, the observed decrease in lifespan is caused by a reduction of p35 and thus Cdk5 activity. Overexpression of p35 had a more severe effect on lifespan than loss of function, as p35-OE flies had a median survival of only 28 days (-40.4% change relative to control, $p<1.0E-15$). Thus, altered Cdk5/p35 activity in either direction drastically shortens lifespan.

Overexpression of p35 also caused strong, age-dependent, progressive loss of motor function, as previously reported for p35 loss of function (Connell-Crowley, Vo et al. 2007). Here, motor function was assayed using an apparatus that gives each fly five sequential opportunities to perform a negative geotaxis task, and reports performance as a partition

coefficient (see Methods; (Benzer 1967, Inagaki, Kamikouchi et al. 2010)). In both gain and loss

of p35, and in controls, flies showed progressive worsening of motor function with age;

however, flies lacking or overexpressing p35 exhibited behavioral decline with a substantially

accelerated time course. Control flies showed slight, insignificant decreases in calculated

partition coefficient from Day 3 through Day 30, and then showed a significant decrease at Day

45 (D10 control = -5.8% change in mean relative to D3 control, D30 control = -7.8%, p=0.83;

D45 control = -54.6%, p<1.0E-15 (two-way ANOVA with Tukey's MTC); Figure 3.3.1D). p35-

null flies were nearly identical to controls at Day 3, but showed significant decreases at each

subsequent timepoint (D3 p35-null = -5.7% change in mean relative to D3 control, p=0.98; D10

p35-null = -44.9%, p=6.9E-14; D30 p35-null = -72.4%, p<1.0E-15; D45 p35-null = -98.5%,

p<1.0E-15). The presence of the p35 genomic transgene in the null background rescued

locomotive ability at each timepoint (D10 = 68.9% rescue, p=6.9E-14; D30 = 48.7% rescue,

p=1.0E-9; D45 rescue = 95.2% rescue, p=1.0E-13). Flies overexpressing p35 actually started out

with severely impaired ability, as their partition coefficient was already significantly lower at

Day 3 (D3 p35-OE = -55.2% change in mean relative to D3 control, p<1.0E-15); their motor

function remained well below that of controls at all time points, further worsening significantly

at Day 45 (D45 p35-OE = -67.9% change in mean relative to D45 control, p=3.9E-9). As such,

both gain and loss of p35 result in accelerated loss of motor function relative to controls.

Disrupted autophagy is strongly associated with many forms of degeneration (Hara,

Nakamura et al. 2006, Komatsu, Waguri et al. 2006, Li, Zhang et al. 2008, Spencer, Potkar et al.

2009, Winslow, Chen et al. 2010). Consistent with this, Cdk5 loss of function was previously

found to result in an increase of autophagic organelles, as well as an increased sensitivity to

starvation, consistent with impaired autophagy (Trunova and Giniger 2012). As more direct

measures, here we assayed Atg8 cleavage and Ref(2)P levels as markers for disrupted

autophagy. Atg8 (LC3 homolog) is cleaved and lipidated before it binds to autophagosomes and

gets degraded (Ichimura, Kirisako et al. 2000); impaired autophagy results in an accumulation of

the cleaved form, assayed as an increase of Atg8-II levels. Both loss and overexpression of p35

resulted in enhanced accumulation of Atg8-II, relative to control samples. Brain homogenate

from control flies revealed a gradual, modest increase in Atg8-II from Day 3 through Day 45,

reaching a maximum 2.5-fold increase at the latest time point (Figure 3.3.2A). p35-null samples

showed a 4.9-fold increase in Atg8-II by Day 45; the increased Atg8-II levels were partially

blocked by the presence of the p35 transgene, as the rescue samples only exhibited a 3.5-fold

increase at Day 45. Samples overexpressing p35 showed further exacerbation, as they surpassed

the maximum levels observed in controls by Day 10, and ultimately reached an 11.1-fold

increase in Atg8-II by the last time point (p=2.7E-5 relative to Day 3 control (two-way ANOVA

with Tukey's MTC)). Both p35-null and p35-OE samples showed trends towards Atg8-II

accumulation, which, while not significant at all time points, is consistent with impaired
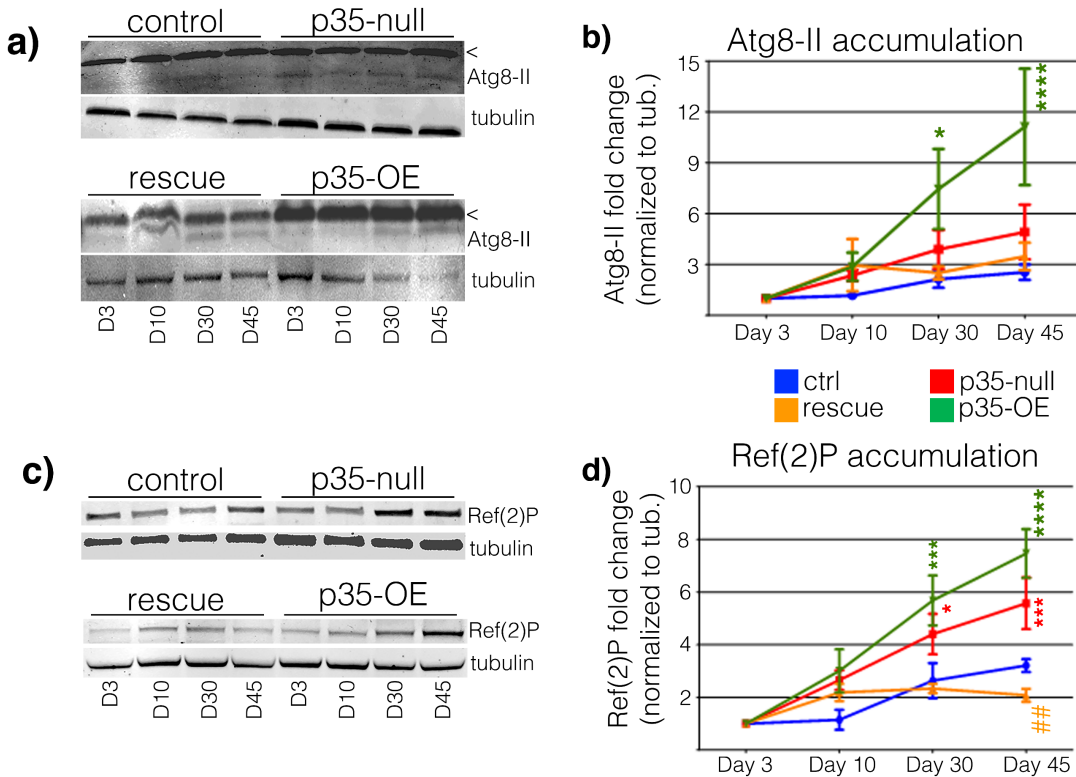
autophagy.

Figure 3.3.2. **Accumulation of autophagic markers indicates inhibition of autophagic flux.**
Representative western blot of **(A)** Atg8-II and **(C)** Ref(2)P levels in brain homogenate of
control, p35-null, p35-OE, and rescue flies; tubulin was used as a loading control. In all cases,
the loading control was probed from the same membrane as the target protein. In **(A)**, bands
marked with '**<**' refer to the uncleaved Atg8-I. Quantification of **(B)** Atg8-II and **(D)** Ref(2)P
accumulation based on WB levels as seen in A and C, respectively; at least three replicate
experiments were analyzed for both. Values presented are mean$\pm$SEM. In **(B)** and **(D)**,
significance relative to the Day 3 control was determined using two-way ANOVA with Tukey's
MTC; *=$p<0.05$; ***=$p<0.001$; ****$p<0.0001$. For the rescue samples, significant differences
between rescue and age-matched p35-null samples are indicated as follows: ##$p<0.008$.

p35-null and p35-OE flies also exhibited elevated Ref(2)P levels. Ref(2)P, a p62

homolog, accumulates on autophagosomes and then gets degraded upon fusion of the

autophagosome with a lysosome. However, if autophagy is impaired, an increase in Ref(2)P

levels is observed (Nezis, Simonsen et al. 2008). While control samples showed age-dependent

increases in levels of Ref(2)P in brain homogenate, both p35-null and p35-OE brains showed

enhanced accumulation at each of the later time points (Figure 3.3.2B). At Day 45, the control

samples showed a 3.2-fold increase in Ref(2)P. In contrast, p35-null samples showed a 5.6-fold increase at Day 45 (p=1.8E-4 relative to Day 3 control (two-way ANOVA with Tukey's MTC)), whereas p35-OE exhibited a 7.5-fold increase in Ref(2)P levels (p=2.4E-7). The p35 genomic transgene blocked the accumulation of Ref(2)P in the p35-null background, as the rescued samples had only a 2.1-fold increase by Day 45, which is comparable to the age-matched control, and significantly different from the age-matched p35-null sample (p=0.008). Deletion and overexpression of p35 both result in significantly elevated levels of Ref(2)P at Day 45; this is consistent with the Atg8-II accumulation, and supports that autophagy is impaired.

Collectively, these data demonstrate that, as in mammals, either increase or decrease of Cdk5 activity results in degeneration of susceptible neurons, and induces a variety of characteristic degeneration-associated phenotypes. Further, many of these phenotypes occur chronologically earlier in the mutant and p35-OE flies than in control flies.

Identification of genes whose expression is altered by p35 levels and aging

The phenotypes we observed from altered p35 levels resembled effects that are also seen in natural aging, but only at advanced ages. This led us to wonder whether altered p35 might be accelerating the absolute rate of aging. To test this hypothesis, we used genome-wide expression profiling to develop a comprehensive, quantitative and unbiased metric for physiological age. In many systems, it has been found that expression levels of ~2-30% of genes change in reproducible ways with age (Pletcher, Macdonald et al. 2002, Girardot, Lasbleiz et al. 2006, de Magalhaes, Curado et al. 2009). We hypothesized that we could characterize the evolution of the gene expression profile with aging in control flies, genome-wide, and use it as a 'standard curve,' comparing the profile of a mutant to that of the reference set to infer physiological age (Figure

3.3.3A). We separately isolated RNA from head and thorax of control flies grown to various

ages and measured the RNA expression profile using microarrays, with the primarily neural

tissue of the head serving as an indicator of neuron-specific changes, and the thorax, which is

dominated by non-neural tissue such as muscle, serving as a proxy for systemic changes. We

then selected aging-related genes by using polyserial correlation to calculate the association of

each gene with aging. Random permutation of expression values with each age class was used to

establish significance cutoffs, ultimately identifying 3,235 and 3,809 probes from control head

and thorax tissue, respectively, that show consistent directional changes in expression with age

(see Methods; Figure 3.3.3B-C). These probes correspond to 2,789 unique genes in the head,

and 3,245 unique genes in the thorax (Supplemental Table 4.3.1).
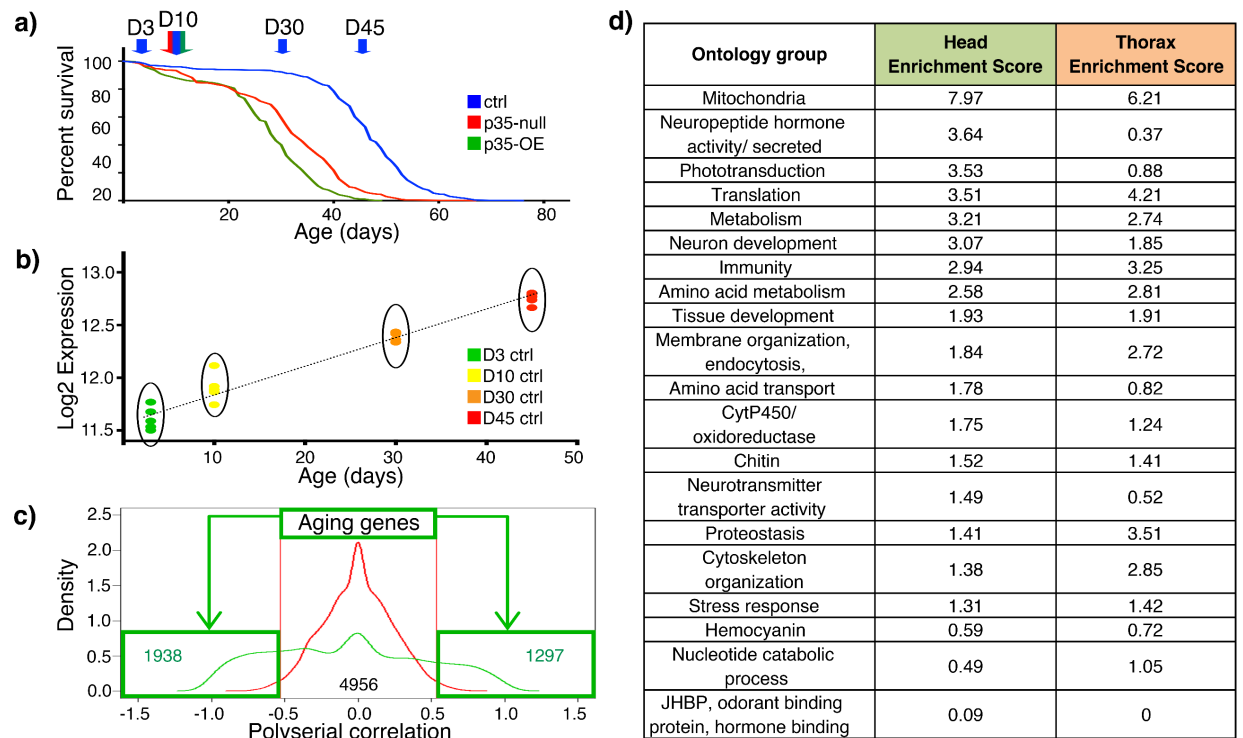
Figure 3.3.3. Identification of aging-related genes and affected biological processes.
(**A**) Experimental outline schematic. RNA samples were extracted from heads and thoraces of 3-, 10-, 30-, and 45-day-old control samples, and from 10-day-old p35-null and p35-OE samples. Five replicates of each sample were collected for microarray analysis. (**B**) An example of a gene (Arc1) showing increased expression with age. Our analysis identified genes with this pattern, or the reverse pattern, as aging-related. (**C**) Identification of genes positively- or negatively-correlated with age in head tissue. The green line represents the observed correlation values; the red line represents the correlation estimates when true age is randomized. The randomized set was used to establish significance cutoffs. The vertical red lines indicate correlation values with a corrected p-value <0.05 (see Materials and methods). The same procedure was used to define aging-related genes in the thorax (not shown). The full list of aging-related probes is available in Supplemental Table 4.3.1. (**D**) Gene ontology (GO) analysis of aging-related genes from head and thorax tissue. GO analysis was performed on each set of affected probes using DAVID. The resulting annotated clusters were grouped together based on similarity of biological modules; only the highest enrichment score for each ontology group is presented here. Full DAVID results are available in Supplemental Tables 4.3.5-4.3.6. By DAVID's statistical analysis, an enrichment score >1.3 has a p-value <0.05.

To validate our set of identified 'aging-related' genes, we first used gene ontology

analysis (**D**atabase for **A**nnotation, **V**isualization and **I**ntegrated **D**iscovery (DAVID)) to identify

biological processes that were over-represented in the set of putative age-correlated genes

(Huang, Sherman et al. 2009a, Huang, Sherman et al. 2009b). The set of processes identified as enriched in our dataset using DAVID enrichment scores (EASE > 1.3) was largely consistent with previous analyses of aging in *Drosophila* (Zou, Meadows et al. 2000, Pletcher, Macdonald et al. 2002, Lai, Parnell et al. 2007) and in other organisms (Lee, Klopp et al. 1999, Lee, Weindruch et al. 2000, Golden and Melov 2004, de Magalhaes, Curado et al. 2009) and included mitochondrial function, immunity, proteostasis, and particular aspects of metabolism, among others (Figure 3.3.3D, Supplemental Tables 4.3.5-4.3.6). Similar results were obtained using other gene ontology databases, including Gene Ontology Consortium and Gene Set Enrichment Analysis, for this and all other gene ontology analyses presented below (data not shown).

We next profiled RNA from head and thorax of 10-day-old flies either lacking or overexpressing p35. As above, overexpression was achieved by introducing four copies of a transgene containing the wild-type p35 genomic locus, while the loss of function was the null mutant. Genes with significantly altered expression were identified by ANOVA under multiple comparison correction condition followed by Tukey-HSD post hoc testing. Significance was defined as corrected $p<0.05$ and $\geq$1.5-fold change in expression level when compared to 10-day-old controls. Loss of p35 significantly altered expression of 198 probes in the head and 193 probes in the thorax, while p35 overexpression affected 328 probes in the head and 405 probes in the thorax (Supplemental Tables 4.3.2-4.3.3).

Three lines of evidence validate the dataset and the identification of affected genes. In a supplemental microarray experiment, we profiled p35-null flies carrying a single copy of the p35 genomic transgene to test whether the transcriptomic effects observed in p35-null flies are indeed p35-specific. The presence of the rescue transgene either fully or partially rescued the expression levels of 81.9% of the p35-null affected probes in head tissue, and 74.1% of probes in

thorax (see Methods, Figure 3.3.4A, Supplemental Table 4.3.4). We used qPCR to validate a

subset of twenty genes showing age-dependent or p35-specific changes, in addition to four

reference genes, and found that nearly 70% (164/240) of conditions tested were concordant with

the array results (Supplemental Table 4.3.8). Lastly, we observed significant overlap of affected

genes between gain and loss of p35, which is consistent with the striking similarity of the

observed degeneration phenotypes. Not only was the size of the intersecting set of probes

significant (80 probes in head, p<2.2E-16; 76 probes in thorax, p<2.2E-16 (Chi-square with

Yates' continuity correction)), but the probes affected in both p35-null and p35-OE flies were

highly concordant (head: R^2=0.60, p<2.2E-16; thorax: R^2=0.56, p=6.7E-15 (Pearson's product-

moment correlation); Figure 3.3.4B). Within these overlapping probes, the magnitude of

expression changes was generally larger in the p35-OE flies, relative to the p35-null samples.

This is also consistent with the physiological assays, where overexpression of p35 typically had

more severe phenotypes than did the mutant.

Altering p35 levels mimics aging: 1. Gene ontology analysis of p35-affected genes strongly

overlaps that of aging-related genes

As a first test of the relationship between the effects of p35 and aging, we examined

biological processes identified by gene ontology and found a strong overlap between categories

enriched by aging or by altered p35. We first compared the list of p35-affected genes and

noticed a strong overlap with the aging-related genes (Figure 3.3.4C). In the p35-OE samples,

153 probes in head and 221 in thorax intersected with the aging set (head: p=0.01, thorax:

p=0.002 (Chi-square with Yates' continuity correction)). In the mutant samples, 92 probes in

head and 112 in thorax overlapped with the aging set (head: p=0.056, thorax: p=0.002). We then

performed gene ontology analysis, which revealed that nine of the top 17 categories enriched in

aging-related genes are also among the top categories affected by altered p35, including

mitochondria, oxidoreductases, metabolism, proteostasis, and immunity (Figure 3.3.4D, 5A,

Supplemental Tables 4.3.6-4.3.9). Some categories that were significantly enriched by the set of

aging-related probes were also enriched by the set of p35-related probes, but at levels further

down the enrichment scale: examples include protein translation in the p35-OE samples, and

proteostatic processes in the p35-null samples. We also found instances of categories

significantly enriched by p35-related probes but not by aging, as well as categories that differed

between head and thorax.

a)

	Head	Thorax
p35-null affected probes	221	228
Fully rescued probes	112 (50.7%)	103 (45.2%)
Partial or fully rescued probes	181 (81.9%)	169 (74.1%)

b) Head (80 gene probes): D10 p35-OE FC vs D10 p35-null FC, $R^2 = 0.5993$, $p < 2.2E\text{-}16$. Thorax (76 gene probes): $R^2 = 0.5620$, $p = 6.7E\text{-}15$.

c) Aging/p35-null Head: 2934, 92#, 106; #p=0.056. Aging/p35-null Thorax: 3408, 112**, 81; **p=0.002. Aging/p35-OE Head: 3082, 153*, 175; *p=0.011. Aging/p35-OE Thorax: 3588, 221**, 184; **p=0.002.

d)

Ontology group	Head Enrichment Score		Thorax Enrichment Score	
	p35-OE	p35-null	p35-OE	p35-null
Immunity	5.86	2.62	4.91	2.25
Hemocyanin	3.33	2.46	2.94	4.04
CytP450/ oxidoreductase	2.78	3.3	1.05	3.41
Metabolism	2.01	---	3.56	---
Mitochondria	2.01	---	0.18	---
Neuropeptide hormone activity/secreted peptides	1.54	---	---	---
Proteostasis	1.53	0.25	0.32	0.64
Amino acid metabolism	1.47	2.93	1.34	---
JHBP, odorant binding protein, hormone binding	1.17	0.16	3.43	---
Stress response	0.41	1.71	0.92	0.72
Chitin	---	0.7	3.56	0.41
Nucleotide catabolic process	---	---	1.68	---

Figure 3.3.4. Identification of genes impacted by altered p35 and affected biological processes.
p35-null, p35-OE, and rescue samples were analyzed for genes with altered expression relative to age-matched controls. The full list of probes with altered expression is available in Supplemental Tables 2-4. **(A)** The presence of the p35 transgene rescues expression changes resulting from loss of p35. Fully-rescued probes are those that are significantly altered in the p35-null samples, but are not altered in the rescue samples. Partially-rescued probes had their expression levels shifted towards control expression values, but still exhibited >1.5 fold change relative to controls. **(B)** Concordance of p35-null and p35-OE intersecting genes in head or thorax tissue. For probes affected by both gain and loss of p35, 91.3% are concordant in head samples, and 96.1% are concordant in thorax samples. Significance of the linear relationship between expression fold change in p35-null versus p35-OE samples was assessed by Pearson's product moment correlation. **(C)** Overlap of aging-related probes and probes affected by either loss (upper row) or overexpression (lower row) of p35 in head (left column) and thorax (right column) samples. The significance of the size of the overlap between sets was determined using a chi-square test with Yates' continuity correction. **(D)** GO analysis of genes affected by gain or loss of p35 in head and thorax tissue samples. Enrichment scores are presented as described in Figure 3.3.3; full DAVID results are available in Supplemental Tables 4.3.9-4.3.12.

Altering p35 levels mimics aging: 2. Expression profile of affected genes in young mutant and

p35-OE flies resembles the profile in the oldest controls

Comparing the mean expression values of genes affected by both aging and by p35 revealed that young flies with altered p35 had expression profiles that correlated better with the oldest control profiles than with age-matched profiles. We compared the Day 10 mutant or p35-OE profiles of intersected probes to the control profile at each of the four time points. In the case of p35 overexpression, comparing the head profiles from Day 10 p35-OE flies with each of the controls yielded average Pearson correlation coefficients of: D3 = 0.34±0.02, D10 = 0.38±0.02, D30 = 0.51±0.02, D45 = 0.63±0.01 (mean±SEM; Figure 3.3.5B). Similar trends were observed in the thorax, and in both the head and thorax of p35-null mutants (Figure 3.3.5B-C): in each case, the correlation value of 'D10 mutant vs. D45 control' was significantly greater than that of 'D10 mutant vs. D3 control' (p35-OE_Head: p=4.6E-10; p35-OE_Thorax: p=4.3E-10; p35-null_Head: p=4.7E-10; p35-null_Thorax: p=0.008 (one-way ANOVA with Tukey's MTC)). These correlations support the hypothesis that young flies with altered p35 have expression profiles more similar to those of older flies, and suggest that aberrant Cdk5/p35 activity does indeed result in an acceleration of at least a portion of aging processes. Given the neuronal specificity of Cdk5/p35 activity, it was unexpected to see such strong effects in thorax tissue: while the thorax includes the thoracic and abdominal ganglia, its cell mass is dominated by muscle, where p35 is not expressed. We note, however, that there is precedent for neuron-specific alterations driving systemic changes, and even shifting lifespan of the entire organism (Bahadorani, Cho et al. 2010, Kumimoto, Fore et al. 2013).
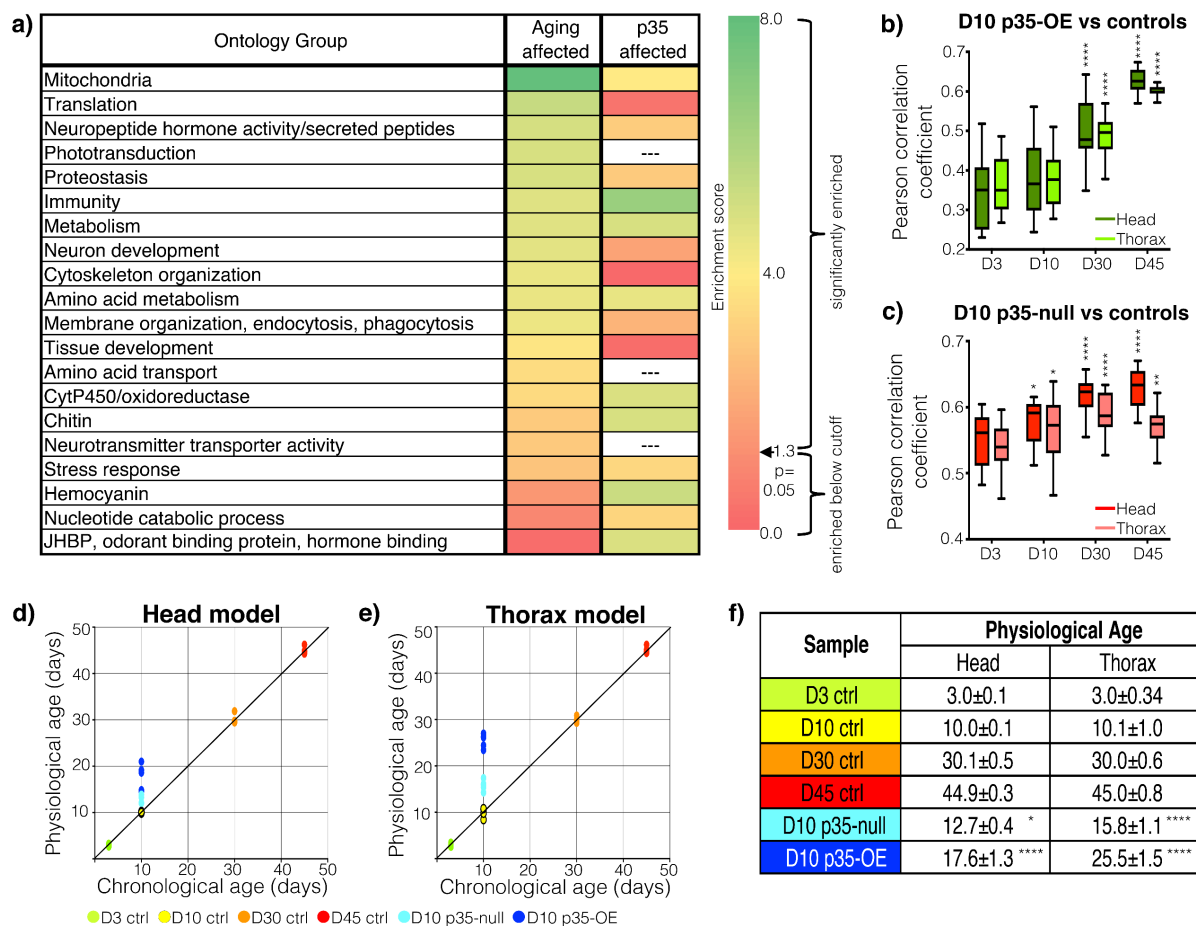
Figure 3.3.5. p35 mutant and p35-OE expression profiles are most similar to older control profiles.
(A) Comparison of significantly enriched GO groups for aging-affected and p35-affected genes. Heatmap is based on DAVID Enrichment scores; cells marked with "---" were not enriched. Annotation clusters with an Enrichment Score >1.3 were significantly enriched; those ≤1.3 were enriched, but not significantly so. For **(B)** p35-OE and **(C)** p35-null samples, the mean expression value of Day 10 p35-modified samples was compared to the mean expression value for each of the four control samples, using the intersecting set of p35-affected and aging-affected probes. Box and whisker plots show minimum and maximum values. Significant differences between samples were determined by one-way ANOVA with Tukey's MTC; presented p-values are from MTC, and are relative to the Day 3 correlation values (*p<0.05, **p<0.01, ****p<0.0001). **(D-F)** Tissue-specific linear models were developed to measure the physiological age of each sample. In **(D)** and **(E)**, the physiological age is graphed against the chronological age for **(D)** head and **(E)** thorax tissue of each sample. The mean physiological age is presented in **(F)** as mean±SEM. Significant differences between samples were determined by one-way ANOVA with Tukey's MTC; presented p-values are from MTC, and are relative to the Day 10 control samples (*p<0.05; ****p<0.0001).

Altering p35 levels mimics aging: 3. p35 mutant and p35-OE flies are physiologically older than age-matched controls

Experiments above show a strong correlation between the gene expression effects of altering p35 and increasing age for a subset of genes; however, it remained unclear whether altered Cdk5/p35 activity mimics specific components of aging, or accelerates aging more globally. To develop a true gene expression metric for aging, we used machine learning to ascertain 'aging classifiers.' Using k-nearest-neighbor (kNN) modeling with leave-one-out (LOO) cross validation, we identified individual probes from the control profiles that can be used to estimate the age of an unknown sample based on gene expression levels (see Methods). We then identified the most robust classifiers that were present in every iteration of the kNN modeling (381 and 882 classifiers in the head and thorax, respectively, Supplemental Table 4.3.13), and used them to derive tissue-specific linear models for physiological age based on principle component analysis of the expression data (Figure 3.3.5D-E). In the head samples, the linear model measured the physiological age of the 10-day-old p35-OE samples as 17.6±1.3 days (mean±SEM; p=7.9E-8, Figure 3.3.5F (one-way ANOVA with Tukey's MTC)), nearly twice the chronological age. The p35-null head samples were measured to be 12.7±0.4 days (p=0.049), corresponding to nearly 30% acceleration of aging. Similar results were obtained for the thorax samples (D10 p35-OE: 25.5±0.7 days, p=1.8E-14; D10 p35-null: 15.8±0.5 days old, p=1.8E-8). These data demonstrate that flies overexpressing p35 exhibit a physiological age that is dramatically older than its chronological age, both in neural and non-neural tissue, while loss of p35 results in a subtler, albeit still significant, acceleration of aging.

Flies with altered p35 show defects in array-identified biological processes

Gene expression data above suggest that there is acceleration of aging with gain-and-loss-of-function of Cdk5/p35. Thus, we performed further physiological tests to challenge this interpretation, drawing on processes highlighted by the expression profiling. The gene ontology analysis revealed that genes affected both by aging and by altered p35 included a variety of oxidoreductases. We therefore assayed the abilities of flies lacking or overexpressing p35 to withstand oxidative stress. Control, p35-null, and p35-OE flies were aged to 3-, 10-, 30-, or 45-days old, and then exposed to hydrogen peroxide (H_2O_2) or paraquat (PQ). p35-null and p35-OE flies of each age show enhanced sensitivity to H_2O_2-induced oxidative stress, relative to controls. For example, 3-day-old mutant and p35-OE flies show significantly altered survival curves following exposure (p35-null: $p<1.0E-15$; p35-OE: $p=6.1E-12$ (Mantel-Cox log rank test)) and reduced median survival times (control median survival time = 100 hours, p35-null = 60 hours ($p=1.4E-5$), p35-OE = 76 hours ($p=0.023$) (two-way ANOVA)). The detrimental effect in p35-null samples was rescued by the presence of the p35 genomic transgene (rescue vs control: $p=0.39$; rescue vs p35-null: $p=<1.0E-10$ (Mantel-cox long rank test), Figure 3.3.6A; rescue median survival time = 100 hours, rescue vs control: $p>0.99$, rescue vs p35-null: $p=1.4E-5$ (two-way ANOVA), Figure 3.3.6A inset). Similar trends were observed with multiple ages, as the median survival time was always lower in p35-null and p35-OE samples than control samples (Figure 3.3.6A inset). Paraquat treatment also significantly shortened survival time of all genotypes following exposure, with the p35-null and p35-OE flies being more susceptible than controls at every time point (Figure 3.3.6B, inset). Together, these data indicate that both increase and decrease of p35 lead to increased susceptibility to various oxidative stresses.
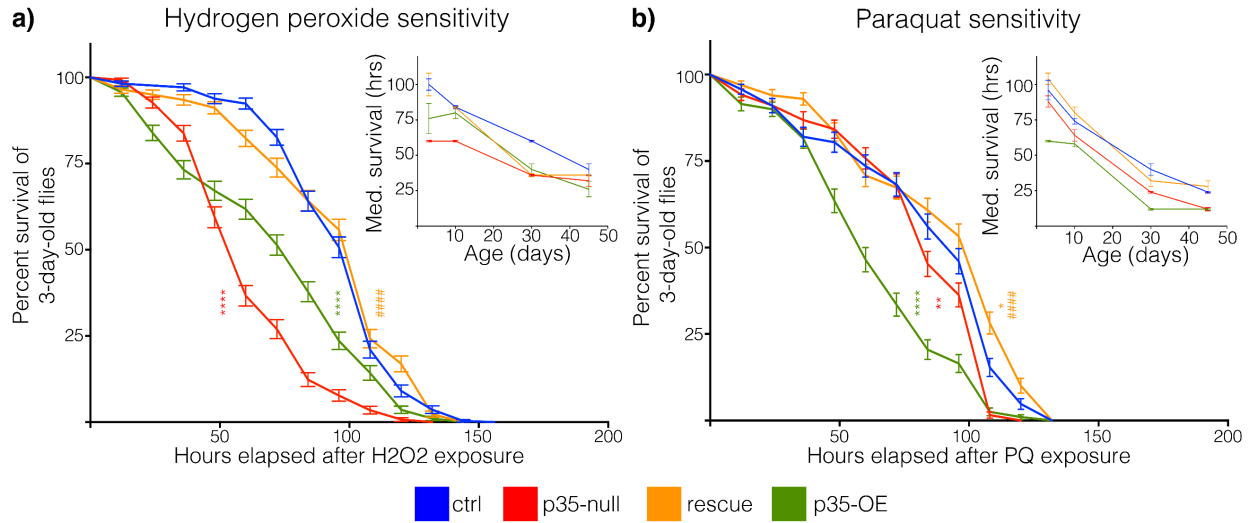
Figure 3.3.6. Altered p35 increases sensitivity to oxidative stress.
(A,B) Survival curves of 3-day-old samples exposed to **(A)** hydrogen peroxide or **(B)** paraquat; error bars represent mean$\pm$SEM. Significant differences in survival curves were determined using the Mantel-Cox log-rank test; *p<0.05, **p<0.01, ****p<0.0001. For the rescue samples, significant differences between rescue and p35-null curves are indicated as follows: ####p<0.0001. Insets demonstrate the median survival time (in hours) following exposure of 3-, 10-, 30-, and 45-day-old flies; error bars represent mean$\pm$SEM. Sample sizes are outlined in Supplemental Table 4.3.14.

3.4 Discussion

We have shown here that aberrant gain or loss of Cdk5/p35 activity accelerates the effective rate of aging in *Drosophila*, and induces multiple age-dependent neurodegenerative phenotypes. We exploit the natural modulation of gene expression across lifespan to define an unbiased, comprehensive, and quantitative metric for physiological age. Applying this metric to flies with altered levels of the Cdk5 activator p35 shows that absence of p35 increases the rate of aging by >25%, while a modest, threefold increase in p35 expression causes the aging rate to double. Change of Cdk5/p35 activity in either direction, and the attendant acceleration of aging, is associated with adult-onset neurodegeneration, marked by a variety of well-characterized degeneration-associated changes in neuronal physiology, including inhibition of autophagy and sensitivity to oxidative stress, as well as loss of neurons from the central brain, progressive decline in motor function, and early death.

It is clearly understood that aging is the greatest risk factor for neurodegeneration, but the mechanistic basis for the relationship between degeneration and aging has remained frustratingly enigmatic. One central challenge to clarifying this relationship is the absence of a metric for the physiological age of a subject. Typically, age is defined chronologically, but chronological age is an imprecise, and sometimes misleading, measurement. The rate of aging can be altered by nearly 30% through a combination of genes, environment, and happenstance in *C. elegans* (Stroustrup, Anthony et al. 2016), for example, and lifespan is equally variable in other organisms. Consequently, we sought a more robust quantification of age. Numerous studies document that the expression levels of a significant portion of genes show reproducible directional change with age. Consistent with this, we assayed multiple points throughout the life of control flies and identified aging-related genes that showed consistent changes in expression

with time. We hypothesized that by comparing a young mutant expression profile to the control profile, we could accurately infer physiological age. This comparison had three potential outcomes: Day 10 mutant profiles could have most closely resembled age-matched control profiles; been too disrupted to resemble any particular control profile; or they might have resembled older control profiles.

Our results here display the last of these options: young, essentially presymptomatic Day 10 p35 mutant and p35-OE samples have an RNA expression profile that strongly resembles that of older control samples. Three separate analyses demonstrate that altered p35 mimics aging. First, there is significant overlap in the gene ontology categories enriched by aging genes and those enriched by p35-affected genes. Second, a correlation analysis of the mean expression of the set of intersecting aging-related genes and p35-related genes revealed that the samples with altered p35 were more strongly correlated with older controls than with the age-matched control; this increased correlation was true in both the head and thorax tissue of both mutant and overexpression samples. Third, using a quantitative metric, we showed that both tissue types of the p35 mutants and p35-overexpressing flies were physiologically 'older' than their chronological age. Whether accelerated aging is a universal mechanism of neurodegeneration remains to be seen. A previous study of *Drosophila* neurodegeneration failed to detect expression changes indicative of accelerated aging; in that case, however, mortality was accelerated profoundly by the experimental manipulations, and the compressed timescale may have obscured the ability to detect any age-related effects (Favrin, Bean et al. 2013). In contrast, other *Drosophila* models of degeneration show a variety of aging phenotypes, as well as demonstrating aging-related effects on the transcriptome (Kumimoto, Fore et al. 2013). Similarly, it has been shown that post-mortem tissue from human AD patients displays a gene

expression profile comparable to the profile predicted for non-demented samples at extreme old age, though in that study it was not possible to distinguish whether this reflects an early, causal step in disease pathogenesis or a late consequence of terminal disease processes (Podtelezhnikov, Tanis et al. 2011).

Our data show that in flies, as in mice and in cultured neurons, gain and loss of Cdk5/p35 activity cause similar degenerative phenotypes and neuron loss. Consistent with this, change of p35 in either direction accelerates the rate of aging. The expression profiles revealed that a significant number of genes were affected by both loss and overexpression of p35, and these overlapping genes showed very high concordance in directionality. Evidence from mammalian systems suggests that cross-regulatory interactions among proline-directed kinases may be responsible for the similar effects of Cdk5 activation and inactivation. Cdk5 is one member of a group of interacting kinases that have related target-site specificity, including glycogen synthase kinase-3 beta (GSK3β) and mitogen activated protein kinases (MAPK) (Anderton, Betts et al. 2001, Hashiguchi, Saito et al. 2002, Liu, Iqbal et al. 2002). Consequently, certain key residues of tau, for example, have the same phosphorylation status in both gain and loss of Cdk5 activity, potentially due to deregulation of GSK3β upon modulation of Cdk5 (Hashiguchi, Saito et al. 2002, Hallows, Chen et al. 2003, Morfini, Szebenyi et al. 2004). If relevant proteins are hyperphosphorylated in similar ways in the context of both increased and decreased Cdk5 activity, it could explain how both conditions modify the same pathways to produce similar degenerative phenotypes. Alternatively, we cannot formally rule out the possibility that gain and loss of p35 lead to degeneration by parallel but distinct mechanisms, much as gain and loss of Rac activity both cause axon stalling during development, but through opposite molecular effects (Luo, Liao et al. 1994).

Although gain and loss of p35 both give rise to similar phenotypes, hyperactivation consistently produces stronger effects than loss of function, and modulates more gene expression categories in a statistically significant way. It may be that compensation by related kinases is less effective at buffering the effects of kinase hyperactivation than kinase insufficiency. It is also worth noting that we focused our analysis on young, essentially pre-symptomatic flies that had yet to show neurodegeneration, and presumably had yet to exhibit the full effects of altered p35 on their transcriptome. Moreover, we set relatively restrictive criteria for significance when identifying p35-affected probes, so the set of genes that are affected by altered p35 is likely to be rather larger than what we identify. Indeed, when we focus on the 17 gene ontology groups that were significantly enriched for our aging probes, all but three (neurotransmitter transporter activity, amino acid transport, and phototransduction) show some level of enrichment among the set of probes altered by aberrant p35 levels. These findings suggest that gain and loss of p35 likely affect a larger percentage of aging-related genes than formally demonstrated in our analysis.

Among the most prominent phenotypes revealed by our expression profiling of altered p35 are a number that are typically considered early events in the mechanism of neurodegeneration. These include impaired autophagy, which we verified by assaying accumulation of autophagosome-related proteins, and oxidative stress, established by measuring sensitivity to oxidative challenge with paraquat or hydrogen peroxide. However, in our paradigm, much of the disruption of these processes can be accounted for by the observed change in aging rate. We must now consider whether oxidative stress and impaired autophagy, which are usually thought of as degeneration phenotypes, might more accurately be characterized as secondary consequences of altered aging. By extension, we must further

consider whether other p35-associated pathological processes should really be considered as downstream consequences of the acceleration of aging rather than as causative, early steps in the degeneration cascade *per se*.

It has been argued that neurodegeneration is not simply 'brain aging' inasmuch as one can have aging without overt degeneration. Our data do not contradict this view, but rather suggest that aging can promote degeneration, in part, by synergistically enhancing the effects of underlying non-aging insults to neuronal integrity. The p35-null head samples exhibited a 27% increase in aging rate, but showed a severe, localized reduction of MB neurons well before any neurodegeneration was observed in controls. We hypothesize that the increase in physiological age either sensitizes neurons to, or synergizes with, cell-intrinsic defects we have documented previously as resulting from the absence of Cdk5/p35 activity, such as modulation of the axon initial segment, aberrant organization of actin and ankyrin, or defects in microtubule stability (Trunova, Baek et al. 2011, Smith-Trunova, Prithviraj et al. 2015). Our findings are consistent with the age-dependent hypothesis of Alzheimer's disease, which proposes that aging aggravates an initial injury that alters the cellular physiology of neurons and primes them for neurodegeneration (Herrup 2010). In the case of p35 overexpression, the aging effect was more pronounced, and appeared sufficient to largely account for the accelerated MB neuron loss and reduction in median survival. It is possible that, in *Drosophila*, a strong enough intervention at key signaling molecules can induce acceleration of aging that alone can drive neurodegeneration, although cell-intrinsic defects likely contribute here as well. Recent experiments with tissue from human AD and PD patients hint that processes similar to those we observe in *Drosophila* may be occurring in human disease, as epigenetic characterization of patient tissue reveals both apparent acceleration of aging (Podtelezhnikov, Tanis et al. 2011, Horvath and Ritz 2015,

Levine, Lu et al. 2015) and alterations in regulatory marks associated with ankyrin genes that are key to neuronal cytoarchitecture (De Jager, Srivastava et al. 2014, Lunnon, Smith et al. 2014). More directed studies of human patient samples will be essential to test this hypothesis.

Using our quantitative metric for physiological age, we observe acceleration of the aging rate upon alteration of proline-directed protein phosphorylation, and crucially, we observe this phenotype prior to evidence of neurodegeneration. This discovery seemingly inverts our picture of the causal relationship of aging and neurodegenerative disease, and raises profound questions for our view of neurodegenerative disease. Is it meaningful to use the consequences of age-dependent processes as biomarkers of disease if aging itself is variably affected by the disease mechanism? If tau pathology and associated kinase dysregulation enhance oxidative stress essentially as a downstream consequence of accelerated aging, does it imply that treatments directed at the consequences of oxidative stress would only protect against disease if they reversed aging itself? It will be essential to fully dissect the relationship of protein phosphorylation to aging, and to neurodegenerative disease, if we are to have a rational basis for advances in treatment of aging-associated disorders, such as Amyotrophic Lateral Sclerosis, Parkinson's disease, and Alzheimer's disease.

Chapter 4

Investigation of the role of the axon initial segment in neurodegeneration

Chapter 4: Investigation of the role of the axon initial segment in neurodegeneration

4.1 Introduction

The axon initial segment (AIS) is a key neuronal domain which lies between the somatodendritic and axonal compartments. The central functions of the AIS include initiating action potentials (APs) and maintaining neuronal polarity, two actions which are essential for optimal neuronal function and excitability. Indeed, the AIS serves as the intersection between neuronal input and output, providing the basis for neuronal circuits. Unsurprisingly, perturbation of the AIS can have significant impacts on the operation of the nervous system, and has been found to play a role in multiple disease and injury paradigms. AIS function in the nervous system, how the AIS is involved in ND, and how the AIS relates to p35-mediated ND in particular will be reviewed below.

Action potential initiation

Communication within the nervous system arises from the release of neurotransmitters from a neuron into a synaptic cleft with another neuron or muscle tissue. A long cascade of events lies upstream of neurotransmission, most notably the initiation of an AP. Nobel-prize winners Hodgkin and Huxley characterized the electrical properties of the squid giant axon over the course of multiple publications; their seminal work resulted in a mathematical model outlining the fundamentals of AP initiation and propagation (Hodgkin and Huxley 1952). At rest, most neurons have a resting membrane potential of approximately -70 millivolts. Upon stimulation, an influx of sodium ($Na+$) or calcium ($Ca2+$) ions from the extracellular space into the neuron raises the membrane potential. Once the membrane potential passes a threshold, an

AP is initiated; if the stimulus fails to depolarize the neuron past this threshold potential, the neuron will not fire. After reaching the threshold, the depolarization causes voltage-gated ion channels to temporarily open, allowing more positively-charged ions to enter the neuron, further raising the membrane potential in the immediate vicinity and inducing neighboring channels to also open. Thus, the depolarization is propagated along the length of the axon. At the synaptic terminal, depolarization causes voltage-gated calcium channels to open; the resultant influx of $Ca2+$ triggers synaptic vesicles holding neurotransmitter to fuse with the presynaptic membrane and release their contents into the synaptic cleft. The released neurotransmitters can then diffuse across the synapse, bind receptors, and stimulate the postsynaptic neuron or muscle cell, or be actively transported back into the presynaptic neuron. This entire process is extremely rapid, as an AP only lasts approximately one millisecond. After depolarization, the sodium and/or calcium channels close, preventing additional ions from entering. Potassium (K+) channels then open, transporting K+ ions from the neuron into the extracellular space, repolarizing the neuron. The neuron will actually hyperpolarize, temporarily preventing additional firing. After this refractory period of about two milliseconds, sodium-potassium ATPases transport K+ and Na+ ions to re-establish the resting membrane potential so that the neuron can fire again upon fresh stimulation.

An essential property of neuronal function is adaptability in response to various stimuli. This plasticity arises in large part from the M-current, a non-inactivating potassium current (Wang, Pan et al. 1998, Rasmussen, Frokjaer-Jensen et al. 2007). The M-current has been found in neurons of both the central and peripheral nervous system (Brown and Adams 1980, Wang, Pan et al. 1998), highlighting its importance to the overall function of the nervous system. In neurons, the conductance of potassium channels is regulated prior to and during depolarization.

The result is a highly-regulated membrane potential that shifts the threshold potential for AP

firing and ultimately determines neuronal excitability.

Following elucidation of the electrical properties of neurons, significant strides were

made in investigating the underlying mechanisms of AP initiation. To do so, it was necessary to

establish the site of AP initiation. Initial work measuring responses of spinal motoneurons to

different stimuli demonstrated that AP initiation occurs within the axon, and specifically starts at

the initial segment. Subsequent experiments further localized the start of AP initiation to the

distal part of the AIS. Using voltage-sensitive dyes, Palmer and Stuart found that APs initiate

~35 microns from the axon hillock, coinciding with the distal AIS (Palmer and Stuart 2006). By

having a primary site for starting AP firing, it is simpler to either enhance or suppress neuronal

excitability, and it is easier to synchronize signaling among multiple neurons.

Electrophysiological properties of the AIS

As the site of AP initiation, the AIS serves as gatekeeper of the nervous system. This

function is achieved by a specialized set of ion channels, which are responsible for the

electrophysiological properties of the AIS that permit APs. Generally, the AIS is characterized

by a high density of sodium channels and a lower number of potassium channels (Figure 4.1.1)

(Khaliq 2006, Shah, Migliore et al. 2008). Kole et al found that the AIS of cortical pyramidal

neurons had a sodium channel density approximately 50 times that of the proximal dendrites

(Kole, Ilschner et al. 2008). This enrichment results from interactions between channels and the

underlying cytoskeleton, anchoring the channels in place. The cytoplasmic loop linking domains

II and III of Nav1.1 channels associates with AnkyrinG (AnkG) and is responsible for targeting

the channel to the AIS (Garrido, Giraud et al. 2003); once there, voltage-gated sodium channels

interact with both AnkG and βIV-spectrin (Kole, Ilschner et al. 2008). While different types of

neurons have varying compositions of channel subtypes, the channels at the AIS usually

comprise a combination of Nav1.1, Nav1.2, and/or Nav1.6 (Ogawa and Rasband 2008).

Notably, the AIS exhibits a further level of polarity as domains within the AIS can have different

compositions and thus, different properties. The low-threshold subunit Nav1.6 locates distally

within the AIS, while Nav1.2, which has a higher threshold, accumulates proximally (Van Wart,

Trimmer et al. 2007, Hu, Tian et al. 2009). This specialized segregation regulates AP initiation,

as the AP initiates from the distal AIS as opposed to the proximal region (Palmer and Stuart

2006).
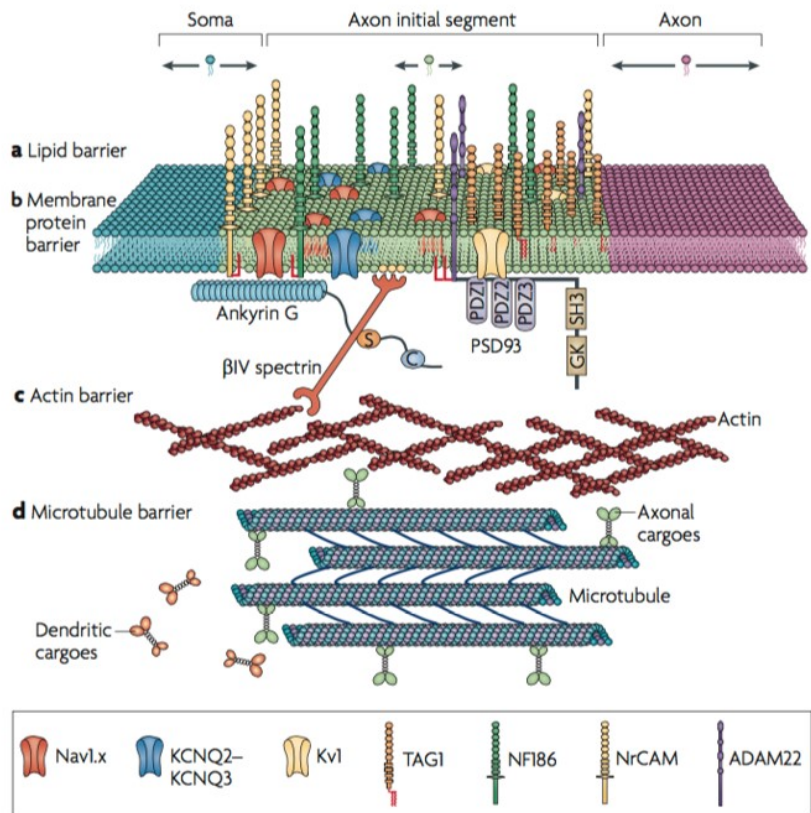
Figure 4.1.1. Molecular composition of the axon initial segment.
The AIS is characterized by a specific composition of ion channels and membrane proteins, its unique cytoskeleton, and accumulation of ankyrin proteins. The AIS is enriched with sodium (Nav) and potassium (KCNQ, Kv) channels, as well as a select group of transmembrane proteins. The underlying cytoskeleton comprises microtubules and actin. AIS interactions with the cytoskeleton are mediated through Ankyrin G and βIV-spectrin. (Reproduced from Rasband, 2010).

The AIS is also home to a specialized collection of potassium channels that modify the properties of APs. These potassium channels function in generating the M-current, which controls membrane excitability. The set of voltage-gated potassium channels found within the AIS includes Kv1.1, Kv1.2, Kv1.4, Kv2.2, Kv7.2 (KCNQ2), and Kv7.3 (KCNQ3) (Ogawa and Rasband 2008). Enrichment of potassium channels at the AIS was more modest than that of sodium channels, as the density of potassium channels within the axon was three to five times the somatic density (Shah, Migliore et al. 2008). Like sodium channels, some potassium

channels show segregation within microdomains of the AIS. Kv1.2 channels accumulate in the distal AIS, but are excluded from the proximal region (Van Wart, Trimmer et al. 2007). Of the potassium channels, Kv7.2 (KCNQ2) and Kv7.3 (KCNQ3) have been identified as essential components for generating the M-current (Wang, Pan et al. 1998, Rasmussen, Frokjaer-Jensen et al. 2007). Kv7.2 (KCNQ2) forms a heterotetramer with Kv7.3 (KCNQ3), and both concentrate at the AIS (Pan, Kao et al. 2006, Rasmussen, Frokjaer-Jensen et al. 2007); this localization is dependent on AnkG, as the AIS accumulation of Kv7.2 (KCNQ2) and Kv7.3 (KCNQ3) in cerebellar neurons from ankG-null mice was completely abolished (Pan, Kao et al. 2006). While both channels can directly bind AnkG, localization at the AIS is only dependent on interactions between AnkG and Kv7.3 (KCNQ3) (Rasmussen, Frokjaer-Jensen et al. 2007). Functionally, these channels help control resting membrane potential and the threshold for AP initiation, thus serving to suppress spontaneous AP firing (Shah, Migliore et al. 2008). Further, these channels also regulate the resting membrane potential by regulating subthreshold currents, preventing repetitive AP firing (Ogawa and Rasband 2008). Taken together, it is clear that changes in potassium channel levels, location, and activity, in conjunction with similar regulation of sodium channels, permits the necessary plasticity necessary for nervous system function.

Establishment of neuronal polarity

The second primary function of the AIS is to establish and uphold neuronal polarity. To maintain polarity and proper neuronal function, the distribution of specific proteins must be restricted to certain domains; specifically, somatodendritic proteins must be constrained proximal to the AIS, while axonal proteins must be contained within axonal projections. Cells can accomplish this segregation by selectively targeting proteins to their final destination

(Nakata and Hirokawa 2003, Sampo, Kaech et al. 2003), distributing proteins non-discriminately and then selectively retaining them in the proper location (Garrido, Fernandes et al. 2001, Sampo, Kaech et al. 2003), or by utilizing localized translation (Jimenez-Diaz, Geranton et al. 2008, Yoon, Jung et al. 2012). Of these possibilities, the AIS has been most associated with selective axonal targeting as it serves as a cytosolic diffusion barrier, effectively separating the cell body and axonal compartments while permitting transport of select cargoes between the two regions. This polarity stems in part from a unique cytoskeletal architecture maintained within the AIS. It has been known for decades that the AIS has a characteristic local microtubule cytoskeleton that distinguishes it from other neuronal domains (Palay, Sotelo et al. 1968) (Figure 4.1.1) . Within the AIS, microtubules are organized into fascicles of usually three to five microtubules, with multiple bundles running parallel to one another through the length of the AIS. These microtubules are oriented such that their plus end is away from the soma and towards the neurite tips (Baas, Deitch et al. 1988). More recently, it has been found that the microtubule skeleton within the AIS also has different post-translational modifications, which alters interactions with motor proteins responsible for trafficking. The microtubules within the somatodendritic domain are heavily tyrosinated, preventing interactions with kinesin-1 (Konishi and Setou 2009). Conversely, axonal microtubules have significantly higher levels of acetylated microtubules, compared to dendrites (Hammond, Huang et al. 2010). The preference of certain motor proteins for specific subpopulations of MT tracks is likely related to the recruitment of the plus-end directed kinesin motor KIF5 to the AIS and its selective buildup in axons (Nakata and Hirokawa 2003). Furthermore, Tapia et al demonstrated that acetylated microtubules localized within the AIS are resistant to detergent treatment (Tapia, Wandosell et al. 2010). As development progresses, F-actin also concentrates locally within the AIS (Nakada, Ritchie et al.

2003, Song, Wang et al. 2009), and this F-actin cytoskeleton remains intact following detergent treatment (Winckler, Forscher et al. 1999). Directly disrupting the actin cytoskeleton with depolymerizing agents results in loss of the diffusion barrier, indicating the significance of the underlying cytoskeleton (Winckler, Forscher et al. 1999, Nakada, Ritchie et al. 2003, Song, Wang et al. 2009).

In addition to F-actin and microtubules, the submembranous cytoskeleton that characterizes the AIS is composed of specific ankyrin and spectrin isoforms (Figure 4.1.1). Ankryin and spectrin proteins are known to link various membrane proteins to the underlying cytoskeleton in a variety of contexts, and are largely associated with establishing and stabilizing specialized membrane domains (Kizhatil and Bennett 2004, Mohler, Davis et al. 2005, Pielage, Fetter et al. 2005). In mammals, there are three separate Ankyrin genes (*Ank1*, *2*, and *3* encoding AnkR, AnkB, and AnkG, respectively), each of which is expressed to some degree in the nervous system. Of the three, AnkG is deemed the master organizer of the AIS. While the distal axonal cytoskeleton contains AnkB, αII-spectrin, and βII-spectrin, AnkG and βIV-spectrin are found in the AIS (Yoshimura and Rasband 2014). AnkG is essential for the clustering and localization of βIV-spectrin, as well as other proteins, to this subcellular domain (Sobotzik, Sie et al. 2009). AnkG directly binds spectrin repeat 15 of βIV-spectrin, and this binding is required for the proper targeting of βIV-spectrin to the AIS, as βIV-spectrin fails to localize to the AIS in AnkG-null mice (Yang, Ogawa et al. 2007). While AnkG can recruit βIV-spectrin to the AIS, the reverse is not true. However, βIV-spectrin does play a role in maintaining the AIS, as its absence leads to loss of stabilization and dispersion of AnkG from the AIS (Komada and Soriano 2002). Without AnkG and βIV-spectrin, the diffusion barrier is lost, and axons exhibit dendritic characteristics, including accumulation of proteins normally restricted to dendrites and the

114

formation of spines with post-synaptic receptors (Hedstrom, Ogawa et al. 2008, Sobotzik, Sie et al. 2009). Thus, the AIS is characterized by a stable cytoskeleton comprising actin, microtubules, ankyrin G, and βIV-spectrin, and is favored by motor proteins moving towards the axon and away from the soma.

Along with the specialized cytoskeleton, a unique composition of transmembrane proteins also contributes to the diffusion barrier separating the somatodendritic region from the axonal compartment (Figure 4.1.1). Indeed, cell adhesion molecules (CAMs) such as neurofascin (NF)-186 and neuron-glia related CAM (NrCAM) are enriched within the AIS (Nakada, Ritchie et al. 2003). Again, AnkG is responsible for the correct recruitment and localization of proteins to the AIS, as NF-186 and NrCAM fail to be retained when their binding with AnkG is disrupted (Zhang, Davis et al. 1998, Lemaillet, Walker et al. 2003) or AnkG expression is silenced (Hedstrom, Ogawa et al. 2008). The high concentration of these transmembrane proteins, in combination with the dense cytoskeleton, prevents diffusion via steric hindrance and hydrodynamic friction-like effects (Nakada, Ritchie et al. 2003). CAMs may also contribute to AIS stability and/or plasticity through interactions with the extracellular matrix (ECM). The C-terminal of CAMs binds with AnkG intracellularly (Dzhashiashvili, Zhang et al. 2007); CAMs also span the plasma membrane and extend into the extracellular space. NF-186 directly interacts with a host of ECM proteins, including brevican, gliomedin, syndecans, laminins, neural/glial antigen 2 (NG2), and versican (Hedstrom, Xu et al. 2007, Nelson and Jenkins 2017). Brevican accumulates around the AIS of cultured hippocampal neurons via an NF-186-dependent mechanism. This specialized brevican-rich milieu is part of a larger 'perineuronal net' surrounding the majority of CNS neurons, and may provide a specialized microenvironment for optimal ion channel function or serve to stabilize axo-axonic

contacts (Hedstrom, Xu et al. 2007). Alternatively, connections to the ECM may function as a stabilizing force for NF-186 and its interacting partners. Altogether, the unique structure and composition of the AIS allow it to effectively segregate different regions of the neuron and to maintain axonal identity.

The role of the AIS in neuronal injury and neurodegeneration

Provided the essential role of the AIS in neuronal function, it is no surprise that recent literature has implicated the AIS as a target of neuronal injury and contributor to neurodegeneration. Exposing mice to ischemic injury, as is seen in strokes, results in the loss of AnkG, βIV-spectrin, and sodium channels from the AIS of cerebral cortex neurons (Schafer, Jha et al. 2009). Loss of these proteins from the AIS was the result of calpain-mediated proteolysis, and occurred independently of axon degeneration or cell death. Expanding on these results, del Puerto et al found that activation of the purinergic P2X7 receptor channel leads to a calcium influx, activation of calpain, and the eventual loss of AnkG from the AIS (del Puerto, Fronzaroli-Molinieres et al. 2015). This disruption of the AIS was accompanied by decreased current amplitudes and excitability. Disruption of the AIS also leads to loss of neuronal polarity. Under normal conditions, tau is primarily restricted to the axons of neurons. In AD, however, the primary constituents of the AIS are downregulated, and tau localization is disrupted, as tau is found in the somatodendritic region as well (Sohn, Tracy et al. 2016). Li et al demonstrated that the microtubule cytoskeleton supporting the AIS is specifically responsible for restricting tau to the axons as it permits anterograde flow of tau, but not retrograde (Li, Kumar et al. 2011). One mechanism through which the AIS is compromised in AD is due to post-translational modifications of tau. Tau acetylated at lys-274 and lys-281 accumulates in post-mortem AD

116

brain samples, and expression of tau mutants that mimic acetylation at these residues was found to decrease AIS-associated proteins and shorten the overall length of the AIS (Sohn, Tracy et al. 2016). Acetylation reduces the affinity of tau for microtubules, leading to destabilization of the microtubule cytoskeleton, disruption of the AIS diffusion barrier, and the eventual redistribution of tau into the somatodendritic region. Once in the dendrites, tau induces decreased expression of AMPA and NMDA receptors, leading to synaptic dysfunction and functional impairments (Hoover, Reed et al. 2010).

The AIS is conserved in Drosophila

The plasticity and polarity provided by the AIS serve as the cornerstones of the intricate vertebrate nervous system; recent literature, however, has also identified AIS-containing neurons in *Drosophila* (Trunova, Baek et al. 2011). Indeed, the AIS domain identified in mushroom body (MB) gamma neurons exhibits the characteristic hallmarks of the mammalian AIS. First, there is selective accumulation of an anchoring protein within this subcellular domain. In mammals, AnkG is the primary organizer of the AIS. In contrast, *Drosophila* only have two Ankyrin genes, the ubiquitous Ank1 and the neuron-specific Ank2 (Bouley, Tian et al. 2000, Hortsch 2002), neither of which is exclusively expressed at the AIS. However, while Ank1 did show ubiquitous expression, it also exhibited elevated levels concentrated within the AIS. Second, the *Drosophila* AIS has a localized enrichment of a unique set of voltage-gated potassium channels. Specifically, Elk, Shaw (Kv3), and Shal (Kv4) channels were enriched in the AIS, while dORK-C2 (Ork1), Shaker (Kv1.3), and EKO (Kv1.3) were selectively excluded. In mammals, Elk channels mediate neuronal excitability by raising the threshold for AP firing (Zhang, Bertaso et al. 2010), while Shaw channels regulate neuronal resting membrane potential

(Hodge and Stanewsky 2008). Shal channels play a role in establishing the A-type current, a

transient inactivating current, as well as regulating action potential waveform (Shibata, Nakahira

et al. 2000). Lastly, there is a specialized F-actin cytoskeleton within the AIS. In the

somatodendritic and axonal regions, actin is highly expressed and ubiquitous; within the AIS,

actin levels are reduced significantly and appear as parallel fibrils (Trunova, Baek et al. 2011).

Similar to mammals, the actin cytoskeleton within the *Drosophila* AIS is more stable than in

surrounding areas, as blocking actin polymerization reduced actin levels within dendrites and

axonal lobes while not visibly affecting the AIS actin cytoskeleton. Taken together, the defined

~20-30 micron domain within *Drosophila* MB neurons satisfies the characteristic hallmarks of

its mammalian counterpart. A similar domain was also observed in multipolar dendritic

arborization neurons. Jegla et al identified a diffusion barrier localized to the proximal axon of

ddaE neurons that coincided with a localized accumulation of Shal and Elk potassium channels

(Jegla, Nguyen et al. 2016). That multiple neuronal subtypes exhibit an AIS in *Drosophila*

supports flies as a valid model, and suggests that more types of neuron will be found to also have

an AIS.

The Drosophila AIS is regulated by Cdk5/p35 kinase activity

The AIS of *Drosophila* mushroom body neurons is regulated by Cdk5 activity. Cdk5

activity modulates the AIS size in a dose-dependent manner: loss of p35 or overexpression of a

dominant-negative Cdk5 results in a shorted or absent AIS, whereas increased p35 levels

significantly elongated the AIS (Trunova, Baek et al. 2011). AIS size was assessed using a

number of somatodendritic markers (Drl, dORK2-C2) and axon-specific labels (Robo2, FasII),

as well as with proteins showing selective accumulation within the AIS (Ank1, Elk). Notably,

p35 perturbation did not alter neuronal polarity or disrupt its function as a diffusion barrier. When the AIS was either shortened or elongated, somatodendritic markers remained localized to the soma and calyx, as the proximal boundary of the AIS remained intact. Conversely, the proximal boundary of axonal markers shifted towards or away from the somatodendritic border, depending on the genetic manipulation. Thus, the proximal border of the axonal compartment shifts in accordance with the distal boundary of the AIS (Trunova, Baek et al. 2011).

Cdk5 also contributes to regulation of the AIS in mammals. Cdk5 phosphorylates the Kvβ2 subunit of the potassium channel Kv1, which is enriched at the AIS (Vacher, Yang et al. 2011). The unphosphorylated subunit interacts more strongly with the microtubule plus-end tracking protein EB1. Cdk5-mediated phosphorylation disrupts this interaction, releasing the channel from its tether and permitting its trafficking to the cell surface. Phosphorylation of serine residues has also been shown to alter AnkG binding. Casein kinase 2 (CSNK2)-mediated phosphorylation of serine residues of sodium channels regulates interaction with AnkG and thus accumulation at the AIS; indeed, blocking CSNK2 activity lead to decreased levels of Nav1.2 at the AIS (Brechet, Fache et al. 2008). Cdk5-mediated phosphorylation of voltage-gated channels could potentially act through similar mechanisms to regulate channel localization. Furthermore, Cdk5 also phosphorylates the voltage-gated potassium channel Kv7.2 at multiple serine residues within its phosphatidylinositol-4,5-bisphosphate (PIP_2)-binding domain by Cdk5 (Salzer, Erdem et al. 2017). The phosphorylation status of the channel alters its sensitivity towards PIP_2, which is required for channel opening. Consequently, Cdk5 helps control potassium channel localization and activity at the AIS, regulating the action potential threshold.

Despite an abundance of research, the underlying molecular mechanisms responsible for establishing the AIS, and those involved in its dysregulation, have yet to be fully untangled.

Exploiting the simpler nervous system of *Drosophila* will allow tremendous gains in parsing apart AIS regulation. To this end, we completed a brief candidate screen for additional modulators of AIS size. We show here that overexpression of a construct encoding the C-terminal tail of an Ank2-L isoform is sufficient to induce shortening of the AIS, and that this shortening mimics the effects of Cdk5/p35 loss of function. Furthermore, we show that Ank2-L-induced effects on the AIS may be sufficient to cause neurodegeneration. Taken together, our data suggest that cell-intrinsic insult, such as shortening of the AIS, stemming from loss of Cdk5 activity likely contributes to p35-mediated neurodegeneration.

4.2 Materials and Methods

Fly stocks

All stocks were generated in an Oregon Red wild-type background (w+). p35 loss of function conditions ($p35^{20C}$) have been previously described (Connell-Crowley, Le Gall et al. 2000, Connell-Crowley, Vo et al. 2007, Trunova, Baek et al. 2011, Trunova and Giniger 2012, Smith-Trunova, Prithviraj et al. 2015). Overexpression of p35 was accomplished using UAS-p35 (Connell-Crowley, Le Gall et al. 2000). Ank2 constructs (UAS-VENUS-Ank2-S, UAS-VENUS-Ank2-L4, UAS-VENUS-Ank2-L4) were graciously provided by Jan Pielage (University of Kaiserslautern, Kaiserslautern, Germany). Ank2-RNAi lines were procured from Dr. Graem Davis (University of California – San Francisco, San Francisco, CA), the Bloomington *Drosophila* Stock Center (BDSC), and from the Harvard Transgenic RNAi Project (TRiP) (Harvard Medical School, Boston, MA). $Ank2^{518}$ stocks were a gift of Dr. Melissa Rolls (Pennsylvania State University, University Park, PA); $Ank2^{2001}$ was provided by the BDSC. Stocks for assessing the AIS included UAS-Act-RFP (BDSC) and UAS-Syt-HA (provided by

Dr. Prokop, University of Manchester, Manchester, UK). In all experiments, MB-specific

expression was accomplished with the gamma-neuron specific Gal4 driver 201Y-Gal4.

To enhance efficacy, RNAi constructs were also co-expressed with UAS-Dcr2. Some

experiments were carried out at 29°C to enhance Gal4 expression and raise the level of Ank2-

RNAi. For select RNAi experiments, ELAV-Gal4 was used to achieve pan-neuronal expression

of constructs (BDSC).

MB cell counting utilized the UAS-nls-mCherry fly stock, which was obtained from the

BDSC. 201Y-Gal4 was used to express UAS-nls-mCherry in control flies (w+; 201Y-Gal4/+;

UAS-nls-mCherry/+ and w+; 201Y-Gal4/+; UAS-nls-mCherry/UAS-GFP) and flies

overexpressing Ank2-L4 (w+; 201Y-Gal4/+; UAS-nls-mCherry/UAS-VENUS-Ank2-L4).

Immunohistochemistry

Third-stage larval brains were dissected in ice-cold PBS (pH 7.4) (Invitrogen), fixed in

4% PFA in PBS for 25 min, and then transferred to 4% PFA in PBS with 0.5% Triton X-100 for

an additional 25 min. Brains were then rinsed once in PBS buffer with 0.5% Triton X-100

(PBST), followed by three five-minute washes in PBST. Brains were incubated in blocking

buffer (PBST, 4% BSA, 4% goat serum, 4% donkey serum) for 1 h, then incubated with primary

antibodies in blocking buffer for 48 hours at 4°C. Primary antibodies included: 1:200 mouse

anti-Fasciclin 2 (Fas2) from Developmental Studies Hybridoma Bank, 1:1000 rabbit anti-myc

(Sigma-Aldrich), and 1:1000 rat anti-HA (Roche). Samples were then rinsed and washed thrice

in PBST, before being incubated with secondary antibodies overnight at 4°C. Secondary

antibodies were diluted 1:500 in blocking buffer, and included goat anti-mouse, anti-rabbit, and

anti-rat conjugated with either A488, A568, or A633 fluorochromes (Invitrogen). Lastly, brains

were rinsed and washed thrice in PBST before being mounted in VectaShield antifade medium. In order to prevent samples from being squished, coverslips were set on number 1 glass chips. Prepared samples were imaged under 40X-oil on a Zeiss NLO510 confocal microscope and analyzed using Imaris.

Mushroom Body Neuron Counting

Control flies and flies overexpressing Ank2-L4 were aged to 3-, 10-, 30-, or 45-days old. Sample preparation and image acquisition were completed as described in the Materials and Methods section of Chapter 2. Following image acquisition, MB cell nuclei were automatically counted using the "Add spots" function in Imaris. For automatic quantification of MB neurons using UAS-nls-mCherry, spot counting diameter was set to "2" and threshold value was set to "2.12." These values were determined through manual testing to yield the most accurate results.

Statistical Analysis

The effects of pan-neuronal expression of constructs were tested genetically; significant differences in ratios of offspring were assessed by chi-square analysis. Mushroom body cell counts were analyzed with GraphPad Prism 7.0b. Differences between groups were assessed by either one-way or two-way ANOVA with post-hoc Tukey multiple comparison testing, as described. All statistical tests were two-tailed, and statistical significance was considered at $p < 0.05$. Experimental groups were determined based on genotype, so no randomization was used; data collect and analysis was not performed blind to the conditions of the experiments. Sample sizes were not predetermined using statistical methods. Data distribution was assumed to be normal with equal variance, although this was not formally tested.

4.3 Results

p35 regulates the size of the axon initial segment in central brain neurons

p35 has previously been shown to regulate the size of the axon initial segment in a dose-dependent manner (Trunova, Baek et al. 2011); we now confirm this regulation in a wild-type (w+) genetic background. The cell adhesion protein fasciclin II (FasII) shows specific patterns of sub-cellular localization in a number of neuronal types. For example, it labels the axonal lobes of mushroom body neurons, but is noticeably absent from the somatodendritic region and the AIS. Here, we see that loss of loss of p35 results in a shift of the distal boundary of the AIS towards the calyx (Figure 4.3.1b). Conversely, overexpressing UAS-p35 with a MB-specific Gal4 driver (201Y-Gal4) results in a shift of the distal boundary away from the calyx (Figure 4.3.1c). Thus, Cdk5/p35 kinase activity regulates the AIS similarly in multiple control genetic backgrounds.
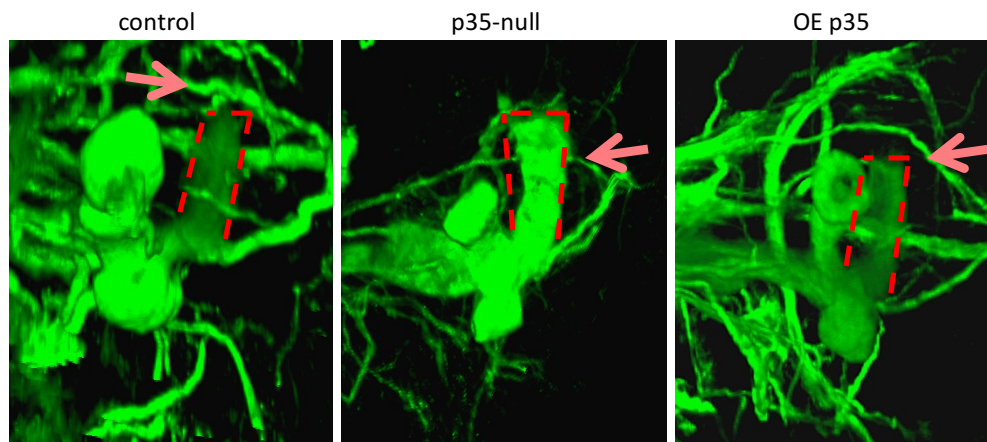
Figure 4.3.1. p35 regulates the size of the AIS in MB neurons.
Third-instar larva brains are stained with anti-FasII. In each panel, the boundaries of the FasII staining in the MB peduncle are outlined by the red-dashed line. The pink arrow indicates a stereotypical nerve that crosses over in front of the MB peduncle. This nerve is used as a landmark to gauge changes in the AIS size. **(A)** FasII staining in control flies stops below the crossover nerve, leaving a small gap. In **(B)** p35-null flies, the FasII boundary is shifted proximally towards the calyx and extends beyond the crossover nerve. In **(C)** flies overexpressing p35, the FasII boundary is shifted distally down the peduncle.

Overexpression of the C-terminal tail of Ank2-L robustly shortens the AIS

A small screen for alternative modifiers of the AIS revealed that constructs encoding the

C-terminal tail of the Ank2-L isoform can alter the size of the AIS. AnkG, the master organizer

of the AIS in mammals, has a giant exon that is essential for assembly of the AIS (Jenkins et al,

2015). In *Drosophila*, Ank2 has specific isoforms that also have giant exons (Ank2-L and Ank2-

XL) and that share structural similarities with AnkG. Ank2-L was found to contribute to axon

caliber and synaptic structure (Stephan et al, 2015), but its relationship to the AIS has yet to be

fully elucidated. Here, we found that expression of Ank2-L4 (UAS-VENUS-Ank2-L4; amino

acids 1530-3005) in the MB results in a shortening of the AIS. Ank2-L4 expression leads to a

proximal shift in FasII staining towards the somatodendritic region of MB neurons (Figure

4.3.2B). Ank2-L8 (UAS-VENUS-Ank2-L8; amino acids 1530-4083) overexpression resulted in

a more severe shortening of the AIS, as FasII staining, which stops at the boundary between the

peduncle and calyx in Ank2-L4 samples, was observed in the calyx of Ank2-L8 samples (Figure

4.3.2C). Notably, Ank2-mediated modulation of the AIS was specific to the distal end of Ank2-

L, as expressing Ank2-S (UAS-VENUS-Ank2-S; amino acids 1-1159), the N-terminal domain of

Ank2, had no effect on the AIS (Figure 4.3.2A). Thus, the C-terminal tail of Ank2-L is both

sufficient and necessary to induce shortening of the AIS.

UAS-VENUS-Ank2-S **UAS-VENUS-Ank2-L4** **UAS-VENUS-Ank2-L8**
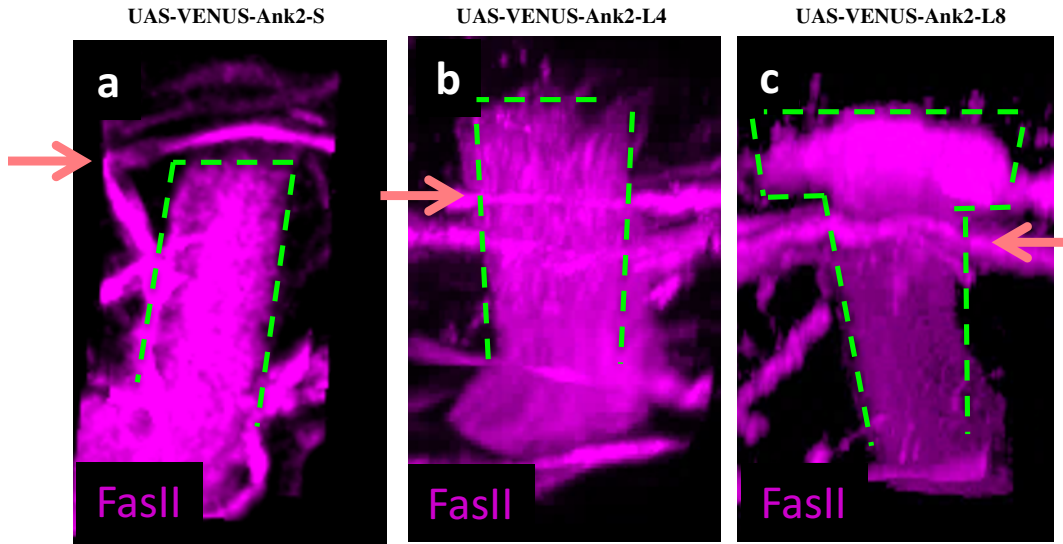
Figure 4.3.2. The C-terminal tail of Ank2-L is necessary and sufficient for modulation of the AIS.
Third-instar larva brains are stained with anti-FasII. Expression of **(A)** UAS-VENUS-Ank2-S, **(B)** UAS-VENUS-Ank2-L4, and **(C)** UAS-VENUS-Ank2-L8 was driven by the MB-specific driver 201Y-Gal4. Ank2-S had no observable effect on the AIS, while both Ank2-L4 and Ank2-L8 shortened the AIS. In each panel, the boundaries of the FasII staining in the MB peduncle are outlined by the green-dashed line. The pink arrow indicates a stereotypical nerve that crosses over in front of the MB peduncle. This nerve is used as a landmark to gauge changes in the AIS size.

Because Ank2-L4-induced shortening of the AIS more closely mimicked the p35-null phenotype, all further experiments utilize this construct. In addition to FasII, we also assessed the AIS with markers labeling different sub-cellular domains within the MB neurons. Actin tagged with RFP (Act-RFP) is expressed throughout control neurons, but shows an altered cytoskeletal architecture within the AIS; the AIS contains stabilized actin organized into parallel fibrils (Figure 4.3.3B; (Trunova, Baek et al. 2011)). Synaptotagmin linked with hemagglutinin (syt-HA) localizes to the axonal lobes and calyx of control neurons while being selectively excluded from the AIS (Figure 4.3.3D). With every marker, the proximal boundary of the axonal label was consistently shifted towards the calyx, indicating robust shortening of the AIS (Figure 4.3.3E-H). Antibody staining of the somatodendritic-specific protein Futsch/MAP1B did

not reveal any alterations (data not shown), indicating that neuronal polarity is maintained even

with the shortened AIS.
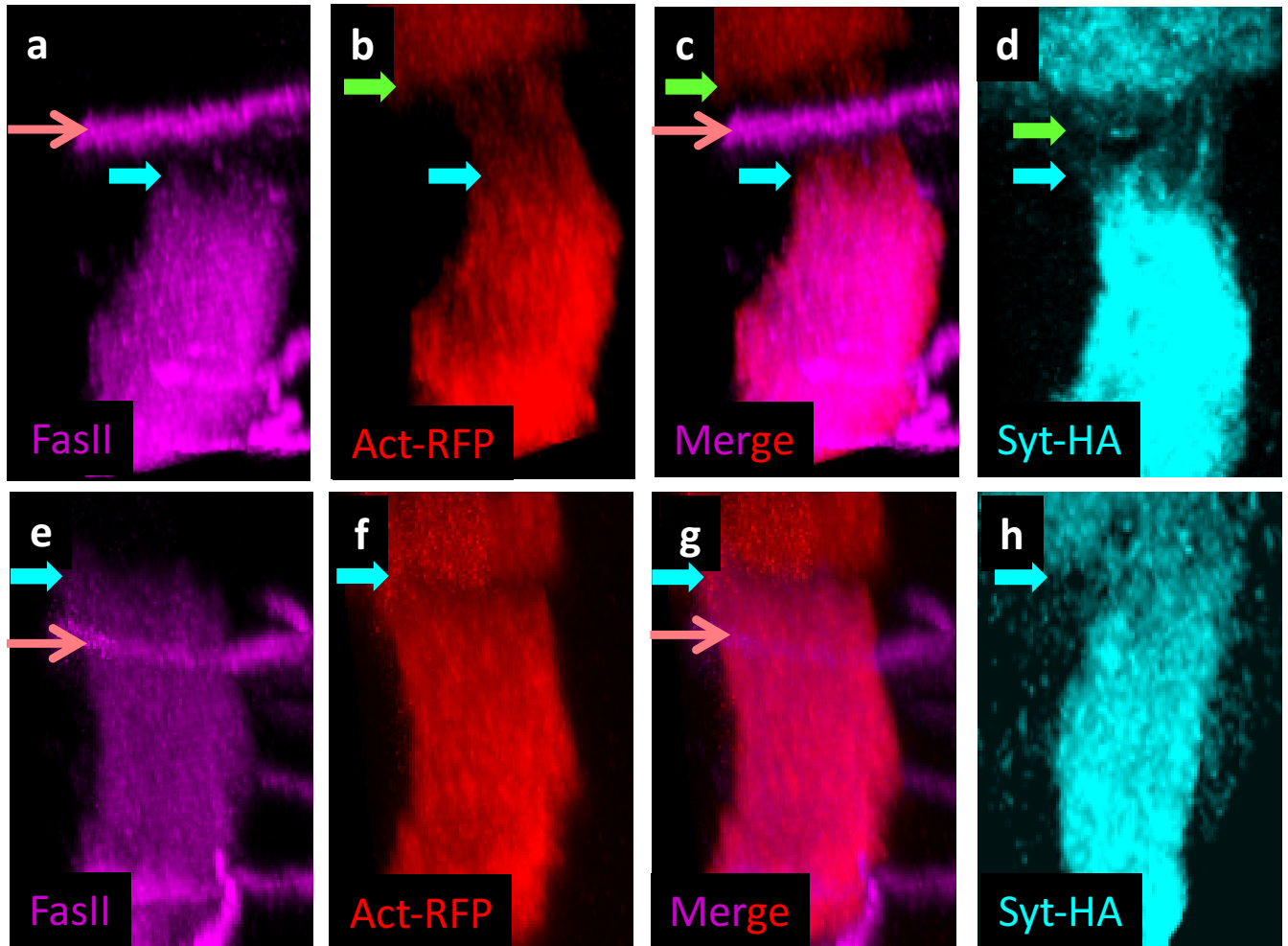
Figure 4.3.3. Ank2-L4 overexpression robustly shortens the AIS.
Labeling of the AIS of MB gamma neurons from **(A-D)** control or **(E-H)** Ank2-L4
overexpressing third instar larva. Panels **(A)** and **(E)** show staining with anti-FasII, panels **(B)**
and **(F)** show Actin-RFP expression, and panels **(C)** and **(G)** show the resulting merged image.
Panels **(D)** and **(H)** outline the AIS using Synaptotagmin-HA. In each panel, the proximal
border of the axonal signal is indicated by the light blue arrow. In **(B-D)**, the somatodendritic
boundary is marked by the green arrow. The pink arrow indicates a stereotypical nerve that
crosses over in front of the MB peduncle. This nerve is used as a landmark to gauge changes in
the AIS size.

Ank2-L4-mediated modulation of the AIS is a neomorphic function

We next sought to discern the underlying mechanism of Ank2-L4-mediated shortening of

the AIS. As expression of Ank2-L4 mimicked the effect of p35 deletion on the AIS, we

hypothesized that the inverse would be true, and that decreasing Ank2 levels would affect the

AIS in a similar manner as increased p35 levels. To address this, we expressed Ank2-RNAi in

the MB, as well as observing the AIS in various Ank2 mutant backgrounds. Multiple Ank2-

RNAi constructs showed some evidence of a partially shortened AIS, but the AIS was never

affected as severely as was seen with loss of p35 or overexpression of Ank2-L4 (Figure 4.3.4A).
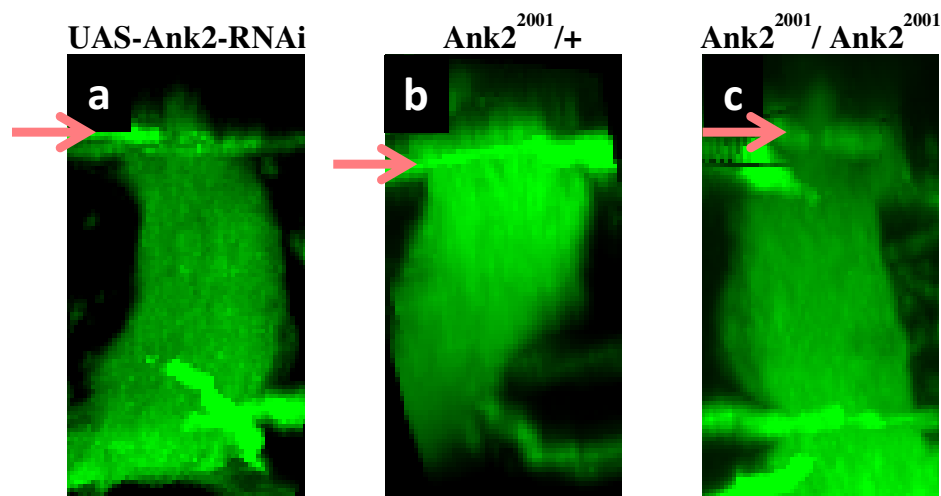
Figure 4.3.4. Reduction of Ank2 levels has modest effects on the AIS.
Brains from third-instar larva **(A)** expressing UAS-Ank2-RNAi, **(B)** heterozygous for Ank2[2001],
or **(C)** homozygous for Ank2[2001] are stained with anti-FasII. In each panel, the pink arrow
indicates a stereotypical nerve that crosses over in front of the MB peduncle. The proximal
boundary of FasII staining in the peduncle is shifted towards the somatodendritic region of the
MB neurons.

The lack of a strong phenotype resulting from knockdown of Ank2 is likely not the result

of ineffective knockdown, as pan-neuronal expression of the RNAi construct mimics larval/pupal

lethality observed in Ank2-null mutants (Pielage, Cheng et al. 2008). Flies carrying UAS-Ank2-

RNAi were crossed to ELAV-Gal4/CyO, and the ratio of CyO to non-CyO offspring was

quantified. Compiled results from multiple experiments revealed that the majority of offspring

were CyO, and therefore not expressing Ank2-RNAi throughout the nervous system (Table

4.3.1; p<0.0001). These results support that pan-neuronal expression of Ank2-RNAi is lethal,

and that the RNAi is being expressed and is functional, at least to a certain degree. Neither the

presence of Dicer2 nor enhancing RNAi levels by raising flies at elevated temperatures to

increase Gal4 activity was sufficient to generate an aberrant AIS phenotype (data not shown).

Alternatively, we also utilized a genetic mutant to decrease Ank2 levels. Ank2^{2001} is selectively

null for the Ank2-L isoform (Pielage, Cheng et al. 2008). Mutants heterozygous for Ank2^{2001}

exhibited a slightly shortened AIS phenotype, while Ank2^{2001} homozygous mutants did not show

an exacerbated phenotype (Figure 4.3.4B-C). Together with the RNAi results, these results

demonstrate that decreased Ank2 levels do not significantly alter the AIS to the extent that

overexpression of Ank2-L4 does.

	CyO offspring	Non-CyO offspring
ELAV-Gal4/CyO ♀ X UAS-Ank2-RNAi ♂	140	62
ELAV-Gal4/CyO ♀ X UAS-VENUS-Ank2-L4 ♂	122	130

Table 4.3.1. Reduction of Ank2 levels in all neurons results in lethality.
Genetic tests were completed to assess viability upon expression of Ank2-RNAi or Ank2-L4.
ELAV/CyO virgins were crossed with males expressing either UAS-Ank2-RNAi or UAS-
VENUS-Ank2-L4. The resultant offspring were collected, and the ratio of CyO to non-CyO
offspring was tallied. The ratios suggest that pan-neuronal knockdown of Ank2 leads to
lethality, whereas pan-neuronal overexpression of Ank2-L4 does not.

Next, we tested if decreasing Ank2 levels could alter the AIS phenotype resulting from

Ank2-L4 overexpression. We combined Ank2-L4 with Ank2-RNAi or with various Ank2

mutants and then assessed the size of the AIS. The shortened AIS observed in MB neurons

expressing Ank2-L4 was not affected by either context of Ank2 reduction (Figure 4.3.5A-B).

The failure of Ank2 reduction to induce an AIS phenotype or to alter the shortened AIS resulting

from Ank2-L4 suggests that Ank2-L4 is neither acting as a gain of function or a loss of function.

Indeed, if Ank2-L4 was acting as a dominant negative, one would expect it to cause lethality

when expressed in all neurons, as was seen in Ank2-null mutants and with pan-neuronal

expression of UAS-Ank2-RNAi. An equal number of CyO and non-CyO offspring were

observed after crossing ELAV-Gal4/CyO with UAS-VENUS-Ank2-L4, indicating that pan-

neuronal Ank2-L4 expression does not induce larval or pupal lethality (Table 4.3.1; p=0.722).

Taken together, these data suggest that Ank2 does not strongly regulate the size of the MB AIS,

at least during development, and that the observed effects resulting from Ank2-L4

overexpression are likely a neomorphic effect.

UAS-VENUS-Ank2-L4 /
UAS-Ank2-RNAi

UAS-VENUS-Ank2-L4 /
Ank2[2001]
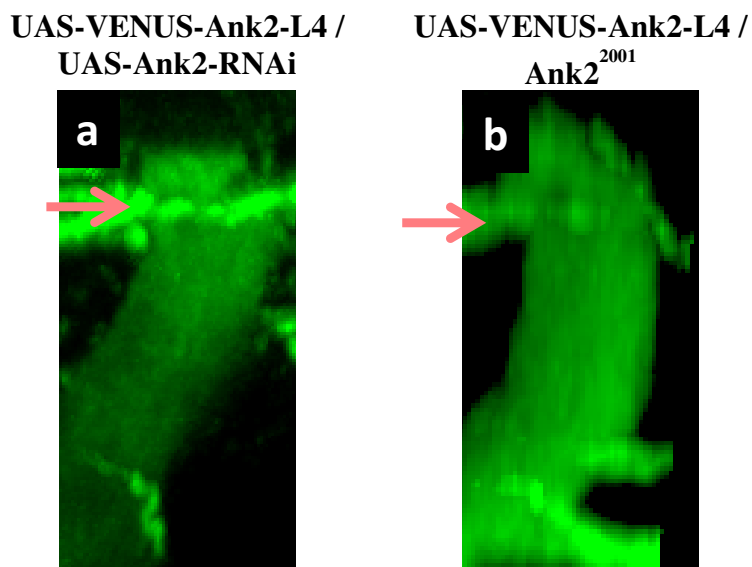
Figure 4.3.5. Reduction of Ank2 levels fail to modify Ank2-L4-induced shortening of the AIS.
Brains from third-instar larva with MB-specific overexpression of UAS-VENUS-Ank2-L4 in combination with **(A)** UAS-Ank2-RNAi or **(B)** the Ank2[2001] allele are stained with anti-FasII. In each panel, the pink arrow indicates a stereotypical nerve that crosses over in front of the MB peduncle. The robust shortening of the AIS resulting from Ank2-L4 overexpression is not altered by RNAi-mediated- or genetic reduction of Ank2-L levels.

Ank2-L4 and p35 regulate the AIS through independent pathways

Ank2-L4 and p35 both alter the size of the AIS, so we investigated whether they do so through common or parallel pathways. We have demonstrated that expression of UAS-p35 in MB neurons extends the AIS, while UAS-Ank2-L4 shortens the AIS. If Ank2-L4 and p35 are epistatic, with one acting downstream of the other, then expressing both constructs would result in an AIS phenotype that mimicked either of the constructs alone. However, Fas2 staining revealed that co-expressing UAS-p35 and UAS-VENUS-Ank2-L4 yields an intermediate phenotype, as these flies exhibit a normal-sized AIS (Figure 4.3.6B). The lack of suppression of phenotypes demonstrates that Ank2-L4 and p35 are not epistatic, and indicates that Ank2-L4 and p35 act independently through parallel pathways to modulate the AIS.
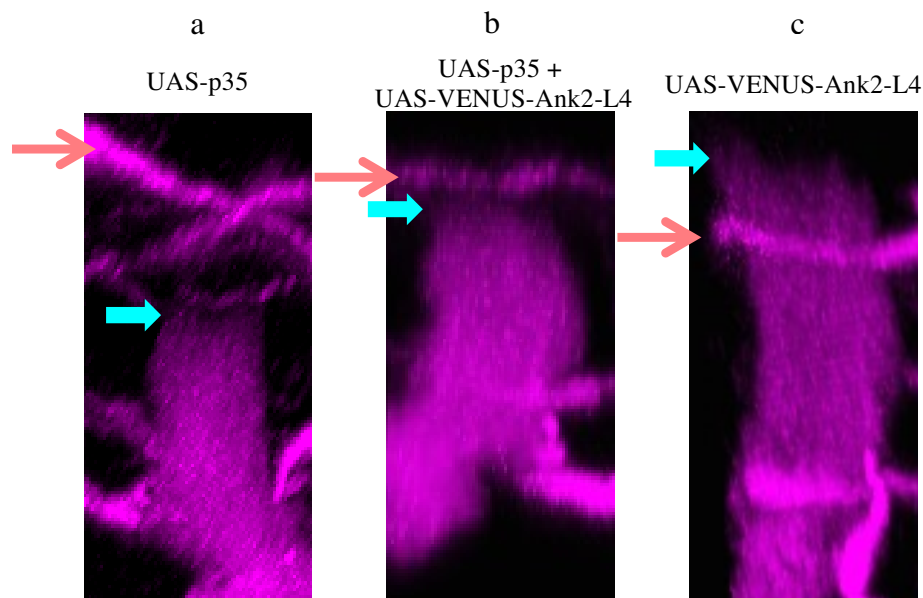
Figure 4.3.6. p35 and Ank2-L4 modify the AIS through independent pathways.
Third-instar larva brains are stained with anti-FasII. The pink arrow indicates a stereotypical nerve that crosses over in front of the MB peduncle. This nerve is used as a landmark to gauge changes in the AIS size. The blue arrows indicate the proximal boundary of the FasII staining. (**A**) FasII staining in flies overexpressing p35 stops below the crossover nerve. In (**B**), flies overexpressing both UAS-p35 and UAS-VENUS-Ank2-L4 exhibit FasII staining that is indistinguishable from wild-type controls. In (**C**), flies overexpressing UAS-VENUS-Ank2-L4 alone show FasII staining that extends above the landmark crossover nerve.

Reduction of Ank2 fails to restore the shortened AIS phenotype in p35-null flies

Next, we sought to test if reducing Ank2 levels could restore or modify the AIS in p35-null flies, even if Ank2 was dispensable for AIS regulation under normal conditions. Using the same MB-specific Gal4 driver (201Y-Gal4), we expressed Ank2-RNAi in p35-null animals. Labeling the AIS with FasII revealed a shortened AIS similar to loss of p35 alone, indicating that the knockdown of Ank2 had no effect on the p35 phenotype. (Figure 4.3.7).

DfC2, 201Y/p3520C; UAS-Ank2-RNAi
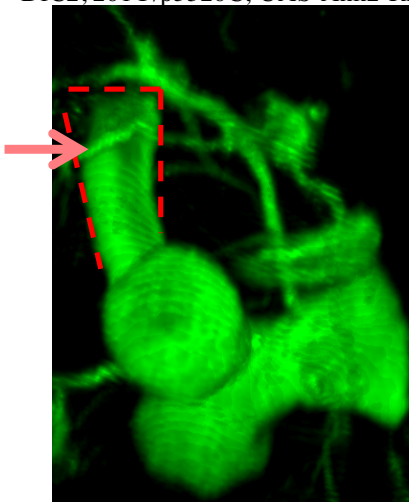
Figure 4.3.7. Ank2-RNAi does not alter the shortened AIS resulting from loss of p35.
Third-instar larva brains are stained with anti-FasII. The boundaries of the FasII staining in the MB peduncle are outlined by the red-dashed line. The pink arrow indicates a stereotypical nerve that crosses over in front of the MB peduncle. This nerve is used as a landmark to gauge changes in the AIS size. Expressing UAS-Ank2-RNAi in a p35-null background does not result in any noticeable alterations to the AIS, relative to deletion of p35 alone.

Shortening of the AIS is sufficient for neurodegeneration

Perturbation of the AIS has been linked to neurodegeneration under a variety of contexts (Li, Kumar et al. 2011, Sun, Wu et al. 2014, Chand, Galliano et al. 2015, del Puerto, Fronzaroli-Molinieres et al. 2015, Sohn, Tracy et al. 2016). We have shown that deletion of p35 leads to a shortening of the AIS in MB neurons and accumulation of axonal swellings in the vicinity of the absent AIS, as well as enhanced loss of MB neurons (Figure 4.3.1B; Figure 3.3.1B). As such,

we hypothesized that aberrant modulation of the AIS could directly lead to neurodegeneration in *Drosophila*. We aged flies co-expressing UAS-VENUS-Ank2-L4 (Ank2-L4) and UAS-nls-mCherry in MB neurons. Additionally, we analyzed flies expressing a cytosolic GFP (UAS-GFP) in place of Ank2-L4. Control flies expressing UAS-nls-mCherry alone showed relatively consistent levels of 201Y-positive MB neurons from Day 3 to Day 30 before declining at Day 45 (Figure 4.3.8). Flies co-expressing UAS-nls-mCherry with UAS-GFP exhibited lower numbers of MB neurons at all time points, although these decreases were not significantly different from the three-day old controls until Day 45. Expression of Ank2-L4 resulted in significant loss of MB neurons by Day 30, and an even further reduction at Day 45. Thus, shortening of the axon initial segment results in accelerated neurodegeneration.
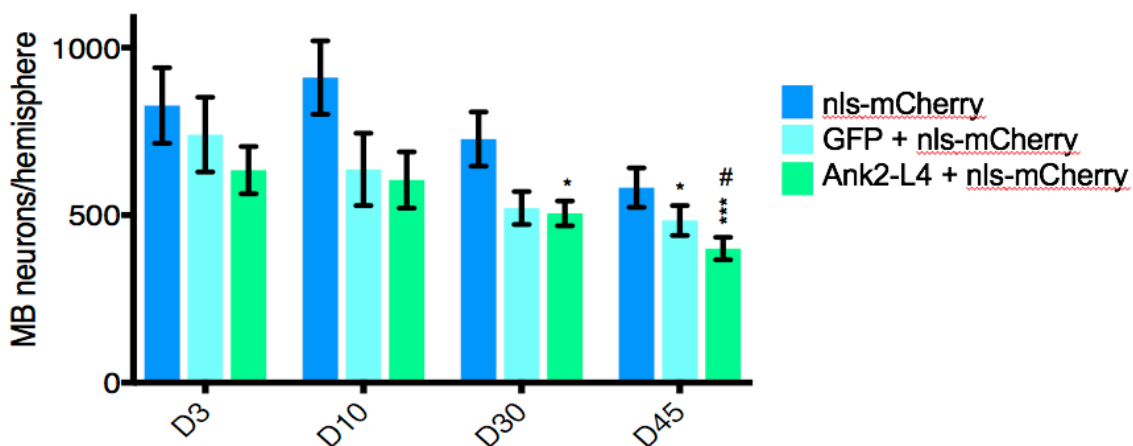
Figure 4.3.8. Ank2-L4 overexpression results in accelerated loss of MB neurons. Overexpression of Ank2-L4 lead to progressive loss of MB neurons. The number of 201Y>nls-mCherry positive MB neurons per hemisphere is presented as mean±SEM. Flies overexpressing Ank2-L4 show a significant reduction in MB cell number at Day 30, with a further reduction at Day 45. Flies expressing cytosolic GFP in place of Ank2-L4 show a significant decrease only at Day 45. Significant differences were assessed by two-way ANOVA; differences labeled with asterisks (*) are relative to the Day 3 UAS-nls-mCherry alone control; differences marked with "#" are relative to the Day 3 sample co-expressing UAS-GFP and UAS-nls-mCherry. *p<0.05; ***p<0.001; #p<0.05.

4.4 Discussion

Here we have identified a novel regulator of the axon initial segment in *Drosophila* central brain neurons. We show that overexpression of the C-terminal portion of the Ank2-L isoform drastically shortens the AIS in MB neurons, and that this modulation of the AIS occurs through a pathway that is parallel to p35-mediated regulation of the AIS. We also provide evidence that disruption of the AIS is sufficient to induce neurodegeneration.

Based on structural similarities and the presence of a giant exon, *Drosophila* Ank2 was proposed to be the ortholog of the mammalian AnkG. Our results here suggest that *Drosophila* Ank2 is not the master organizer of the AIS; however, we do see evidence that Ank2 at least plays a role. In mammals, deletion of AnkG results in the complete loss of the AIS; consistent with this, we observe a partial shortening of the AIS when we reduce Ank2 levels, either through RNAi or genetically with mutants. However, we fail to see the complete absence of the AIS by reduced Ank2 levels, even when those levels are decreased enough to cause lethality. This discrepancy could stem from the differing sets of ankyrin genes between flies and mammals. *Drosophila* only have two identified ankyrins while mammals carry three ankyrin genes. As mammals have an expanded ankyrin repertoire with more specialized functions for each gene, the loss of one completely ablates the associated function. In *Drosophila,* the neuron-specific Ank2 is accompanied by Ank1, which is enriched at the AIS. It is possible that deletion of Ank2 disrupts the AIS to a certain degree, but there is compensation by Ank1, preventing the complete dissolution of the AIS. Interplay between multiple ankyrins at the AIS has been shown in mammals, as overexpression of AnkB in cultured hippocampal neurons resulted in a more restricted distribution of AnkG at the AIS (Galiano, Jha et al. 2012). Another possibility is that Ank1 plays a significant role in the organization of the *Drosophila* AIS. However, Ank1 lacks

the giant exons common to mammalian AnkG, so if it were to be the sole organizer of the AIS, it would likely do so through novel mechanisms. Experiments utilizing MB-specific RNAi to decrease Ank1 levels will reveal the specific contributions of Ank1 in establishment and maintenance of the AIS. Furthermore, it will be interesting to see if Ank1 is altered in MB neurons when Ank2-L levels are perturbed or Ank2-L4 is overexpressed.

Unlike reduction of Ank2 levels, overexpression of Ank2-L4 in MB neurons drastically shortened the axon initial segment, as measured with various AIS markers. This was unexpected, as overexpression of AnkG in cultured hippocampal neurons nearly tripled the length of the AIS (Galiano, Jha et al. 2012). Independent experiments reducing levels of endogenous Ank2 failed to match the severity of Ank2-L4 overexpression despite being sufficient to induce lethality, suggesting that Ank2-L4 likely does not shorten the AIS by acting as a dominant negative. Conversely, expressing Ank2-RNAi with Ank2-L4 fails to rescue the AIS phenotype observed when Ank2-L4 is expressed alone, suggesting that Ank2-L4 also does not act as a gain-of-function. Therefore, we have concluded that Ank2-L4-mediated shortening of the axon initial segment is a neomorphic effect. It has been previously demonstrated that the C-terminal domain of Ank2 also exhibits neomorphic activity during neuromuscular junction (NMJ) development, as expression of Ank2-L8 in presynaptic neurons at the NMJ results in the formation of small, highly ramified satellite boutons at the synapse (Pielage, Cheng et al. 2008).

In motoneurons at the *Drosophila* neuromuscular junction, Ank2-L was localized to the axon and pre-synaptic terminal at the NMJ (Pielage, Cheng et al. 2008). Both Ank2-L4 and Ank2-L8 also trafficked to the presynaptic nerve terminal in motoneurons, indicating that the C-terminal domain of Ank2 is sufficient for this localization. As the Ank2-S domain remained restricted to the cell body, it was concluded that the C-terminal region is also necessary for nerve

terminal targeting. However, Ank2-L4 exhibited different expression patterns in multiple

neuronal subtypes. In ddaE neurons, Ank2-L4 was accumulated in the proximal axon and

regulated the diffusion barrier, while Ank2-S appeared ubiquitously throughout the entire neuron

(Jegla, Nguyen et al. 2016). In our hands, neither Ank2-S, Ank2-L4, or Ank2-L8 showed any

specific localization within MB gamma neurons, as expression was observed in the cell bodies,

dendrites, and axonal lobes. Thus, it is apparent that different neuronal subtypes utilize different

targeting paradigms. Interactions with specific sets of proteins or specific isoforms could result

in altered localizations between neurons. The N-terminal domain of Ank2 contains 24 ankyrin

repeats, a membrane-binding domain, and a spectrin-binding domain, while the C-terminal

region can interact with microtubules (Bennett and Baines 2001, Pielage, Cheng et al. 2008). As

Ank2-L4 lacks the membrane- and spectrin-binding domains, its localization is likely driven by

interactions with microtubules. Indeed, expressing Ank2-L4 in *Drosophila* S2 cells severely

perturbed the microtubule cytoskeleton, generating spike-like processes innervated by bundles of

microtubules (Pielage, Cheng et al. 2008). Similar perturbation of the underlying microtubule

cytoskeleton could be the mechanism through which Ank2-L4 shortens the AIS. Alternatively,

Ank2-L4 could also interface with microtubule-binding proteins. End-binding (EB) protein EB3

accumulates at the AIS of cultured rat hippocampal neurons, and directly binds to AnkG

(Leterrier, Vacher et al. 2011). shRNA-mediated reduction of EB3, and of EB1, resulted in

decreased AnkG levels at the AIS.

Perturbation of the AIS has been implicated in neurodegenerative diseases; we show here

that direct shortening of the AIS may be sufficient to induce neurodegeneration. Overexpression

of Ank2-L4 induces accelerated loss of MB neurons, as flies carrying the construct showed

significant reductions in MB cell number at 30 days, well before control samples. While

expression of cytosolic GFP in place of Ank2-L4 did result in enhanced neurodegeneration

relative to controls only expressing a nuclear label, the effects were not as severe as those

observed with Ank2-L4. One possibility is that expression of fluorescent proteins causes

photocytotoxicity; indeed, multiple studies have demonstrated GFP toxicity (Liu, Jan et al. 1999,

Ansari, Ahmed et al. 2016). Ongoing experiments will address this by aging control flies and

flies overexpressing Ank2-L4 in total darkness to prevent excitation of the fluorescent proteins.

Alternatively, the increased protein levels from Gal4-driven expression could induce

proteotoxicity and contribute to degeneration. Regardless, Ank2-L4 caused greater cell loss than

was seen in either control, suggesting that at least some of the observed neurodegeneration stems

from shortening of the AIS. This neurodegeneration is also likely a direct result of the AIS

modulation, and not due to any non-specific detrimental effects on neuronal morphology or

physiology. Expression of neither Ank2-L4 nor Ank2-L8, which had a more severe effect on the

AIS, significantly altered the gross morphological structure of the MB neurons, indicating that

any phenotypes are largely restricted to subcellular domains. Furthermore, using the same AIS

markers, we were unable to identify an AIS in dopaminergic (DA) neurons, and expressing the

same Ank2-L4 construct in DA neurons did not result in accelerated neuronal loss (Arvind

Shukla, personal communication). Potentially, only neurons with an AIS are susceptible to

Ank2-L4-induced ND. It is worth noting that even with the apparent loss of the AIS, Futsch

remained restricted to the somatodendritic region when Ank2-L4 was overexpressed. Thus, it is

likely that the observed ND stems from alterations in neuronal excitability or axon structural

integrity rather than disruption of polarity.

Cdk5 activity has been extensively linked to the AIS in both mammals and *Drosophila*.

Further, a common link among many neurodegenerative diseases is the aberrant activation of

Cdk5. In flies, upregulation of Cdk5/p35 activity has been found to elongate the AIS (Figure 4.3.1; (Trunova, Baek et al. 2011)). It is possible that perturbation of AIS size and/or function contributes to disease progression. Therefore, any mechanism that could restore the AIS could potentially alleviate detrimental aspects of these diseases. Because Ank2-L4 modulates the AIS independently of Cdk5/p35, it may be capable of restoring the AIS to its normal size in contexts of Cdk5 hyperactivity. Furthermore, the fact that Ank2-L4 seems to target the AIS specifically, without obvious non-specific effects, make it a plausible therapeutic agent.

Using a novel reagent, we have unlocked a new method for modulating the AIS independent of the only known AIS regulator in *Drosophila* MB neurons, and shown that this modulation is sufficient to induce neurodegeneration. By expanding the toolbox, we have made it easier to investigate the underlying mechanisms establishing and maintaining the AIS. In the MB neurons, Ank2-L does not appear to be functionally homologous to the mammalian master organizer AnkG; thus, researching AIS regulation in *Drosophila* could reveal mechanisms that have previously been overlooked. Future investigations of these mechanisms, and of interactions between the involved proteins, will likely lead to the development of new therapeutic strategies for diseases stemming from AIS dysfunction, including Angelman syndrome and epilepsy, diseases related to altered Cdk5 activity, neuronal injuries caused by ischemic stroke, or even age-dependent loss of cognition.

Chapter 5

Concluding Remarks and Future Directions

Chapter 5. Concluding Remarks and Future Directions

Cdk5 plays significant roles in neurodevelopment, neuronal homeostasis, and neurotransmission. Given the importance of Cdk5, it is not surprising that its dysfunction has been linked to multiple neurodegenerative diseases. Despite, or perhaps because of, the wide range of established and putative functions of Cdk5, however, the mechanisms underlying Cdk5-mediated neurodegeneration remain opaque. Through the study of Cdk5 in a simpler biological model, we can gain an appreciation of physiologically relevant functions that contribute to neurodegeneration.

Work in this thesis characterized the effects of Cdk5 gain and loss of function at the organismal, cellular, and molecular levels. In both cases, we have observed severe declines in motor function and lifespan, accompanied by robust loss of central brain neurons, impairment of autophagy, and increased susceptibility to oxidative stress. At the gene expression level, young presymptomatic animals with deletion or hyperactivation of Cdk5 activity both exhibited transcriptional changes consistent with chronologically older control flies. Indeed, construction of a linear model based on the expression data revealed significantly elevated physiological ages of the p35-null and p35-OE samples. Provided the precocious effects on the transcriptome, we propose that Cdk5 dysfunction accelerates the intrinsic rate of aging, and that this serves as one mechanism for the observed neurodegeneration.

Separately, we demonstrate that loss of Cdk5 function results in shortening of the axon initial segment, and that this phenotype is mimicked by overexpression of Ank2-L4 through a Cdk5-independent mechanism. Subsequently, we show that shortening of the AIS is sufficient to induce neurodegeneration, as Ank2-L4 overexpression caused enhanced MB cell loss relative to controls. Combining multiple experiments discussed throughout this thesis, we see that aging

139

alone results in a low level of neurodegeneration within the MBs, and that Ank2-L4 overexpression causes degeneration, but absence of Cdk5 activity causes more robust neurodegeneration. Put simply, aging and cell-intrinsic insult alone can result in neurodegeneration, but neither is sufficient to reach the severity of ND observed in p35-null mutants. Further, our lab previously demonstrated that p35-null flies only exhibited localized vacuolization, rather than degeneration throughout the entire brain (Trunova and Giniger 2012), suggesting that some neurons are more susceptible than others. Collectively, these findings support the hypothesis that synergy between aging and neuronal insults exacerbates neurodegeneration in flies lacking Cdk5 activity.

It is notable that transcriptomic changes and elevated physiological age were evidenced in both head and thorax tissue. As Cdk5 activity has only been demonstrated in neuronal tissue of *Drosophila*, this suggests that the systemic effects are secondary to neuronal dysfunction; systemic effects resulting from neuron-specific perturbations has been demonstrated previously (Bahadorani, Cho et al. 2010, Kumimoto, Fore et al. 2013). Our data are consistent with several mechanisms by which this may occur. Cdk5-mediated neuronal dysfunction could disrupt neuroendocrine secretion, either directly or through defects in relevant neural circuits. It is well established that the aging program is regulated by insulin-like peptides in *Drosophila*, as well as other systems. *Drosophila* Insulin-like Protein 2 (DILP-2), DILP-3, and DILP-5 showed altered expression in the p35-OE head samples. In p35-null head samples, DILPs 3 and 5 were significantly altered, while DILP2 exhibited changes just below our 1.5 magnitude fold change cutoff. Alternatively, dysregulation of Cdk5 could induce an inflammation-like response, which could then spread systemically. Our gene ontology results revealed that affected genes from both mutant contexts showed significant enrichment of immunity-related processes, in both head

and thorax tissue. To discern if specific neuronal subpopulations are driving the effect, or if it is the result of general neuronal dysfunction, it will be necessary to alter Cdk5 in individual populations. Conditional deletion or overexpression of p35 will reveal if there are any regions where expression of p35 is sufficient to recapitulate the observed systemic effects or any of the other degenerative phenotypes. Further, conditional mutants will permit us to rule out the hypothesis that adult-onset neurodegeneration is a delayed manifestation of developmental defects.

Now that we have demonstrated that Cdk5 dysfunction accelerates the intrinsic rate of aging, the next step is to delineate the mechanisms responsible. Future experiments will focus on determining if the observed gene expression changes stem directly from Cdk5 activity on transcription factors, are secondary effects of altered neuronal physiology, or more likely, a combination of both. To date, only a handful of studies have identified physiologically relevant modification of transcription factor activity by Cdk5. In mice, Cdk5 phosphorylates FOXO3a, leading to elevated FOXO3a levels and nuclear translocation (Shi, Viccaro et al. 2016). FOXO3a initially upregulates MnSOD, protecting neurons from oxidative stress. However, prolonged FOXO3a activation eventually led to increased expression of Bim and FasL, and ultimately neuronal death. Cdk5 has also been linked to STAT3 (Fu, Fu et al. 2004) and MEF2 (Gong, Tang et al. 2003), each of which could also contribute to Cdk5-mediated transcriptomic effects. A subset of the observed expression changes is consistent with studies characterizing physiological perturbations, such as oxidative stress and impaired autophagy (Zou, Meadows et al. 2000) (Landis, Abdueva et al. 2004, Érdi, Nagy et al. 2012), suggesting that a portion of the altered transcriptome arises from secondary effects of Cdk5 dysfunction. Analyzing gene

expression at earlier time points will highlight the progression of changes in the profile and could pinpoint targets involved in the initiation of the degenerative processes.

A separate method for elucidating the pathways underpinning Cdk5-mediated neurodegeneration is to identify the physiologically relevant substrates of Cdk5. Examining the phosphoproteomes of p35-null and p35-OE flies and comparing them to an age-matched control phosphoproteome will reveal differentially phosphorylated proteins. Screening of the sequences of these proteins for the Cdk5 target motif will suggest direct targets, which can then be biochemically validated and genetically tested. One such substrate that has a well-documented interplay with Cdk5 is GSK3β. These two proteins are known to phosphorylate one another, resulting in inhibition of the target. Additional experiments are underway to test whether aberrant GSK3β activity can recapitulate any of the observed degenerative phenotypes, and if double mutants reveal any signs of rescue or exacerbation.

Experiments described here reveal that Cdk5 is capable of regulating a number of aging-related processes, highlighting multiple pathways that are perturbed by Cdk5 dysfunction, and that could serve as potential therapeutic targets in diseases linked to altered Cdk5 activity. Further, our data show that perturbation of these processes precedes robust neurodegeneration and the onset of various degenerative phenotypes. These findings upset the current view that aging causes degeneration by outlining a degenerative mechanism through which neuronal dysfunction itself can drive acceleration of aging. Therapeutic advances for treating aging-related and neurodegenerative diseases will hinge on our full understanding of this relationship, and the role of kinase regulation.

References

Anderton, B. H., J. Betts, W. P. Blackstock, J. P. Brion, S. Chapman, J. Connell, R. Dayanandan, J. M. Gallo, G. Gibb, D. P. Hanger, M. Hutton, E. Kardalinou, K. Leroy, S. Lovestone, T. Mack, C. H. Reynolds and M. Van Slegtenhorst (2001). "Sites of phosphorylation in tau and factors affecting their regulation." Biochem Soc Symp(67): 73-80.

Abeliovich, A., Y. Schmitz, I. Farinas, D. Choi-Lundberg, W. H. Ho, P. E. Castillo, N. Shinsky, J. M. Verdugo, M. Armanini, A. Ryan, M. Hynes, H. Phillips, D. Sulzer and A. Rosenthal (2000). "Mice lacking alpha-synuclein display functional deficits in the nigrostriatal dopamine system." Neuron 25(1): 239-252.

Amor, S., F. Puentes, D. Baker and P. van der Valk (2010). "Inflammation in neurodegenerative diseases." Immunology 129(2): 154-169.

Angevine, J. B., Jr. and R. L. Sidman (1961). "Autoradiographic study of cell migration during histogenesis of cerebral cortex in the mouse." Nature 192: 766-768.

Ansari, A. M., A. K. Ahmed, A. E. Matsangos, F. Lay, L. J. Born, G. Marti, J. W. Harmon and Z. Sun (2016). "Cellular GFP Toxicity and Immunogenicity: Potential Confounders in in Vivo Cell Tracking Experiments." Stem Cell Reviews and Reports 12(5): 553-559.

Asada, A., N. Yamamoto, M. Gohda, T. Saito, N. Hayashi and S.-i. Hisanaga (2008). "Myristoylation of p39 and p35 is a determinant of cytoplasmic or nuclear localization of active cycline-dependent kinase 5 complexes." Journal of Neurochemistry 106(3): 1325-1336.

Aso, Y., K. Grübel, S. Busch, A. B. Friedrich, I. Siwanowicz and H. Tanimoto (2009). "The Mushroom Body of Adult Drosophila Characterized by GAL4 Drivers." Journal of Neurogenetics 23(1-2): 156-172.

Avraham, E., R. Rott, E. Liani, R. Szargel and S. Engelender (2007). "Phosphorylation of Parkin by the Cyclin-dependent Kinase 5 at the Linker Region Modulates Its Ubiquitin-Ligase Activity and Aggregation." Journal of Biological Chemistry 282(17): 12842-12850.

Baas, P. W., J. S. Deitch, M. M. Black and G. A. Banker (1988). "Polarity orientation of microtubules in hippocampal neurons: uniformity in the axon and nonuniformity in the dendrite." Proc Natl Acad Sci U S A 85(21): 8335-8339.

Bahadorani, S., J. Cho, T. Lo, H. Contreras, H. O. Lawal, D. E. Krantz, T. J. Bradley and D. W. Walker (2010). "Neuronal expression of a single-subunit yeast NADH-ubiquinone oxidoreductase (Ndi1) extends Drosophila lifespan." Aging Cell 9(2): 191-202.

Balaban, R. S., S. Nemoto and T. Finkel (2005). "Mitochondria, oxidants, and aging." Cell 120(4): 483-495.

Barber, S. C. and P. J. Shaw (2010). "Oxidative stress in ALS: Key role in motor neuron injury and therapeutic target." Free Radical Biology and Medicine 48(5): 629-641.

Beaudette, K. N., J. Lew and J. H. Wang (1993). "Substrate specificity characterization of a cdc2-like protein kinase purified from bovine brain." J Biol Chem **268**(28): 20825-20830.

Bender, A., K. J. Krishnan, C. M. Morris, G. A. Taylor, A. K. Reeve, R. H. Perry, E. Jaros, J. S. Hersheson, J. Betts, T. Klopstock, R. W. Taylor and D. M. Turnbull (2006). "High levels of mitochondrial DNA deletions in substantia nigra neurons in aging and Parkinson disease." Nature Genetics **38**(5): 515-517.

Bendor, Jacob T., Todd P. Logan and Robert H. Edwards (2013). "The Function of α-Synuclein." Neuron **79**(6): 1044-1066.

Bennett, V. and A. J. Baines (2001). "Spectrin and ankyrin-based pathways: metazoan inventions for integrating cells into tissues." Physiol Rev **81**(3): 1353-1392.

Benzer, S. (1967). "BEHAVIORAL MUTANTS OF Drosophila ISOLATED BY COUNTERCURRENT DISTRIBUTION." Proc Natl Acad Sci U S A **58**(3): 1112-1119.

Bibb, J. A., G. L. Snyder, A. Nishi, Z. Yan, L. Meijer, A. A. Fienberg, L. H. Tsai, Y. T. Kwon, J. A. Girault, A. J. Czernik, R. L. Huganir, H. C. Hemmings, Jr., A. C. Nairn and P. Greengard (1999). "Phosphorylation of DARPP-32 by Cdk5 modulates dopamine signalling in neurons." Nature **402**(6762): 669-671.

Birben, E., U. M. Sahiner, C. Sackesen, S. Erzurum and O. Kalayci (2012). "Oxidative stress and antioxidant defense." World Allergy Organ J **5**(1): 9-19.

Blasco, M. A. (2007). "Telomere length, stem cells and aging." Nat Chem Biol **3**(10): 640-649.

Bloom, G. S. (2014). "Amyloid-beta and tau: the trigger and bullet in Alzheimer disease pathogenesis." JAMA Neurol **71**(4): 505-508.

Borthwick, G. M., M. A. Johnson, P. G. Ince, P. J. Shaw and D. M. Turnbull (1999). "Mitochondrial enzyme activity in amyotrophic lateral sclerosis: implications for the role of mitochondria in neuronal cell death." Ann Neurol **46**(5): 787-790.

Bouley, M., M. Z. Tian, K. Paisley, Y. C. Shen, J. D. Malhotra and M. Hortsch (2000). "The L1-type cell adhesion molecule neuroglian influences the stability of neural ankyrin in the Drosophila embryo but not its axonal localization." J Neurosci **20**(12): 4515-4523.

Brechet, A., M. P. Fache, A. Brachet, G. Ferracci, A. Baude, M. Irondelle, S. Pereira, C. Leterrier and B. Dargent (2008). "Protein kinase CK2 contributes to the organization of sodium channels in axonal membranes by regulating their interactions with ankyrin G." J Cell Biol **183**(6): 1101-1114.

Brinkkoetter, P. T., J. S. Wu, T. Ohse, R. D. Krofft, B. Schermer, T. Benzing, J. W. Pippin and S. J. Shankland (2010). "p35, the non-cyclin activator of Cdk5, protects podocytes against apoptosis in vitro and in vivo." Kidney international **77**(8): 690-699.

Brinkkoetter, P. T., P. Olivier, J. S. Wu, S. Henderson, R. D. Krofft, J. W. Pippin, D. Hockenbery, J. M. Roberts and S. J. Shankland (2009). "Cyclin I activates Cdk5 and regulates expression of Bcl-2 and Bcl-XL in postmitotic mouse cells." Journal of Clinical Investigation **119**(10): 3089-3101.

Brion, J. P. and A. M. Couck (1995). "Cortical and brainstem-type Lewy bodies are immunoreactive for the cyclin-dependent kinase 5." Am J Pathol **147**(5): 1465-1476.

Brochard, V., B. Combadiere, A. Prigent, Y. Laouar, A. Perrin, V. Beray-Berthat, O. Bonduelle, D. Alvarez-Fischer, J. Callebert, J. M. Launay, C. Duyckaerts, R. A. Flavell, E. C. Hirsch and S. Hunot (2009). "Infiltration of CD4+ lymphocytes into the brain contributes to neurodegeneration in a mouse model of Parkinson disease." J Clin Invest **119**(1): 182-192.

Brown, D. A. and P. R. Adams (1980). "Muscarinic suppression of a novel voltage-sensitive K+ current in a vertebrate neurone." Nature **283**(5748): 673-676.

Bruijn, L. I., M. K. Houseweart, S. Kato, K. L. Anderson, S. D. Anderson, E. Ohama, A. G. Reaume, R. W. Scott and D. W. Cleveland (1998). "Aggregation and motor neuron toxicity of an ALS-linked SOD1 mutant independent from wild-type SOD1." Science **281**(5384): 1851-1854.

Cabin, D. E., K. Shimazu, D. Murphy, N. B. Cole, W. Gottschalk, K. L. McIlwain, B. Orrison, A. Chen, C. E. Ellis, R. Paylor, B. Lu and R. L. Nussbaum (2002). "Synaptic vesicle depletion correlates with attenuated synaptic responses to prolonged repetitive stimulation in mice lacking alpha-synuclein." J Neurosci **22**(20): 8797-8807.

Casley, C. S., L. Canevari, J. M. Land, J. B. Clark and M. A. Sharpe (2002). "β-Amyloid inhibits integrated mitochondrial respiration and key enzyme activities." Journal of neurochemistry **80**(1): 91-100.

Celsi, F., P. Pizzo, M. Brini, S. Leo, C. Fotino, P. Pinton and R. Rizzuto (2009). "Mitochondria, calcium and cell death: A deadly triad in neurodegeneration." Biochimica et Biophysica Acta (BBA) - Bioenergetics **1787**(5): 335-344.

Chae, T., Y. T. Kwon, R. Bronson, P. Dikkes, E. Li and L.-H. Tsai (1997). "Mice lacking p35, a neuronal specific activator of Cdk5, display cortical lamination defects, seizures, and adult lethality." Neuron **18**(1): 29-42.

Chand, A. N., E. Galliano, R. A. Chesters and M. S. Grubb (2015). "A Distinct Subtype of Dopaminergic Interneuron Displays Inverted Structural Plasticity at the Axon Initial Segment." Journal of Neuroscience **35**(4): 1573-1590.

Chen, C. and W. G. Regehr (2000). "Developmental remodeling of the retinogeniculate synapse." Neuron **28**(3): 955-966.

Chen, F., Q. Wang, X. Wang and G. P. Studzinski (2004). "Up-regulation of Egr1 by 1,25-dihydroxyvitamin D3 contributes to increased expression of p35 activator of cyclin-

dependent kinase 5 and consequent onset of the terminal phase of HL60 cell differentiation." <u>Cancer Res</u> **64**(15): 5425-5433.

Chergui, K., P. Svenningsson and P. Greengard (2004). "Cyclin-dependent kinase 5 regulates dopaminergic and glutamatergic transmission in the striatum." <u>Proceedings of the National Academy of Sciences</u> **101**(7): 2191-2196.

Cheung, Z. H., W. H. Chin, Y. Chen, Y. P. Ng and N. Y. Ip (2007). "Cdk5 is involved in BDNF-stimulated dendritic growth in hippocampal neurons." <u>PLoS Biol</u> **5**(4): e63.

Chevalier-Larsen, E. and E. L. F. Holzbaur (2006). "Axonal transport and neurodegenerative disease." <u>Biochimica et Biophysica Acta (BBA) - Molecular Basis of Disease</u> **1762**(11-12): 1094-1108.

Chintapalli, V. R., J. Wang and J. A. Dow (2007). "Using FlyAtlas to identify better Drosophila melanogaster models of human disease." <u>Nat Genet</u> **39**(6): 715-720.

Chiti, F., M. Stefani, N. Taddei, G. Ramponi and C. M. Dobson (2003). "Rationalization of the effects of mutations on peptide and protein aggregation rates." <u>Nature</u> **424**(6950): 805-808.

Chow, H.-m. and K. Herrup (2015). "Genomic integrity and the ageing brain." <u>Nature Reviews Neuroscience</u> **16**(11): 672-684.

Christensen, D. Z., M. Huettenrauch, M. Mitkovski, L. Pradier and O. Wirths (2014). "Axonal degeneration in an Alzheimer mouse model is PS1 gene dose dependent and linked to intraneuronal Abeta accumulation." <u>Front Aging Neurosci</u> **6**: 139.

Chu, Y., G. A. Morfini, L. B. Langhamer, Y. He, S. T. Brady and J. H. Kordower (2012). "Alterations in axonal transport motor proteins in sporadic and experimental Parkinson's disease." <u>Brain</u> **135**(7): 2058-2073.

Chung, C. Y., J. B. Koprich, H. Siddiqi and O. Isacson (2009). "Dynamic changes in presynaptic and axonal transport proteins combined with striatal neuroinflammation precede dopaminergic neuronal loss in a rat model of AAV alpha-synucleinopathy." <u>J Neurosci</u> **29**(11): 3365-3373.

Colledge, M., E. M. Snyder, R. A. Crozier, J. A. Soderling, Y. Jin, L. K. Langeberg, H. Lu, M. F. Bear and J. D. Scott (2003). "Ubiquitination regulates PSD-95 degradation and AMPA receptor surface expression." <u>Neuron</u> **40**(3): 595-607.

Connell-Crowley, L., D. Vo, L. Luke and E. Giniger (2007). "Drosophila lacking the Cdk5 activator, p35, display defective axon guidance, age-dependent behavioral deficits and reduced lifespan." <u>Mechanisms of Development</u> **124**(5): 341-349.

Connell-Crowley, L., M. Le Gall, D. J. Vo and E. Giniger (2000). "The cyclin-dependent kinase Cdk5 controls multiple aspects of axon patterning in vivo." <u>Current Biology</u> **10**(10): 599-603.

Contreras-Vallejos, E., E. Utreras and C. Gonzalez-Billault (2012). "Going out of the brain: Non-nervous system physiological and pathological functions of Cdk5." Cellular Signalling **24**(1): 44-52.

Coskun, P. E., M. F. Beal and D. C. Wallace (2004). "Alzheimer's brains harbor somatic mtDNA control-region mutations that suppress mitochondrial transcription and replication." Proceedings of the National Academy of Sciences of the United States of America **101**(29): 10726-10731.

Cottet-Rousselle, C., X. Ronot, X. Leverve and J.-F. Mayol (2011). "Cytometric assessment of mitochondria using fluorescent probes." Cytometry Part A **79A**(6): 405-425.

Coyle, J. T. and P. Puttfarcken (1993). "Oxidative stress, glutamate, and neurodegenerative disorders." Science **262**(5134): 689-695.

Cruz, J. C., H.-C. Tseng, J. A. Goldman, H. Shih and L.-H. Tsai (2003). "Aberrant Cdk5 activation by p25 triggers pathological events leading to neurodegeneration and neurofibrillary tangles." Neuron **40**(3): 471-483.

Cuervo, A. M., L. Stefanis, R. Fredenburg, P. T. Lansbury and D. Sulzer (2004). "Impaired degradation of mutant alpha-synuclein by chaperone-mediated autophagy." Science **305**(5688): 1292-1295.

Czapski, G. A., M. Gassowska, A. Wilkaniec, M. Cieslik and A. Adamczyk (2013). "Extracellular alpha-synuclein induces calpain-dependent overactivation of cyclin-dependent kinase 5 in vitro." FEBS Lett **587**(18): 3135-3141.

Davie, C. A. (2008). "A review of Parkinson's disease." British Medical Bulletin **86**(1): 109-127.

De Jager, P. L., G. Srivastava, K. Lunnon, J. Burgess, L. C. Schalkwyk, L. Yu, M. L. Eaton, B. T. Keenan, J. Ernst, C. McCabe, A. Tang, T. Raj, J. Replogle, W. Brodeur, S. Gabriel, H. S. Chai, C. Younkin, S. G. Younkin, F. Zou, M. Szyf, C. B. Epstein, J. A. Schneider, B. E. Bernstein, A. Meissner, N. Ertekin-Taner, L. B. Chibnik, M. Kellis, J. Mill and D. A. Bennett (2014). "Alzheimer's disease: early alterations in brain DNA methylation at ANK1, BIN1, RHBDF2 and other loci." Nature Neuroscience **17**(9): 1156-1163.

de Magalhaes, J. P., J. Curado and G. M. Church (2009). "Meta-analysis of age-related gene expression profiles identifies common signatures of aging." Bioinformatics **25**(7): 875-881.

De Olmos, J. S. (1969). "A cupric-silver method for impregnation of terminal axon degeneration and its further use in staining granular argyrophilic neurons." Brain, Behavior, and Evolution **2**: 213-237.

DeKosky, S. T. and S. W. Scheff (1990). "Synapse loss in frontal cortex biopsies in Alzheimer's disease: correlation with cognitive severity." Ann Neurol **27**(5): 457-464.

del Puerto, A., L. Fronzaroli-Molinieres, M. J. Perez-Alvarez, P. Giraud, E. Carlier, F. Wandosell, D. Debanne and J. J. Garrido (2015). "ATP-P2X7 Receptor Modulates Axon Initial Segment Composition and Function in Physiological Conditions and Brain Injury." Cerebral Cortex **25**(8): 2282-2294.

Del Rio, J. A., C. Gonzalez-Billault, J. M. Urena, E. M. Jimenez, M. J. Barallobre, M. Pascual, L. Pujadas, S. Simo, A. La Torre, F. Wandosell, J. Avila and E. Soriano (2004). "MAP1B is required for Netrin 1 signaling in neuronal migration and axonal guidance." Curr Biol **14**(10): 840-850.

Delisle, M. B. and S. Carpenter (1984). "Neurofibrillary axonal swellings and amyotrophic lateral sclerosis." J Neurol Sci **63**(2): 241-250.

Deng, H. X., A. Hentati, J. A. Tainer, Z. Iqbal, A. Cayabyab, W. Y. Hung, E. D. Getzoff, P. Hu, B. Herzfeldt, R. P. Roos and et al. (1993). "Amyotrophic lateral sclerosis and structural defects in Cu,Zn superoxide dismutase." Science **261**(5124): 1047-1051.

Desai, B. S., A. J. Monahan, P. M. Carvey and B. Hendey (2007). "Blood-brain barrier pathology in Alzheimer's and Parkinson's disease: implications for drug therapy." Cell Transplant **16**(3): 285-299.

Desplats, P., H.-J. Lee, E.-J. Bae, C. Patrick, E. Rockenstein, L. Crews, B. Spencer, E. Masliah and S.-J. Lee (2009). "Inclusion formation and neuronal cell death through neuron-to-neuron transmission of α-synuclein." Proceedings of the National Academy of Sciences **106**(31): 13010-13015.

DeVorkin, L. and S. M. Gorski (2014). "Monitoring autophagy in Drosophila using fluorescent reporters in the UAS-GAL4 system." Cold Spring Harb Protoc **2014**(9): 967-972.

Dhavan, R. and L. H. Tsai (2001). "A decade of CDK5." Nat Rev Mol Cell Biol **2**(10): 749-759.

Diaconeasa, A. G., M. Rachita and R.-I. Stefan-van Staden (2015). "A new hypothesis of aging." Medical Hypotheses **84**(3): 252-257.

Du, H. and S. S. Yan (2010). "Mitochondrial permeability transition pore in Alzheimer's disease: Cyclophilin D and amyloid beta." Biochimica et Biophysica Acta (BBA) - Molecular Basis of Disease **1802**(1): 198-204.

Du, H., L. Guo, F. Fang, D. Chen, A. A Sosunov, G. M McKhann, Y. Yan, C. Wang, H. Zhang, J. D. Molkentin, F. J. Gunn-Moore, J. P. Vonsattel, O. Arancio, J. X. Chen and S. D. Yan (2008). "Cyclophilin D deficiency attenuates mitochondrial and neuronal perturbation and ameliorates learning and memory in Alzheimer's disease." Nature Medicine **14**(10): 1097-1105.

Dudoit, S., J. Fridlyand and T. P. Speed (2002). "Comparison of discrimination methods for the classification of tumors using gene expression data." Journal of the American statistical association **97**(457): 77-87.

Dzhashiashvili, Y., Y. Zhang, J. Galinska, I. Lam, M. Grumet and J. L. Salzer (2007). "Nodes of Ranvier and axon initial segments are ankyrin G-dependent domains that assemble by distinct mechanisms." J Cell Biol **177**(5): 857-870.

Edgar, D., I. Shabalina, Y. Camara, A. Wredenberg, M. A. Calvaruso, L. Nijtmans, J. Nedergaard, B. Cannon, N. G. Larsson and A. Trifunovic (2009). "Random point mutations with major effects on protein-coding genes are the driving force behind premature aging in mtDNA mutator mice." Cell Metab **10**(2): 131-138.

El Khoury, J., M. Toft, S. E. Hickman, T. K. Means, K. Terada, C. Geula and A. D. Luster (2007). "Ccr2 deficiency impairs microglial accumulation and accelerates progression of Alzheimer-like disease." Nat Med **13**(4): 432-438.

Elkon, H., J. Don, E. Melamed, I. Ziv, A. Shirvan and D. Offen (2002). "Mutant and wild-type α-synuclein interact with mitochondrial cytochrome C oxidase." Journal of Molecular Neuroscience **18**(3): 229-238.

Érdi, B., P. Nagy, Á. Zvara, Á. Varga, K. Pircs, D. Ménesi, L. G. Puskás and G. Juhász (2012). "Loss of the starvation-induced gene Rack1 leads to glycogen deficiency and impaired autophagic responses in Drosophila." Autophagy **8**(7): 1124-1135.

Evans, D. B., K. B. Rank, K. Bhattacharya, D. R. Thomsen, M. E. Gurney and S. K. Sharma (2000). "Tau Phosphorylation at Serine 396 and Serine 404 by Human Recombinant Tau Protein Kinase II Inhibits Tau's Ability to Promote Microtubule Assembly." Journal of Biological Chemistry **275**(32): 24977-24983.

Farrington, J. A., M. Ebert, E. J. Land and K. Fletcher (1973). "Bipyridylium quaternary salts and related compounds. V. Pulse radiolysis studies of the reaction of paraquat radical with oxygen. Implications for the mode of action of bipyridyl herbicides." Biochimica et Biophysica Acta (BBA)-Bioenergetics **314**(3): 372-381.

Favrin, G., D. M. Bean, E. Bilsland, H. Boyer, B. E. Fischer, S. Russell, D. C. Crowther, H. A. Baylis, S. G. Oliver and M. E. Giannakou (2013). "Identification of novel modifiers of Abeta toxicity by transcriptomic analysis in the fruitfly." Sci Rep **3**: 3512.

Feany, M. B. and W. W. Bender (2000). "A Drosophila model of Parkinson's disease." Nature **404**(6776): 394-398.

Fischer, A., F. Sananbenesi, P. T. Pang, B. Lu and L.-H. Tsai (2005). "Opposing Roles of Transient and Prolonged Expression of p25 in Synaptic Plasticity and Hippocampus-Dependent Memory." Neuron **48**(5): 825-838.

Fletcher, A. I., R. Shuang, D. R. Giovannucci, L. Zhang, M. A. Bittner and E. L. Stuenkel (1999). "Regulation of exocytosis by cyclin-dependent kinase 5 via phosphorylation of Munc18." Journal of Biological Chemistry **274**(7): 4027-4035.

Floyd, S. R., E. B. Porro, V. I. Slepnev, G.-C. Ochoa, L.-H. Tsai and P. De Camilli (2001). "Amphiphysin 1 Binds the Cyclin-dependent Kinase (cdk) 5 Regulatory Subunit p35 and

Is Phosphorylated by cdk5 and cdc2." Journal of Biological Chemistry **276**(11): 8104-8110.

Fontana, L., B. K. Kennedy, V. D. Longo, D. Seals and S. Melov (2014). "Medical research: treat ageing." Nature **511**(7510): 405-407.

Fornai, F., P. Lenzi, M. Gesi, M. Ferrucci, G. Lazzeri, C. L. Busceti, R. Ruffoli, P. Soldani, S. Ruggieri, M. G. Alessandrì and others (2003). "Fine structure and biochemical mechanisms underlying nigrostriatal inclusions and cell death after proteasome inhibition." Journal of Neuroscience **23**(26): 8955-8966.

Fridovich, I. (1986). "Superoxide dismutases." Adv Enzymol Relat Areas Mol Biol **58**: 61-97.

Frost, B., R. L. Jacks and M. I. Diamond (2009). "Propagation of Tau Misfolding from the Outside to the Inside of a Cell." Journal of Biological Chemistry **284**(19): 12845-12852.

Fu, A. K. Y., F. C. F. Ip, W.-Y. Fu, J. Cheung, J. H. Wang, W.-H. Yung and N. Y. Ip (2005). "Aberrant motor axon projection, acetylcholine receptor clustering, and neurotransmission in cyclin-dependent kinase 5 null mice." Proceedings of the National Academy of Sciences of the United States of America **102**(42): 15224-15230.

Fu, A. K., W. Y. Fu, J. Cheung, K. W. Tsim, F. C. Ip, J. H. Wang and N. Y. Ip (2001). "Cdk5 is involved in neuregulin-induced AChR expression at the neuromuscular junction." Nat Neurosci **4**(4): 374-381.

Fu, A. K. Y., W.-Y. Fu, A. K. Y. Ng, W. W. Y. Chien, Y.-P. Ng, J. H. Wang and N. Y. Ip (2004). "Cyclin-dependent kinase 5 phosphorylates signal transducer and activator of transcription 3 and regulates its transcriptional activity." Proceedings of the National Academy of Sciences of the United States of America **101**(17): 6728-6733.

Fu, X., R. Liu, I. Sanchez, C. Silva-Sanchez, N. L. Hepowit, S. Cao, S. Chen and J. Maupin-Furlow (2016). "Ubiquitin-Like Proteasome System Represents a Eukaryotic-Like Pathway for Targeted Proteolysis in Archaea." mBio **7**(3): e00379-00316.

Fumagalli, M., F. Rossiello, M. Clerici, S. Barozzi, D. Cittaro, J. M. Kaplunov, G. Bucci, M. Dobreva, V. Matti, C. M. Beausejour, U. Herbig, M. P. Longhese and F. d'Adda di Fagagna (2012). "Telomeric DNA damage is irreparable and causes persistent DNA-damage-response activation." Nat Cell Biol **14**(4): 355-365.

Fuortes, M. G. F., K. Frank and M. C. Becker (1957). "Steps in the production of motoneuron spikes." The Journal of general physiology **40**(5): 735-752.

Furuya, T., M. Kim, M. Lipinski, J. Li, D. Kim, T. Lu, Y. Shen, L. Rameh, B. Yankner, L.-H. Tsai and J. Yuan (2010). "Negative Regulation of Vps34 by Cdk Mediated Phosphorylation." Molecular Cell **38**(4): 500-511.

Galiano, Mauricio R., S. Jha, Tammy S.-Y. Ho, C. Zhang, Y. Ogawa, K.-J. Chang, Michael C. Stankewich, Peter J. Mohler and Matthew N. Rasband (2012). "A Distal Axonal

Cytoskeleton Forms an Intra-Axonal Boundary that Controls Axon Initial Segment Assembly." <u>Cell</u> **149**(5): 1125-1139.

Garrido, J. J., F. Fernandes, P. Giraud, I. Mouret, E. Pasqualini, M.-P. Fache, F. Jullien and B. Dargent (2001). "Identification of an axonal determinant in the C-terminus of the sodium channel Nav1. 2." <u>The EMBO journal</u> **20**(21): 5950-5961.

Garrido, J. J., P. Giraud, E. Carlier, F. Fernandes, A. Moussif, M.-P. Fache, D. Debanne and B. Dargent (2003). "A Targeting Motif Involved in Sodium Channel Clustering at the Axonal Initial Segment." <u>Science</u> **300**(5628): 2091-2094.

Ghee, M., A. Fournier and J. Mallet (2000). "Rat α-Synuclein Interacts with Tat Binding Protein 1, a Component of the 26S Proteasomal Complex." <u>Journal of neurochemistry</u> **75**(5): 2221-2224.

Gilmore, E. C., T. Ohshima, A. M. Goffinet, A. B. Kulkarni and K. Herrup (1998). "Cyclin-dependent kinase 5-deficient mice demonstrate novel developmental arrest in cerebral cortex." <u>The Journal of neuroscience</u> **18**(16): 6370-6377.

Girardot, F., C. Lasbleiz, V. Monnier and H. Tricoire (2006). "Specific age related signatures in Drosophila body parts transcriptome." <u>BMC genomics</u> **7**(1): 69.

Giunta, B., F. Fernandez, W. V. Nikolic, D. Obregon, E. Rrapo, T. Town and J. Tan (2008). "Inflammaging as a prodrome to Alzheimer's disease." <u>Journal of Neuroinflammation</u> **5**(1): 51.

Golden, T. R. and S. Melov (2004). "Microarray analysis of gene expression with age in individual nematodes." <u>Aging Cell</u> **3**(3): 111-124.

Goldsmith, T. C. (2014). <u>Aging by design: how new thinking on aging will change your life</u>. Crownsville, MD, Azinet Press.

Goldsmith, T. C. (2014). "Modern evolutionary mechanics theories and resolving the programmed/non-programmed aging controversy." <u>Biochemistry (Moscow)</u> **79**(10): 1049-1055.

Gong, X., X. Tang, M. Wiedmann, X. Wang, J. Peng, D. Zheng, L. A. C. Blair, J. Marshall and Z. Mao (2003). "Cdk5-mediated inhibition of the protective effects of transcription factor MEF2 in neurotoxicity-induced apoptosis." <u>Neuron</u> **38**(1): 33-46.

Gorbunova, V., A. Seluanov, Z. Mao and C. Hine (2007). "Changes in DNA repair during aging." <u>Nucleic Acids Res</u> **35**(22): 7466-7474.

Gorman, A. M. (2008). "Neuronal cell death in neurodegenerative diseases: recurring themes around protein handling." <u>Journal of Cellular and Molecular Medicine</u> **12**(6a): 2263-2280.

Graeber, M. B. and W. J. Streit (2010). "Microglia: biology and pathology." <u>Acta Neuropathol</u> **119**(1): 89-105.

Greene, L. A., D. X. Liu, C. M. Troy and S. C. Biswas (2007). "Cell cycle molecules define a pathway required for neuron death in development and disease." <u>Biochim Biophys Acta</u> **1772**(4): 392-401.

Greenfield, J. G. (2008). <u>Greenfield's Neuropathology</u>. London, Hodder Arnold.

Grether, M. E., J. M. Abrams, J. Agapite, K. White and H. Steller (1995). "The head involution defective gene of Drosophila melanogaster functions in programmed cell death." <u>Genes & Development</u> **9**(14): 1694-1708.

Grewal, S. I. and D. Moazed (2003). "Heterochromatin and epigenetic control of gene expression." <u>Science</u> **301**(5634): 798-802.

Guan, J.-S., S. C. Su, J. Gao, N. Joseph, Z. Xie, Y. Zhou, O. Durak, L. Zhang, J. J. Zhu, K. R. Clauser, S. A. Carr and L.-H. Tsai (2011). "Cdk5 Is Required for Memory Function and Hippocampal Plasticity via the cAMP Signaling Pathway." <u>PLoS ONE</u> **6**(9): e25735.

Guidato, S., D. M. McLoughlin, A. J. Grierson and C. C. J. Miller (1998). "Cyclin D2 interacts with cdk-5 and modulates cellular cdk-5/p35 activity." <u>Journal of neurochemistry</u> **70**(1): 335-340.

Guillot-Sestier, M.-V. and T. Town (2013). "Innate immunity in Alzheimer's disease: a complex affair." <u>CNS & Neurological Disorders-Drug Targets (Formerly Current Drug Targets-CNS & Neurological Disorders)</u> **12**(5): 593-607.

Gunawardena, S. and L. S. B. Goldstein (2001). "Disruption of axonal transport and neuronal viability by amyloid precursor protein mutations in Drosophila." <u>Neuron</u> **32**(3): 389-401.

Halliwell, B. and J. M. C. Gutteridge (1984). "Oxygen toxicity, oxygen radicals, transition metals and disease." <u>Biochemical journal</u> **219**(1): 1-14.

Hallows, J. L., K. Chen, R. A. DePinho and I. Vincent (2003). "Decreased cyclin-dependent kinase 5 (cdk5) activity is accompanied by redistribution of cdk5 and cytoskeletal proteins and increased cytoskeletal protein phosphorylation in p35 null mice." <u>The Journal of neuroscience</u> **23**(33): 10633-10644.

Hammond, J. W., C.-F. Huang, S. Kaech, C. Jacobson, G. Banker and K. J. Verhey (2010). "Posttranslational modifications of tubulin and the polarized transport of kinesin-1 in neurons." <u>Molecular biology of the cell</u> **21**(4): 572-583.

Hara, T., K. Nakamura, M. Matsui, A. Yamamoto, Y. Nakahara, R. Suzuki-Migishima, M. Yokoyama, K. Mishima, I. Saito, H. Okano and N. Mizushima (2006). "Suppression of basal autophagy in neural cells causes neurodegenerative disease in mice." <u>Nature</u> **441**(7095): 885-889.

Harada, T., T. Morooka, S. Ogawa and E. Nishida (2001). "ERK induces p35, a neuron-specific activator of Cdk5, through induction of Egr1." Nature cell biology **3**(5): 453-459.

Hashiguchi, M., T. Saito, S. i. Hisanaga and T. Hashiguchi (2002). "Truncation of CDK5 Activator p35 Induces Intensive Phosphorylation of Ser202/Thr205 of Human Tau." Journal of Biological Chemistry **277**(46): 44525-44530.

Hashimoto, M., L. J. Hsu, Y. Xia, A. Takeda, A. Sisk, M. Sundsmo and E. Masliah (1999). "Oxidative stress induces amyloid-like aggregate formation of NACP/alpha-synuclein in vitro." Neuroreport **10**(4): 717-721.

Hata, Y., C. A. Slaughter and T. C. Sudhof (1993). "Synaptic vesicle fusion complex contains unc-18 homologue bound to syntaxin." Nature **366**(6453): 347-351.

Hawasli, A. H., D. R. Benavides, C. Nguyen, J. W. Kansy, K. Hayashi, P. Chambon, P. Greengard, C. M. Powell, D. C. Cooper and J. A. Bibb (2007). "Cyclin-dependent kinase 5 governs learning and synaptic plasticity via control of NMDAR degradation." Nature Neuroscience **10**(7): 880-886.

Hayflick, L. and P. S. Moorhead (1961). "The serial cultivation of human diploid cell strains." Exp Cell Res **25**: 585-621.

Hazelrigg, T. (1987). " The Drosophila white gene: a molecular update." Trends in Genetics **3**(2): 43-47.

Hedstrom, K. L., X. Xu, Y. Ogawa, R. Frischknecht, C. I. Seidenbecher, P. Shrager and M. N. Rasband (2007). "Neurofascin assembles a specialized extracellular matrix at the axon initial segment." The Journal of Cell Biology **178**(5): 875-886.

Hedstrom, K. L., Y. Ogawa and M. N. Rasband (2008). "AnkyrinG is required for maintenance of the axon initial segment and neuronal polarity." The Journal of Cell Biology **183**(4): 635-640.

Heilbronn, L. K. and E. Ravussin (2003). "Calorie restriction and aging: review of the literature and implications for studies in humans." The American journal of clinical nutrition **78**(3): 361-369.

Hellmich, M. R., H. C. Pant, E. Wada and J. F. Battey (1992). "Neuronal cdc2-like kinase: a cdc2-related protein kinase with predominantly neuronal expression." Proc Natl Acad Sci U S A **89**(22): 10867-10871.

Herrup, K. (2010). "Reimagining Alzheimer's disease--an age-based hypothesis." J Neurosci **30**(50): 16755-16762.

Hewitt, G., D. Jurk, F. D. Marques, C. Correia-Melo, T. Hardy, A. Gackowska, R. Anderson, M. Taschuk, J. Mann and J. F. Passos (2012). "Telomeres are favoured targets of a persistent DNA damage response in ageing and stress-induced senescence." Nat Commun **3**: 708.

Heydari, A. R., B. Wu, R. Takahashi, R. Strong and A. Richardson (1993). "Expression of heat shock protein 70 is altered by age and diet at the level of transcription." Mol Cell Biol **13**(5): 2909-2918.

Hisanaga, S., K. Ishiguro, T. Uchida, E. Okumura, T. Okano and T. Kishimoto (1993). "Tau protein kinase II has a similar characteristic to cdc2 kinase for phosphorylating neurofilament proteins." Journal of Biological Chemistry **268**(20): 15056-15060.

Hodge, J. J. and R. Stanewsky (2008). "Function of the Shaw potassium channel within the Drosophila circadian clock." PLoS One **3**(5): e2274.

Hodgkin, A. L. and A. F. Huxley (1952). "A quantitative description of membrane current and its application to conduction and excitation in nerve." J Physiol **117**(4): 500-544.

Hoeijmakers, J. H. (2009). "DNA damage, aging, and cancer." N Engl J Med **361**(15): 1475-1485.

Hoover, B. R., M. N. Reed, J. Su, R. D. Penrod, L. A. Kotilinek, M. K. Grant, R. Pitstick, G. A. Carlson, L. M. Lanier, L.-L. Yuan, K. H. Ashe and D. Liao (2010). "Tau Mislocalization to Dendritic Spines Mediates Synaptic Dysfunction Independently of Neurodegeneration." Neuron **68**(6): 1067-1081.

Hortsch, M. (2002). "The Axonal Localization of Large Drosophila Ankyrin2 Protein Isoforms Is Essential for Neuronal Functionality." Molecular and Cellular Neuroscience **20**(1): 43-55.

Horvath, S. and B. R. Ritz (2015). "Increased epigenetic age and granulocyte counts in the blood of Parkinson's disease patients." Aging (Albany NY) **7**(12): 1130-1142.

Hou, Z., L. He and R. Z. Qi (2007). "Regulation of s6 kinase 1 activation by phosphorylation at ser-411." J Biol Chem **282**(10): 6922-6928.

Hu, W., C. Tian, T. Li, M. Yang, H. Hou and Y. Shu (2009). "Distinct contributions of Nav1.6 and Nav1.2 in action potential initiation and backpropagation." Nature Neuroscience **12**(8): 996-1002.

Huang, D. W., B. T. Sherman and R. A. Lempicki (2009). "Bioinformatics enrichment tools: paths toward the comprehensive functional analysis of large gene lists." Nucleic Acids Research **37**(1): 1-13.

Huang, D. W., B. T. Sherman and R. A. Lempicki (2009). "Systematic and integrative analysis of large gene lists using DAVID bioinformatics resources." Nature Protocols **4**(1): 44-57.

Humbert, S., R. Dhavan and L. Tsai (2000). "p39 activates cdk5 in neurons, and is associated with the actin cytoskeleton." J Cell Sci **113**(6): 975-983.

Hung, W. W., J. S. Ross, K. S. Boockvar and A. L. Siu (2011). "Recent trends in chronic disease, impairment and disability among older adults in the United States." BMC Geriatr **11**: 47.

Ichimura, Y., T. Kirisako, T. Takao, Y. Satomi, Y. Shimonishi, N. Ishihara, N. Mizushima, I. Tanida, E. Kominami, M. Ohsumi, T. Noda and Y. Ohsumi (2000). "A ubiquitin-like system mediates protein lipidation." Nature **408**(6811): 488-492.

Iijima, K., H.-C. Chiang, S. A. Hearn, I. Hakker, A. Gatt, C. Shenton, L. Granger, A. Leung, K. Iijima-Ando and Y. Zhong (2008). "Aβ42 Mutants with Different Aggregation Profiles Induce Distinct Pathologies in Drosophila." PLoS ONE **3**(2): e1703.

Iijima, K., H.-P. Liu, A.-S. Chiang, S. A. Hearn, M. Konsolaki and Y. Zhong (2004). "Dissecting the pathological effects of human Aβ40 and Aβ42 in Drosophila: a potential model for Alzheimer's disease." Proceedings of the National Academy of Sciences of the United States of America **101**(17): 6623-6628.

Inagaki, H. K., A. Kamikouchi and K. Ito (2010). "Methods for quantifying simple gravity sensing in Drosophila melanogaster." Nature Protocols **5**(1): 20-25.

Ingre, C., P. M. Roos, F. Piehl, F. Kamel and F. Fang (2015). "Risk factors for amyotrophic lateral sclerosis." Clin Epidemiol **7**: 181-193.

Ino, H., T. Ishizuka, T. Chiba and M. Tatibana (1994). "Expression of CDK5 (PSSALRE kinase), a neural cdc2-related protein kinase, in the mature and developing mouse central and peripheral nervous systems." Brain Res **661**(1-2): 196-206.

Ishizuka, K., T. Kimura, R. Igata-yi, S. Katsuragi, J. Takamatsu and T. Miyakawa (1997). "Identification of monocyte chemoattractant protein-1 in senile plaques and reactive microglia of Alzheimer's disease." Psychiatry Clin Neurosci **51**(3): 135-138.

Itoh, K., K. Nakamura, M. Iijima and H. Sesaki (2013). "Mitochondrial dynamics in neurodegeneration." Trends in Cell Biology **23**(2): 64-71.

Jegla, T., M. M. Nguyen, C. Feng, D. J. Goetschius, E. Luna, D. B. van Rossum, B. Kamel, A. Pisupati, E. S. Milner and M. M. Rolls (2016). "Bilaterian Giant Ankyrins Have a Common Evolutionary Origin and Play a Conserved Role in Patterning the Axon Initial Segment." PLOS Genetics **12**(12): e1006457.

Jellinger, K. A. (2010). "Basic mechanisms of neurodegeneration: a critical update." J Cell Mol Med **14**(3): 457-487.

Jensen, P. H., M. S. Nielsen, R. Jakes, C. G. Dotti and M. Goedert (1998). "Binding of alpha-synuclein to brain vesicles is abolished by familial Parkinson's disease mutation." J Biol Chem **273**(41): 26292-26294.

Jimenez-Diaz, L., S. M. Geranton, G. M. Passmore, J. L. Leith, A. S. Fisher, L. Berliocchi, A. K. Sivasubramaniam, A. Sheasby, B. M. Lumb and S. P. Hunt (2008). "Local Translation in Primary Afferent Fibers Regulates Nociception." PLoS ONE **3**(4): e1961.

Jin, C., J. Li, C. D. Green, X. Yu, X. Tang, D. Han, B. Xian, D. Wang, X. Huang, X. Cao, Z. Yan, L. Hou, J. Liu, N. Shukeir, P. Khaitovich, C. D. Chen, H. Zhang, T. Jenuwein and J.

D. Han (2011). "Histone demethylase UTX-1 regulates C. elegans life span by targeting the insulin/IGF-1 signaling pathway." Cell Metab **14**(2): 161-172.

Jin, K. (2010). "Modern Biological Theories of Aging." Aging Dis **1**(2): 72-74.

Kadavath, H., R. V. Hofele, J. Biernat, S. Kumar, K. Tepper, H. Urlaub, E. Mandelkow and M. Zweckstetter (2015). "Tau stabilizes microtubules by binding at the interface between tubulin heterodimers." Proc Natl Acad Sci U S A **112**(24): 7501-7506.

Kanaan, N. M., G. Morfini, G. Pigino, N. E. LaPointe, A. Andreadis, Y. Song, E. Leitman, L. I. Binder and S. T. Brady (2012). "Phosphorylation in the amino terminus of tau prevents inhibition of anterograde axonal transport." Neurobiol Aging **33**(4): 826 e815-830.

Kansy, J. W., S. C. Daubner, A. Nishi, N. Sotogaku, M. D. Lloyd, C. Nguyen, L. Lu, J. W. Haycock, B. T. Hope, P. F. Fitzpatrick and J. A. Bibb (2004). "Identification of tyrosine hydroxylase as a physiological substrate for Cdk5." J Neurochem **91**(2): 374-384.

Kaushik, S., U. Bandyopadhyay, S. Sridhar, R. Kiffin, M. Martinez-Vicente, M. Kon, S. J. Orenstein, E. Wong and A. M. Cuervo (2011). "Chaperone-mediated autophagy at a glance." J Cell Sci **124**(Pt 4): 495-499.

Kennedy, S. R., L. A. Loeb and A. J. Herr (2012). "Somatic mutations in aging, cancer and neurodegeneration." Mechanisms of Ageing and Development **133**(4): 118-126.

Kesavapany, S., K.-F. Lau, D. M. McLoughlin, J. Brownlees, S. Ackerley, P. N. Leigh, C. E. Shaw and C. C. J. Miller (2001). "p35/cdk5 binds and phosphorylates β-catenin and regulates β-catenin/presenilin-1 interaction." European Journal of Neuroscience **13**(2): 241-247.

Khaliq, Z. M. (2006). "Relative Contributions of Axonal and Somatic Na Channels to Action Potential Initiation in Cerebellar Purkinje Neurons." Journal of Neuroscience **26**(7): 1935-1944.

Kim, E., S. Naisbitt, Y. P. Hsueh, A. Rao, A. Rothschild, A. M. Craig and M. Sheng (1997). "GKAP, a novel synaptic protein that interacts with the guanylate kinase-like domain of the PSD-95/SAP90 family of channel clustering molecules." J Cell Biol **136**(3): 669-678.

Kim, G. H., J. E. Kim, S. J. Rhie and S. Yoon (2015). "The Role of Oxidative Stress in Neurodegenerative Diseases." Exp Neurobiol **24**(4): 325-340.

Kim, Y., J. Y. Sung, I. Ceglia, K. W. Lee, J. H. Ahn, J. M. Halford, A. M. Kim, S. P. Kwak, J. B. Park, S. Ho Ryu, A. Schenck, B. Bardoni, J. D. Scott, A. C. Nairn and P. Greengard (2006). "Phosphorylation of WAVE1 regulates actin polymerization and dendritic spine morphology." Nature **442**(7104): 814-817.

Kitada, T., S. Asakawa, N. Hattori, H. Matsumine, Y. Yamamura, S. Minoshima, M. Yokochi, Y. Mizuno and N. Shimizu (1998). "Mutations in the parkin gene cause autosomal recessive juvenile parkinsonism." Nature **392**(6676): 605-608.

Kizhatil, K. and V. Bennett (2004). "Lateral membrane biogenesis in human bronchial epithelial cells requires 190-kDa ankyrin-G." J Biol Chem **279**(16): 16706-16714.

Ko, J., S. Humbert, R. T. Bronson, S. Takahashi, A. B. Kulkarni, E. Li and L.-H. Tsai (2001). "p35 and p39 are essential for cyclin-dependent kinase 5 function during neurodevelopment." The Journal of Neuroscience **21**(17): 6758-6771.

Koffie, R. M., B. T. Hyman and T. L. Spires-Jones (2011). "Alzheimer's disease: synapses gone cold." Molecular neurodegeneration **6**(1): 63.

Koga, H., S. Kaushik and A. M. Cuervo (2011). "Protein homeostasis and aging: The importance of exquisite quality control." Ageing Res Rev **10**(2): 205-215.

Kole, M. H. P., S. U. Ilschner, B. M. Kampa, S. R. Williams, P. C. Ruben and G. J. Stuart (2008). "Action potential generation requires a high sodium channel density in the axon initial segment." Nature Neuroscience **11**(2): 178-186.

Komada, M. and P. Soriano (2002). "[Beta]IV-spectrin regulates sodium channel clustering through ankyrin-G at axon initial segments and nodes of Ranvier." J Cell Biol **156**(2): 337-348.

Komatsu, M., S. Waguri, T. Chiba, S. Murata, J.-i. Iwata, I. Tanida, T. Ueno, M. Koike, Y. Uchiyama, E. Kominami and K. Tanaka (2006). "Loss of autophagy in the central nervous system causes neurodegeneration in mice." Nature **441**(7095): 880-884.

Konishi, Y. and M. Setou (2009). "Tubulin tyrosination navigates the kinesin-1 motor domain to axons." Nature Neuroscience **12**(5): 559-567.

Kosel, S., R. Egensperger, U. von Eitzen, P. Mehraein and M. B. Graeber (1997). "On the question of apoptosis in the parkinsonian substantia nigra." Acta Neuropathol **93**(2): 105-108.

Kowald, A. and T. B. Kirkwood (2011). "Evolution of the mitochondrial fusion-fission cycle and its role in aging." Proc Natl Acad Sci U S A **108**(25): 10237-10242.

Kramer, M. L. and W. J. Schulz-Schaeffer (2007). "Presynaptic alpha-synuclein aggregates, not Lewy bodies, cause neurodegeneration in dementia with Lewy bodies." J Neurosci **27**(6): 1405-1410.

Kroemer, G., L. Galluzzi, P. Vandenabeele, J. Abrams, E. S. Alnemri, E. H. Baehrecke, M. V. Blagosklonny, W. S. El-Deiry, P. Golstein, D. R. Green, M. Hengartner, R. A. Knight, S. Kumar, S. A. Lipton, W. Malorni, G. Nuñez, M. E. Peter, J. Tschopp, J. Yuan, M. Piacentini, B. Zhivotovsky and G. Melino (2009). "Classification of cell death: recommendations of the Nomenclature Committee on Cell Death 2009." Cell Death and Differentiation **16**(1): 3-11.

Kumimoto, E. L., T. R. Fore and B. Zhang (2013). "Transcriptome Profiling Following Neuronal and Glial Expression of ALS-Linked SOD1 in Drosophila." G3: Genes, Genomes, Genetics **3**(4): 695-708.

Kuo, C. T., L. Y. Jan and Y. N. Jan (2005). "Dendrite-specific remodeling of Drosophila sensory neurons requires matrix metalloproteases, ubiquitin-proteasome, and ecdysone signaling." Proceedings of the National Academy of Sciences of the United States of America **102**(42): 15230-15235.

Kwon, Y. T. and L. H. Tsai (1998). "A novel disruption of cortical development in p35(-/-) mice distinct from reeler." J Comp Neurol **395**(4): 510-522.

Lai, C.-Q., L. D. Parnell, R. F. Lyman, J. M. Ordovas and T. F. C. Mackay (2007). "Candidate genes affecting Drosophila life span identified by integrating microarray gene expression analysis and QTL mapping." Mechanisms of Ageing and Development **128**(3): 237-249.

Lai, K. O., A. S. Wong, M. C. Cheung, P. Xu, Z. Liang, K. C. Lok, H. Xie, M. E. Palko, W. H. Yung, L. Tessarollo, Z. H. Cheung and N. Y. Ip (2012). "TrkB phosphorylation by Cdk5 is required for activity-dependent structural plasticity and spatial memory." Nat Neurosci **15**(11): 1506-1515.

Lalioti, V., D. Pulido and I. V. Sandoval (2010). "Cdk5, the multifunctional surveyor." Cell Cycle **9**(2): 284-311.

Landis, G. N., D. Abdueva, D. Skvortsov, J. Yang, B. E. Rabin, J. Carrick, S. Tavare and J. Tower (2004). "Similar gene expression patterns characterize aging and oxidative stress in Drosophila melanogaster." Proc Natl Acad Sci U S A **101**(20): 7663-7668.

LaPointe, N. E., G. Morfini, G. Pigino, I. N. Gaisina, A. P. Kozikowski, L. I. Binder and S. T. Brady (2009). "The amino terminus of tau inhibits kinesin-dependent axonal transport: Implications for filament toxicity." Journal of Neuroscience Research **87**(2): 440-451.

Laske, C., E. Stransky, N. Hoffmann, W. Maetzler, G. Straten, G. W. Eschweiler and T. Leyhe (2010). "Macrophage colony-stimulating factor (M-CSF) in plasma and CSF of patients with mild cognitive impairment and Alzheimer's disease." Curr Alzheimer Res **7**(5): 409-414.

Lau, L.-F. and M. K. Ahlijanian (2003). "Role of cdk5 in the Pathogenesis of Alzheimer's Disease." Neurosignals **12**(4-5): 209-214.

Lazarov, O., G. A. Morfini, G. Pigino, A. Gadadhar, X. Chen, J. Robinson, H. Ho, S. T. Brady and S. S. Sisodia (2007). "Impairments in fast axonal transport and motor neuron deficits in transgenic mice expressing familial Alzheimer's disease-linked mutant presenilin 1." J Neurosci **27**(26): 7011-7020.

Lebel, M. and M. Cyr (2011). "Molecular and cellular events of dopamine D1 receptor-mediated tau phosphorylation in SK-N-MC cells." Synapse **65**(1): 69-76.

Lee, C. K., R. G. Klopp, R. Weindruch and T. A. Prolla (1999). "Gene expression profile of aging and its retardation by caloric restriction." Science **285**(5432): 1390-1393.

Lee, C. K., R. Weindruch and T. A. Prolla (2000). "Gene-expression profile of the ageing brain in mice." Nat Genet **25**(3): 294-297.

Lee, H.-g., G. Casadesus, X. Zhu, R. J. Castellani, A. McShea, G. Perry, R. B. Petersen, V. Bajic and M. A. Smith (2009). "Cell cycle re-entry mediated neurodegeneration and its treatment role in the pathogenesis of Alzheimer's disease." Neurochemistry International **54**(2): 84-88.

Lee, K. Y., A. W. Clark, J. L. Rosales, K. Chapman, T. Fung and R. N. Johnston (1999). "Elevated neuronal Cdc2-like kinase activity in the Alzheimer disease brain." Neurosci Res **34**(1): 21-29.

Lee, S. Y., M. R. Wenk, Y. Kim, A. C. Nairn and P. De Camilli (2004). "Regulation of synaptojanin 1 by cyclin-dependent kinase 5 at synapses." Proc Natl Acad Sci U S A **101**(2): 546-551.

Lehman, N. L. (2009). "The ubiquitin proteasome system in neuropathology." Acta Neuropathol **118**(3): 329-347.

Lemaillet, G., B. Walker and S. Lambert (2003). "Identification of a conserved ankyrin-binding motif in the family of sodium channel alpha subunits." J Biol Chem **278**(30): 27333-27339.

Leterrier, C., H. Vacher, M. P. Fache, S. A. d'Ortoli, F. Castets, A. Autillo-Touati and B. Dargent (2011). "End-binding proteins EB3 and EB1 link microtubules to ankyrin G in the axon initial segment." Proc Natl Acad Sci U S A **108**(21): 8826-8831.

Leuner, K., S. Hauptmann, R. Abdel-Kader, I. Scherping, U. Keil, J. B. Strosznajder, A. Eckert and W. E. Müller (2007). "Mitochondrial Dysfunction: The First Domino in Brain Aging and Alzheimer's Disease?" Antioxidants & Redox Signaling **9**(10): 1659-1676.

Leutner, S., A. Eckert and W. E. Muller (2001). "ROS generation, lipid peroxidation and antioxidant enzyme activities in the aging brain." J Neural Transm (Vienna) **108**(8-9): 955-967.

Levine, M. E., A. T. Lu, D. A. Bennett and S. Horvath (2015). "Epigenetic age of the pre-frontal cortex is associated with neuritic plaques, amyloid load, and Alzheimer's disease related cognitive functioning." Aging (Albany NY) **7**(12): 1198-1211.

Levy, O. A., C. Malagelada and L. A. Greene (2009). "Cell death pathways in Parkinson's disease: proximal triggers, distal effectors, and final steps." Apoptosis **14**(4): 478-500.

Lew, J., Z. Qi, Q. Q. Huang, H. Paudel, I. Matsuura, M. Matsushita, X. Zhu and J. H. Wang (1995). "Structure, function, and regulation of neuronal Cdc2-like protein kinase." Neurobiol Aging **16**(3): 263-268; discussion 268-270.

Li, B.-S., M.-K. Sun, L. Zhang, S. Takahashi, W. Ma, L. Vinade, A. B. Kulkarni, R. O. Brady and H. C. Pant (2001). "Regulation of NMDA receptors by cyclin-dependent kinase-5." Proceedings of the National Academy of Sciences **98**(22): 12742-12747.

Li, C., Y. Sasaki, K. Takei, H. Yamamoto, M. Shouji, Y. Sugiyama, T. Kawakami, F. Nakamura, T. Yagi, T. Ohshima and Y. Goshima (2004). "Correlation between semaphorin3A-induced facilitation of axonal transport and local activation of a translation initiation factor eukaryotic translation initiation factor 4E." J Neurosci **24**(27): 6161-6170.

Li, L., X. Zhang and W. Le (2008). "Altered macroautophagy in the spinal cord of SOD1 mutant mice." Autophagy **4**(3): 290-293.

Li, X., Y. Kumar, H. Zempel, E.-M. Mandelkow, J. Biernat and E. Mandelkow (2011). "Novel diffusion barrier for axonal retention of Tau in neurons and its failure in neurodegeneration." The EMBO journal **30**(23): 4825-4837.

Lilja, L., J. U. Johansson, J. Gromada, S. A. Mandic, G. Fried, P. O. Berggren and C. Bark (2004). "Cyclin-dependent kinase 5 associated with p39 promotes Munc18-1 phosphorylation and Ca(2+)-dependent exocytosis." J Biol Chem **279**(28): 29534-29541.

Lim, K. L. (2007). "Ubiquitin-proteasome system dysfunction in Parkinson's disease: current evidence and controversies." Expert Rev Proteomics **4**(6): 769-781.

Lin, M. T. and M. F. Beal (2006). "Mitochondrial dysfunction and oxidative stress in neurodegenerative diseases." Nature **443**(7113): 787-795.

Lin, W., B. Dominguez, J. Yang, P. Aryal, E. P. Brandon, F. H. Gage and K.-F. Lee (2005). "Neurotransmitter Acetylcholine Negatively Regulates Neuromuscular Synapse Formation by a Cdk5-Dependent Mechanism." Neuron **46**(4): 569-579.

Liu, F., K. Iqbal, I. Grundke-Iqbal and C. X. Gong (2002). "Involvement of aberrant glycosylation in phosphorylation of tau by cdk5 and GSK-3beta." FEBS Lett **530**(1-3): 209-214.

Liu, H. S., M. S. Jan, C. K. Chou, P. H. Chen and N. J. Ke (1999). "Is green fluorescent protein toxic to the living cells?" Biochem Biophys Res Commun **260**(3): 712-717.

Liu, J., D. W. Killilea and B. N. Ames (2002). "Age-associated mitochondrial oxidative decay: improvement of carnitine acetyltransferase substrate-binding affinity and activity in brain by feeding old rats acetyl-L- carnitine and/or R-alpha -lipoic acid." Proc Natl Acad Sci U S A **99**(4): 1876-1881.

Liu, Y., K. Cheng, K. Gong, A. K. Fu and N. Y. Ip (2006). "Pctaire1 phosphorylates N-ethylmaleimide-sensitive fusion protein: implications in the regulation of its hexamerization and exocytosis." J Biol Chem **281**(15): 9852-9858.

Livak, K. J. and T. D. Schmittgen (2001). "Analysis of Relative Gene Expression Data Using Real-Time Quantitative PCR and the $2-\Delta\Delta CT$ Method." Methods **25**(4): 402-408.

Long-Smith, C. M., A. M. Sullivan and Y. M. Nolan (2009). "The influence of microglia on the pathogenesis of Parkinson's disease." Prog Neurobiol **89**(3): 277-287.

López-Otín, C., M. A. Blasco, L. Partridge, M. Serrano and G. Kroemer (2013). "The Hallmarks of Aging." Cell **153**(6): 1194-1217.

Lord, C. J. and A. Ashworth (2012). "The DNA damage response and cancer therapy." Nature **481**(7381): 287-294.

Luk, K. C., C. Song, P. O'Brien, A. Stieber, J. R. Branch, K. R. Brunden, J. Q. Trojanowski and V. M. Y. Lee (2009). "Exogenous α-synuclein fibrils seed the formation of Lewy body-like intracellular inclusions in cultured cells." Proceedings of the National Academy of Sciences **106**(47): 20051-20056.

Lund, E. T., R. McKenna, D. B. Evans, S. K. Sharma and W. R. Mathews (2001). "Characterization of the in vitro phosphorylation of human tau by tau protein kinase II (cdk5/p20) using mass spectrometry." Journal of neurochemistry **76**(4): 1221-1232.

Lunnon, K., R. Smith, E. Hannon, P. L. De Jager, G. Srivastava, M. Volta, C. Troakes, S. Al-Sarraj, J. Burrage, R. Macdonald, D. Condliffe, L. W. Harries, P. Katsel, V. Haroutunian, Z. Kaminsky, C. Joachim, J. Powell, S. Lovestone, D. A. Bennett, L. C. Schalkwyk and J. Mill (2014). "Methylomic profiling implicates cortical deregulation of ANK1 in Alzheimer's disease." Nature Neuroscience **17**(9): 1164-1170.

Luo, L., Y. J. Liao, L. Y. Jan and Y. N. Jan (1994). "Distinct morphogenetic functions of similar small GTPases: Drosophila Drac1 is involved in axonal outgrowth and myoblast fusion." Genes & development **8**(15): 1787-1802.

Luskin, M. B. and C. J. Shatz (1985). "Studies of the earliest generated cells of the cat's visual cortex: cogeneration of subplate and marginal zones." J Neurosci **5**(4): 1062-1075.

Maegawa, S., G. Hinkal, H. S. Kim, L. Shen, L. Zhang, J. Zhang, N. Zhang, S. Liang, L. A. Donehower and J. P. Issa (2010). "Widespread and tissue specific age-related DNA methylation changes in mice." Genome Res **20**(3): 332-340.

Maestre, C., M. Delgado-Esteban, J. C. Gomez-Sanchez, J. P. Bolanos and A. Almeida (2008). "Cdk5 phosphorylates Cdh1 and modulates cyclin B1 stability in excitotoxicity." EMBO J **27**(20): 2736-2745.

Manczak, M., Y. Jung, B. S. Park, D. Partovi and P. H. Reddy (2005). "Time-course of mitochondrial gene expressions in mice brains: implications for mitochondrial dysfunction, oxidative damage, and cytochrome c in aging." J Neurochem **92**(3): 494-504.

Martin, H. L. and P. Teismann (2009). "Glutathione--a review on its role and significance in Parkinson's disease." The FASEB Journal **23**(10): 3263-3272.

Martins, R., G. J. Lithgow and W. Link (2016). "Long live FOXO: unraveling the role of FOXO proteins in aging and longevity." Aging Cell **15**(2): 196-207.

Masliah, E., M. Mallory, M. Alford, R. DeTeresa, L. A. Hansen, D. W. McKeel and J. C. Morris (2001). "Altered expression of synaptic proteins occurs early during progression of Alzheimer's disease." Neurology **56**(1): 127-129.

Matsubara, M., M. Kusubata, K. Ishiguro, T. Uchida, K. Titani and H. Taniguchi (1996). "Site-specific phosphorylation of synapsin I by mitogen-activated protein kinase and Cdk5 and its effects on physiological functions." J Biol Chem **271**(35): 21108-21113.

Matsuura, I. and J. H. Wang (1996). "Demonstration of cyclin-dependent kinase inhibitory serine/threonine kinase in bovine thymus." J Biol Chem **271**(10): 5443-5450.

Mattson, M. P., S. L. Chan and W. Duan (2002). "Modification of brain aging and neurodegenerative disorders by genes, diet, and behavior." Physiol Rev **82**(3): 637-672.

McCarroll, S. A., C. T. Murphy, S. Zou, S. D. Pletcher, C. S. Chin, Y. N. Jan, C. Kenyon, C. I. Bargmann and H. Li (2004). "Comparing genomic expression patterns across species identifies shared transcriptional profile in aging." Nat Genet **36**(2): 197-204.

McLinden, K. A. (2012). "At the Fulcrum in Health and Disease: Cdk5 and the Balancing Acts of Neuronal Structure and Physiology." Brain Disorders & Therapy **01**(S1).

McNaught, K. S. P., L. M. Björklund, R. Belizaire, O. Isacson, P. Jenner and C. W. Olanow (2002). "Proteasome inhibition causes nigral degeneration with inclusion bodies in rats." Neuroreport **13**(11): 1437-1441.

Menzies, F. M., A. Fleming and D. C. Rubinsztein (2015). "Compromised autophagy and neurodegenerative diseases." Nature Reviews Neuroscience **16**(6): 345-357.

Mesquita, A., M. Weinberger, A. Silva, B. Sampaio-Marques, B. Almeida, C. Leao, V. Costa, F. Rodrigues, W. C. Burhans and P. Ludovico (2010). "Caloric restriction or catalase inactivation extends yeast chronological lifespan by inducing H2O2 and superoxide dismutase activity." Proc Natl Acad Sci U S A **107**(34): 15123-15128.

Meyerson, M., G. H. Enders, C. L. Wu, L. K. Su, C. Gorka, C. Nelson, E. Harlow and L. H. Tsai (1992). "A family of human cdc2-related protein kinases." EMBO J **11**(8): 2909-2917.

Michel, G., M. Mercken, M. Murayama, K. Noguchi, K. Ishiguro, K. Imahori and A. Takashima (1998). "Characterization of tau phosphorylation in glycogen synthase kinase-3beta and cyclin dependent kinase-5 activator (p23) transfected cells." Biochim Biophys Acta **1380**(2): 177-182.

Min, J. N., R. A. Whaley, N. E. Sharpless, P. Lockyer, A. L. Portbury and C. Patterson (2008). "CHIP Deficiency Decreases Longevity, with Accelerated Aging Phenotypes Accompanied by Altered Protein Quality Control." Molecular and Cellular Biology **28**(12): 4018-4025.

Minegishi, S., A. Asada, S. Miyauchi, T. Fuchigami, T. Saito and S. Hisanaga (2010). "Membrane association facilitates degradation and cleavage of the cyclin-dependent kinase 5 activators p35 and p39." Biochemistry **49**(26): 5482-5493.

Miwa, H., T. Kubo, A. Suzuki, K. Nishi and T. Kondo (2005). "Retrograde dopaminergic neuron degeneration following intrastriatal proteasome inhibition." Neuroscience Letters **380**(1-2): 93-98.

Miyajima, M., H. O. Nornes and T. Neuman (1995). "Cyclin E is expressed in neurons and forms complexes with cdk5." Neuroreport **6**(8): 1130-1132.

Mohler, P. J., J. Q. Davis and V. Bennett (2005). "Ankyrin-B coordinates the Na/K ATPase, Na/Ca exchanger, and InsP3 receptor in a cardiac T-tubule/SR microdomain." PLoS Biol **3**(12): e423.

Moreno, H., E. Yu, G. Pigino, A. I. Hernandez, N. Kim, J. E. Moreira, M. Sugimori and R. R. Llinas (2009). "Synaptic transmission block by presynaptic injection of oligomeric amyloid beta." Proc Natl Acad Sci U S A **106**(14): 5901-5906.

Morfini, G., G. Szebenyi, H. Brown, H. C. Pant, G. Pigino, S. DeBoer, U. Beffert and S. T. Brady (2004). "A novel CDK5-dependent pathway for regulating GSK3 activity and kinesin-driven motility in neurons." The EMBO journal **23**(11): 2235-2245.

Morfini, G., G. Szebenyi, R. Elluru, N. Ratner and S. T. Brady (2002). "Glycogen synthase kinase 3 phosphorylates kinesin light chains and negatively regulates kinesin-based motility." EMBO J **21**(3): 281-293.

Morrow, G., M. Samson, S. Michaud and R. M. Tanguay (2004). "Overexpression of the small mitochondrial Hsp22 extends Drosophila life span and increases resistance to oxidative stress." FASEB J **18**(3): 598-599.

Moy, L. Y. and L. H. Tsai (2004). "Cyclin-dependent Kinase 5 Phosphorylates Serine 31 of Tyrosine Hydroxylase and Regulates Its Stability." Journal of Biological Chemistry **279**(52): 54487-54493.

Muller, D. C., D. Elahi, J. D. Tobin and R. Andres (1996). "The effect of age on insulin resistance and secretion: a review." Semin Nephrol **16**(4): 289-298.

Muller, W. E., A. Eckert, C. Kurz, G. P. Eckert and K. Leuner (2010). "Mitochondrial dysfunction: common final pathway in brain aging and Alzheimer's disease--therapeutic aspects." Mol Neurobiol **41**(2-3): 159-171.

Nakada, C., K. Ritchie, Y. Oba, M. Nakamura, Y. Hotta, R. Iino, R. S. Kasai, K. Yamaguchi, T. Fujiwara and A. Kusumi (2003). "Accumulation of anchored proteins forms membrane diffusion barriers during neuronal polarization." Nat Cell Biol **5**(7): 626-632.

Nakamura, K., V. M. Nemani, F. Azarbal, G. Skibinski, J. M. Levy, K. Egami, L. Munishkina, J. Zhang, B. Gardner, J. Wakabayashi, H. Sesaki, Y. Cheng, S. Finkbeiner, R. L.

Nussbaum, E. Masliah and R. H. Edwards (2011). "Direct Membrane Association Drives Mitochondrial Fission by the Parkinson Disease-associated Protein α-Synuclein." Journal of Biological Chemistry **286**(23): 20710-20726.

Nakamura, S., Y. Kawamoto, S. Nakano, I. Akiguchi and J. Kimura (1997). "p35nck5a and cyclin-dependent kinase 5 colocalize in Lewy bodies of brains with Parkinson's disease." Acta Neuropathol **94**(2): 153-157.

Nakata, T. and N. Hirokawa (2003). "Microtubules provide directional cues for polarized axonal transport through interaction with kinesin motor head." The Journal of Cell Biology **162**(6): 1045-1055.

Nelson, A. D. and P. M. Jenkins (2017). "Axonal Membranes and Their Domains: Assembly and Function of the Axon Initial Segment and Node of Ranvier." Front Cell Neurosci **11**: 136.

Nezis, I. P., A. Simonsen, A. P. Sagona, K. Finley, S. Gaumer, D. Contamine, T. E. Rusten, H. Stenmark and A. Brech (2008). "Ref(2)P, the Drosophila melanogaster homologue of mammalian p62, is required for the formation of protein aggregates in adult brain." The Journal of Cell Biology **180**(6): 1065-1071.

Nguyen, M. D., R. C. Larivière and J.-P. Julien (2001). "Deregulation of Cdk5 in a mouse model of ALS: toxicity alleviated by perikaryal neurofilament inclusions." Neuron **30**(1): 135-148.

Nielsen, A. L., M. Oulad-Abdelghani, J. A. Ortiz, E. Remboutsika, P. Chambon and R. Losson (2001). "Heterochromatin formation in mammalian cells: interaction between histones and HP1 proteins." Molecular cell **7**(4): 729-739.

Niethammer, M., D. S. Smith, R. Ayala, J. Peng, J. Ko, M.-S. Lee, M. Morabito and L.-H. Tsai (2000). "NUDEL is a novel Cdk5 substrate that associates with LIS1 and cytoplasmic dynein." Neuron **28**(3): 697-711.

Nikolic, M., H. Dudek, Y. T. Kwon, Y. F. Ramos and L.-H. Tsai (1996). "The cdk5/p35 kinase is essential for neurite outgrowth during neuronal differentiation." Genes & development **10**(7): 816-825.

Nikolic, M., M. Chou, W. Lu, B. Mayer and L.-H. Tsai (1998). "The p35/cdk5 kinase is a neuron-specific Rac effector that inhibits Pak1 activity." Nature **395**(6698): 194-198.

Noble, W., V. Olm, K. Takata, E. Casey, O. Mary, J. Meyerson, K. Gaynor, J. LaFrancois, L. Wang, T. Kondo and others (2003). "Cdk5 is a key factor in tau aggregation and tangle formation in vivo." Neuron **38**(4): 555-565.

O'Hare, K., C. Murphy, R. Levis and G. M. Rubin (1984). "DNA sequence of the white locus of Drosophila melanogaster." J Mol Biol **180**(3): 437-455.

Odajima, J., Zachary P. Wills, Yasmine M. Ndassa, M. Terunuma, K. Kretschmannova, Tarek Z. Deeb, Y. Geng, S. Gawrzak, Isabel M. Quadros, J. Newman, M. Das, Marie E. Jecrois,

Q. Yu, N. Li, F. Bienvenu, Stephen J. Moss, Michael E. Greenberg, Jarrod A. Marto and P. Sicinski (2011). "Cyclin E Constrains Cdk5 Activity to Regulate Synaptic Plasticity and Memory Formation." Developmental Cell **21**(4): 655-668.

Oddo, S. (2008). "The ubiquitin-proteasome system in Alzheimer's disease." J Cell Mol Med **12**(2): 363-373.

Ogawa, Y. and M. N. Rasband (2008). "The functional organization and assembly of the axon initial segment." Current Opinion in Neurobiology **18**(3): 307-313.

Ohshima, T., J. M. Ward, C.-G. Huh, G. Longenecker, H. C. Pant, R. O. Brady, L. J. Martin and A. B. Kulkarni (1996). "Targeted disruption of the cyclin-dependent kinase 5 gene results in abnormal corticogenesis, neuronal pathology and perinatal death." Proceedings of the National Academy of Sciences **93**(20): 11173-11178.

Osorio, F. G., C. Barcena, C. Soria-Valles, A. J. Ramsay, F. de Carlos, J. Cobo, A. Fueyo, J. M. Freije and C. Lopez-Otin (2012). "Nuclear lamina defects cause ATM-dependent NF-kappaB activation and link accelerated aging to a systemic inflammatory response." Genes Dev **26**(20): 2311-2324.

Paglini, G., G. Pigino, P. Kunda, G. Morfini, R. Maccioni, S. Quiroga, A. Ferreira and A. Caceres (1998). "Evidence for the participation of the neuron-specific CDK5 activator P35 during laminin-enhanced axonal growth." J Neurosci **18**(23): 9858-9869.

Palay, S. L., C. Sotelo, A. Peters and P. M. Orkand (1968). "The axon hillock and the initial segment." J Cell Biol **38**(1): 193-201.

Palmer, L. M. and G. Stuart (2006). "Site of Action Potential Initiation in Layer 5 Pyramidal Neurons." Journal of Neuroscience **26**(6): 1854-1863.

Pan, Z., T. Kao, Z. Horvath, J. Lemos, J. Y. Sul, S. D. Cranstoun, V. Bennett, S. S. Scherer and E. C. Cooper (2006). "A common ankyrin-G-based mechanism retains KCNQ and NaV channels at electrically active domains of the axon." J Neurosci **26**(10): 2599-2613.

Patel, N. S., D. Paris, V. Mathura, A. N. Quadros, F. C. Crawford and M. J. Mullan (2005). "Inflammatory cytokine levels correlate with amyloid load in transgenic mouse models of Alzheimer's disease." J Neuroinflammation **2**(1): 9.

Patrick, G. N., L. Zukerberg, M. Nikolic, S. de la Monte, P. Dikkes and L. H. Tsai (1999). "Conversion of p35 to p25 deregulates Cdk5 activity and promotes neurodegeneration." Nature **402**(6762): 615-622.

Patrick, G. N., P. Zhou, Y. T. Kwon, P. M. Howley and L.-H. Tsai (1998). "p35, the neuronal-specific activator of cyclin-dependent kinase 5 (Cdk5) is degraded by the ubiquitin-proteasome pathway." Journal of Biological Chemistry **273**(37): 24057-24064.

Paudel, H. K., J. Lew, Z. Ali and J. H. Wang (1993). "Brain proline-directed protein kinase phosphorylates tau on sites that are abnormally phosphorylated in tau associated with

Alzheimer's paired helical filaments." <u>Journal of Biological Chemistry</u> **268**(31): 23512-23518.

Paul, S. (2008). "Dysfunction of the ubiquitin-proteasome system in multiple disease conditions: therapeutic approaches." <u>BioEssays</u> **30**(11-12): 1172-1184.

Pegoraro, G., N. Kubben, U. Wickert, H. Gohler, K. Hoffmann and T. Misteli (2009). "Ageing-related chromatin defects through loss of the NURD complex." <u>Nat Cell Biol</u> **11**(10): 1261-1267.

Perez, V. I., H. Van Remmen, A. Bokov, C. J. Epstein, J. Vijg and A. Richardson (2009). "The overexpression of major antioxidant enzymes does not extend the lifespan of mice." <u>Aging Cell</u> **8**(1): 73-75.

Perry, S., J. Norman, J. Barbieri, E. Brown and H. Gelbard (2011). "Mitochondrial membrane potential probes and the proton gradient: a practical usage guide." <u>BioTechniques</u> **50**(2): 98-115.

Pickrell, Alicia M. and Richard J. Youle (2015). "The Roles of PINK1, Parkin, and Mitochondrial Fidelity in Parkinson's Disease." <u>Neuron</u> **85**(2): 257-273.

Pielage, J., L. Cheng, R. D. Fetter, P. M. Carlton, J. W. Sedat and G. W. Davis (2008). "A Presynaptic Giant Ankyrin Stabilizes the NMJ through Regulation of Presynaptic Microtubules and Transsynaptic Cell Adhesion." <u>Neuron</u> **58**(2): 195-209.

Pielage, J., R. D. Fetter and G. W. Davis (2005). "Presynaptic spectrin is essential for synapse stabilization." <u>Curr Biol</u> **15**(10): 918-928.

Pigino, G., G. Morfini, A. Pelsman, M. P. Mattson, S. T. Brady and J. Busciglio (2003). "Alzheimer's presenilin 1 mutations impair kinesin-based axonal transport." <u>J Neurosci</u> **23**(11): 4499-4508.

Pigino, G., G. Morfini, Y. Atagi, A. Deshpande, C. Yu, L. Jungbauer, M. LaDu, J. Busciglio and S. Brady (2009). "Disruption of fast axonal transport is a pathogenic mechanism for intraneuronal amyloid beta." <u>Proc Natl Acad Sci U S A</u> **106**(14): 5907-5912.

Pigino, G., G. Paglini, L. Ulloa, J. Avila and A. Cáceres (1997). "Analysis of the expression, distribution and function of cyclin dependent kinase 5 (cdk5) in developing cerebellar macroneurons." <u>Journal of Cell Science</u> **110**(2): 257-270.

Pletcher, S. D., S. J. Macdonald, R. Marguerie, U. Certa, S. C. Stearns, D. B. Goldstein and L. Partridge (2002). "Genome-Wide Transcript Profiles in Aging and Calorically Restricted Drosophila melanogaster." <u>Current Biology</u> **12**(9): 712-723.

Podtelezhnikov, A. A., K. Q. Tanis, M. Nebozhyn, W. J. Ray, D. J. Stone and A. P. Loboda (2011). "Molecular insights into the pathogenesis of Alzheimer's disease and its relationship to normal aging." <u>PLoS One</u> **6**(12): e29610.

Poole, A. C., R. E. Thomas, L. A. Andrews, H. M. McBride, A. J. Whitworth and L. J. Pallanck (2008). "The PINK1/Parkin pathway regulates mitochondrial morphology." Proceedings of the National Academy of Sciences **105**(5): 1638-1643.

Poon, R. Y. C., J. Lew and T. Hunter (1997). "Identification of functional domains in the neuronal Cdk5 activator protein." Journal of Biological Chemistry **272**(9): 5703-5708.

Powers, E. T., R. I. Morimoto, A. Dillin, J. W. Kelly and W. E. Balch (2009). "Biological and Chemical Approaches to Diseases of Proteostasis Deficiency." Annual Review of Biochemistry **78**(1): 959-991.

Qu, D., J. Rashidian, M. P. Mount, H. Aleyasin, M. Parsanejad, A. Lira, E. Haque, Y. Zhang, S. Callaghan, M. Daigle, M. W. C. Rousseaux, R. S. Slack, P. R. Albert, I. Vincent, J. M. Woulfe and D. S. Park (2007). "Role of Cdk5-Mediated Phosphorylation of Prx2 in MPTP Toxicity and Parkinson's Disease." Neuron **55**(1): 37-52.

Raichle, M. E. and D. A. Gusnard (2002). "Appraising the brain's energy budget." Proc Natl Acad Sci U S A **99**(16): 10237-10239.

Ranganathan, S. and R. Bowser (2003). "Alterations in G(1) to S phase cell-cycle regulators during amyotrophic lateral sclerosis." Am J Pathol **162**(3): 823-835.

Rasmussen, H. B., C. Frokjaer-Jensen, C. S. Jensen, H. S. Jensen, N. K. Jorgensen, H. Misonou, J. S. Trimmer, S. P. Olesen and N. Schmitt (2007). "Requirement of subunit co-assembly and ankyrin-G for M-channel localization at the axon initial segment." Journal of Cell Science **120**(6): 953-963.

Reddi, A. R. and V. C. Culotta (2013). "SOD1 Integrates Signals from Oxygen and Glucose to Repress Respiration." Cell **152**(1-2): 224-235.

Reeve, A., E. Simcox and D. Turnbull (2014). "Ageing and Parkinson's disease: Why is advancing age the biggest risk factor?" Ageing Research Reviews **14**: 19-30.

Reynolds, A. D., J. G. Glanzer, I. Kadiu, M. Ricardo-Dukelow, A. Chaudhuri, P. Ciborowski, R. Cerny, B. Gelman, M. P. Thomas, R. L. Mosley and H. E. Gendelman (2008). "Nitrated alpha-synuclein-activated microglial profiling for Parkinson's disease." J Neurochem **104**(6): 1504-1525.

Ristow, M. and S. Schmeisser (2011). "Extending life span by increasing oxidative stress." Free Radic Biol Med **51**(2): 327-336.

Rohn, T. T., V. Vyas, T. Hernandez-Estrada, K. E. Nichol, L. A. Christie and E. Head (2008). "Lack of Pathology in a Triple Transgenic Mouse Model of Alzheimer's Disease after Overexpression of the Anti-Apoptotic Protein Bcl-2." Journal of Neuroscience **28**(12): 3051-3059.

Roselli, F., P. Livrea and O. F. Almeida (2011). "CDK5 is essential for soluble amyloid beta-induced degradation of GKAP and remodeling of the synaptic actin cytoskeleton." PLoS One **6**(7): e23097.

Rosen, D. R., T. Siddique, D. Patterson, D. A. Figlewicz, P. Sapp, A. Hentati, D. Donaldson, J. Goto, J. P. O'Regan, H. X. Deng and et al. (1993). "Mutations in Cu/Zn superoxide dismutase gene are associated with familial amyotrophic lateral sclerosis." Nature **362**(6415): 59-62.

Ross, C. A. and M. A. Poirier (2004). "Protein aggregation and neurodegenerative disease." Nat Med **10 Suppl**: S10-17.

Rubinsztein, David C., G. Mariño and G. Kroemer (2011). "Autophagy and Aging." Cell **146**(5): 682-695.

Rui, Y. N., Z. Xu, B. Patel, Z. Chen, D. Chen, A. Tito, G. David, Y. Sun, E. F. Stimming, H. J. Bellen, A. M. Cuervo and S. Zhang (2015). "Huntingtin functions as a scaffold for selective macroautophagy." Nat Cell Biol **17**(3): 262-275.

Sadleir, K. R. and R. Vassar (2012). "Cdk5 protein inhibition and Abeta42 increase BACE1 protein level in primary neurons by a post-transcriptional mechanism: implications of CDK5 as a therapeutic target for Alzheimer disease." J Biol Chem **287**(10): 7224-7235.

Sahlgren, C. M., A. Mikhailov, S. Vaittinen, H. M. Pallari, H. Kalimo, H. C. Pant and J. E. Eriksson (2003). "Cdk5 Regulates the Organization of Nestin and Its Association with p35." Molecular and Cellular Biology **23**(14): 5090-5106.

Salminen, A., K. Kaarniranta and A. Kauppinen (2012). "Inflammaging: disturbed interplay between autophagy and inflammasomes." Aging (Albany NY) **4**(3): 166-175.

Salzer, I., F. A. Erdem, W. Q. Chen, S. Heo, X. Koenig, K. W. Schicker, H. Kubista, G. Lubec, S. Boehm and J. W. Yang (2017). "Phosphorylation regulates the sensitivity of voltage-gated Kv7.2 channels towards phosphatidylinositol-4,5-bisphosphate." J Physiol **595**(3): 759-776.

Sampo, B., S. Kaech, S. Kunz and G. Banker (2003). "Two distinct mechanisms target membrane proteins to the axonal surface." Neuron **37**(4): 611-624.

Sasaki, S., A. Shionoya, M. Ishida, M. J. Gambello, J. Yingling, A. Wynshaw-Boris and S. Hirotsune (2000). "A LIS1/NUDEL/cytoplasmic dynein heavy chain complex in the developing and adult nervous system." Neuron **28**(3): 681-696.

Sasaki, S., S. Maruyama, K. Yamane, H. Sakuma and M. Takeishi (1990). "Ultrastructure of swollen proximal axons of anterior horn neurons in motor neuron disease." J Neurol Sci **97**(2-3): 233-240.

Sasaki, Y., C. Cheng, Y. Uchida, O. Nakajima, T. Ohshima, T. Yagi, M. Taniguchi, T. Nakayama, R. Kishida, Y. Kudo, S. Ohno, F. Nakamura and Y. Goshima (2002). "Fyn

and Cdk5 mediate semaphorin-3A signaling, which is involved in regulation of dendrite orientation in cerebral cortex." Neuron **35**(5): 907-920.

Sawada, M., H. Sawada and T. Nagatsu (2008). "Effects of Aging on Neuroprotective and Neurotoxic Properties of Microglia in Neurodegenerative Diseases." Neurodegenerative Diseases **5**(3-4): 254-256.

Schafer, D. P., S. Jha, F. Liu, T. Akella, L. D. McCullough and M. N. Rasband (2009). "Disruption of the Axon Initial Segment Cytoskeleton Is a New Mechanism for Neuronal Injury." Journal of Neuroscience **29**(42): 13242-13254.

Schlossmacher, M. G., M. P. Frosch, W. P. Gai, M. Medina, N. Sharma, L. Forno, T. Ochiishi, H. Shimura, R. Sharon, N. Hattori, J. W. Langston, Y. Mizuno, B. T. Hyman, D. J. Selkoe and K. S. Kosik (2002). "Parkin localizes to the Lewy bodies of Parkinson disease and dementia with Lewy bodies." Am J Pathol **160**(5): 1655-1667.

Schuldiner, O. and A. Yaron (2015). "Mechanisms of developmental neurite pruning." Cellular and Molecular Life Sciences **72**(1): 101-119.

Sesti, F. (2016). "Oxidation of K(+) Channels in Aging and Neurodegeneration." Aging Dis **7**(2): 130-135.

Shah, M. M., M. Migliore, I. Valencia, E. C. Cooper and D. A. Brown (2008). "Functional significance of axonal Kv7 channels in hippocampal pyramidal neurons." Proceedings of the National Academy of Sciences **105**(22): 7869-7874.

Shea, T. B., Y. L. Zheng, D. Ortiz and H. C. Pant (2004). "Cyclin-dependent kinase 5 increases perikaryal neurofilament phosphorylation and inhibits neurofilament axonal transport in response to oxidative stress." J Neurosci Res **76**(6): 795-800.

Shelly, S., N. Lukinova, S. Bambina, A. Berman and S. Cherry (2009). "Autophagy is an essential component of Drosophila immunity against vesicular stomatitis virus." Immunity **30**(4): 588-598.

Shelton, S. B. and G. V. W. Johnson (2004). "Cyclin-dependent kinase-5 in neurodegeneration." Journal of Neurochemistry **88**(6): 1313-1326.

Shi, C., K. Viccaro, H. G. Lee and K. Shah (2016). "Cdk5-Foxo3 axis: initially neuroprotective, eventually neurodegenerative in Alzheimer's disease models." J Cell Sci **129**(9): 1815-1830.

Shibata, R., K. Nakahira, K. Shibasaki, Y. Wakazono, K. Imoto and K. Ikenaka (2000). "A-type K+ current mediated by the Kv4 channel regulates the generation of action potential in developing cerebellar granule cells." J Neurosci **20**(11): 4145-4155.

Shigenaga, M. K., T. M. Hagen and B. N. Ames (1994). "Oxidative damage and mitochondrial decay in aging." Proc Natl Acad Sci U S A **91**(23): 10771-10778.

Sinclair, D. A. (2005). "Toward a unified theory of caloric restriction and longevity regulation." Mech Ageing Dev **126**(9): 987-1002.

Smith-Trunova, S., R. Prithviraj, J. Spurrier, I. Kuzina, Q. Gu and E. Giniger (2015). "Cdk5 regulates developmental remodeling of mushroom body neurons in Drosophila: CDK5 Regulates Neuronal Remodeling." Developmental Dynamics **244**(12): 1550-1563.

Sobotzik, J.-M., J. M. Sie, C. Politi, D. Del Turco, V. Bennett, T. Deller and C. Schultz (2009). "AnkyrinG is required to maintain axo-dendritic polarity in vivo." Proceedings of the National Academy of Sciences **106**(41): 17564-17569.

Sohal, R. S. and R. Weindruch (1996). "Oxidative stress, caloric restriction, and aging." Science **273**(5271): 59-63.

Sohal, R. S., P. L. Toy and R. G. Allen (1986). "Relationship between life expectancy, endogenous antioxidants and products of oxygen free radical reactions in the housefly, Musca domestica." Mech Ageing Dev **36**(1): 71-77.

Sohn, P. D., T. E. Tracy, H. I. Son, Y. Zhou, R. E. Leite, B. L. Miller, W. W. Seeley, L. T. Grinberg and L. Gan (2016). "Acetylated tau destabilizes the cytoskeleton in the axon initial segment and is mislocalized to the somatodendritic compartment." Mol Neurodegener **11**(1): 47.

Song, A.-h., D. Wang, G. Chen, Y. Li, J. Luo, S. Duan and M.-m. Poo (2009). "A Selective Filter for Cytoplasmic Transport at the Axon Initial Segment." Cell **136**(6): 1148-1160.

Spencer, B., R. Potkar, M. Trejo, E. Rockenstein, C. Patrick, R. Gindi, A. Adame, T. Wyss-Coray and E. Masliah (2009). "Beclin 1 gene transfer activates autophagy and ameliorates the neurodegenerative pathology in alpha-synuclein models of Parkinson's and Lewy body diseases."

Spires-Jones, T. L., W. H. Stoothoff, A. de Calignon, P. B. Jones and B. T. Hyman (2009). "Tau pathophysiology in neurodegeneration: a tangled issue." Trends in Neurosciences **32**(3): 150-159.

Stefani, M. and C. M. Dobson (2003). "Protein aggregation and aggregate toxicity: new insights into protein folding, misfolding diseases and biological evolution." J Mol Med (Berl) **81**(11): 678-699.

Stokin, G. B., C. Lillo, T. L. Falzone, R. G. Brusch, E. Rockenstein, S. L. Mount, R. Raman, P. Davies, E. Masliah, D. S. Williams and L. S. Goldstein (2005). "Axonopathy and transport deficits early in the pathogenesis of Alzheimer's disease." Science **307**(5713): 1282-1288.

Stroustrup, N., W. E. Anthony, Z. M. Nash, V. Gowda, A. Gomez, I. F. López-Moyado, J. Apfeld and W. Fontana (2016). "The temporal scaling of Caenorhabditis elegans ageing." Nature **530**(7588): 103-107.

Sun, X., Y. Wu, M. Gu, Z. Liu, Y. Ma, J. Li and Y. Zhang (2014). "Selective filtering defect at the axon initial segment in Alzheimer's disease mouse models." Proc Natl Acad Sci U S A **111**(39): 14271-14276.

Swerdlow, R. H. (2011). "Brain aging, Alzheimer's disease, and mitochondria." Biochimica et Biophysica Acta (BBA) - Molecular Basis of Disease **1812**(12): 1630-1639.

Switzer, R. C. (2000). "Application of Silver Degeneration Stains for Neurotoxicity Testing." Toxicologic Pathology **28**(1): 70-83.

Taanman, J. W. (1999). "The mitochondrial genome: structure, transcription, translation and replication." Biochim Biophys Acta **1410**(2): 103-123.

Tak, P. P. and G. S. Firestein (2001). "NF-kappaB: a key role in inflammatory diseases." J Clin Invest **107**(1): 7-11.

Takahashi, M., E. Iseki and K. Kosaka (2000). "Cyclin-dependent kinase 5 (Cdk5) associated with Lewy bodies in diffuse Lewy body disease." Brain Res **862**(1-2): 253-256.

Takahashi, S., T. Ohshima, M. Hirasawa, T. K. Pareek, T. H. Bugge, A. Morozov, K. Fujieda, R. O. Brady and A. B. Kulkarni (2010). "Conditional Deletion of Neuronal Cyclin-Dependent Kinase 5 in Developing Forebrain Results in Microglial Activation and Neurodegeneration." The American Journal of Pathology **176**(1): 320-329.

Takahashi, Y., D. Coppola, N. Matsushita, H. D. Cualing, M. Sun, Y. Sato, C. Liang, J. U. Jung, J. Q. Cheng, J. J. Mule, W. J. Pledger and H. G. Wang (2007). "Bif-1 interacts with Beclin 1 through UVRAG and regulates autophagy and tumorigenesis." Nat Cell Biol **9**(10): 1142-1151.

Talens, R. P., K. Christensen, H. Putter, G. Willemsen, L. Christiansen, D. Kremer, H. E. Suchiman, P. E. Slagboom, D. I. Boomsma and B. T. Heijmans (2012). "Epigenetic variation during the adult lifespan: cross-sectional and longitudinal data on monozygotic twin pairs." Aging Cell **11**(4): 694-703.

Tan, T. C., V. A. Valova, C. S. Malladi, M. E. Graham, L. A. Berven, O. J. Jupp, G. Hansra, S. J. McClure, B. Sarcevic, R. A. Boadle, M. R. Larsen, M. A. Cousin and P. J. Robinson (2003). "Cdk5 is essential for synaptic vesicle endocytosis." Nat Cell Biol **5**(8): 701-710.

Tanaka, T., F. F. Serneo, H.-C. Tseng, A. B. Kulkarni, L.-H. Tsai and J. G. Gleeson (2004). "Cdk5 phosphorylation of doublecortin ser297 regulates its effect on neuronal migration." Neuron **41**(2): 215-227.

Tanaka, T., Veeranna, T. Ohshima, P. Rajan, N. D. Amin, A. Cho, T. Sreenath, H. C. Pant, R. O. Brady and A. B. Kulkarni (2001). "Neuronal cyclin-dependent kinase 5 activity is critical for survival." J Neurosci **21**(2): 550-558.

Tang, D., J. Yeung, K.-Y. Lee, M. Matsushita, H. Matsui, K. Tomizawa, O. Hatase and J. H. Wang (1995). "An isoform of the neuronal cyclin-dependent kinase 5 (Cdk5) activator." Journal of Biological Chemistry **270**(45): 26897-26903.

Tapia, M., F. Wandosell and J. J. Garrido (2010). "Impaired function of HDAC6 slows down axonal growth and interferes with axon initial segment development." PLoS One **5**(9): e12908.

Tarricone, C., R. Dhavan, J. Peng, L. B. Areces, L.-H. Tsai and A. Musacchio (2001). "Structure and regulation of the CDK5-p25 nck5a complex." Molecular cell **8**(3): 657-669.

Tatton, N. A. (2000). "Increased Caspase 3 and Bax Immunoreactivity Accompany Nuclear GAPDH Translocation and Neuronal Apoptosis in Parkinson's Disease." Experimental Neurology **166**(1): 29-43.

Taylor, R. C. (2016). "Aging and the UPR(ER)." Brain Res **1648**(Pt B): 588-593.

Taylor, R. C. and A. Dillin (2011). "Aging as an event of proteostasis collapse." Cold Spring Harb Perspect Biol **3**(5).

Tenkova, T. I. and M. P. Goldberg (2007). "A modified silver technique (de Olmos stain) for assessment of neuronal and axonal degeneration." Methods Mol Biol **399**: 31-39.

Terni, B., J. Boada, M. Portero-Otin, R. Pamplona and I. Ferrer (2010). "Mitochondrial ATP-Synthase in the Entorhinal Cortex Is a Target of Oxidative Stress at Stages I/II of Alzheimer's Disease Pathology: ATP-Synthase Oxidation in AD Stages I/II." Brain Pathology **20**(1): 222-233.

Tessier, C. R. and K. Broadie (2009). "Activity-dependent modulation of neural circuit synaptic connectivity." Front Mol Neurosci **2**: 8.

Tomaru, U., S. Takahashi, A. Ishizu, Y. Miyatake, A. Gohda, S. Suzuki, A. Ono, J. Ohara, T. Baba, S. Murata, K. Tanaka and M. Kasahara (2012). "Decreased proteasomal activity causes age-related phenotypes and promotes the development of metabolic abnormalities." Am J Pathol **180**(3): 963-972.

Tomizawa, K., S. Sunada, Y.-F. Lu, Y. Oda, M. Kinuta, T. Ohshima, T. Saito, F.-Y. Wei, M. Matsushita, S.-T. Li, K. Tsutsui, S.-i. Hisanaga, K. Mikoshiba, K. Takei and H. Matsui (2003). "Cophosphorylation of amphiphysin I and dynamin I by Cdk5 regulates clathrin-mediated endocytosis of synaptic vesicles." The Journal of Cell Biology **163**(4): 813-824.

Tompkins, M. M., E. J. Basgall, E. Zamrini and W. D. Hill (1997). "Apoptotic-like changes in Lewy-body-associated disorders and normal aging in substantia nigral neurons." Am J Pathol **150**(1): 119-131.

Trifunovic, A., A. Hansson, A. Wredenberg, A. T. Rovio, E. Dufour, I. Khvorostov, J. N. Spelbrink, R. Wibom, H. T. Jacobs and N. G. Larsson (2005). "Somatic mtDNA

mutations cause aging phenotypes without affecting reactive oxygen species production." Proc Natl Acad Sci U S A **102**(50): 17993-17998.

Trunova, S. and E. Giniger (2012). "Absence of the Cdk5 activator p35 causes adult-onset neurodegeneration in the central brain of Drosophila." Disease Models & Mechanisms **5**(2): 210-219.

Trunova, S., B. Baek and E. Giniger (2011). "Cdk5 Regulates the Size of an Axon Initial Segment-Like Compartment in Mushroom Body Neurons of the Drosophila Central Brain." Journal of Neuroscience **31**(29): 10451-10462.

Tsai, J., J. Grutzendler, K. Duff and W. B. Gan (2004). "Fibrillar amyloid deposition leads to local synaptic abnormalities and breakage of neuronal branches." Nat Neurosci **7**(11): 1181-1183.

Tsai, L. H., T. Takahashi, V. S. Caviness, Jr. and E. Harlow (1993). "Activity and expression pattern of cyclin-dependent kinase 5 in the embryonic mouse nervous system." Development **119**(4): 1029-1040.

Tsai, L. H., I. Delalle, V. S. Caviness, Jr., T. Chae and E. Harlow (1994). "p35 is a neural-specific regulatory subunit of cyclin-dependent kinase 5." Nature **371**(6496): 419-423.

Uttara, B., A. V. Singh, P. Zamboni and R. T. Mahajan (2009). "Oxidative stress and neurodegenerative diseases: a review of upstream and downstream antioxidant therapeutic options." Curr Neuropharmacol **7**(1): 65-74.

Uversky, V. N. (2009). "Intrinsic disorder in proteins associated with neurodegenerative diseases." Front Biosci (Landmark Ed) **14**: 5188-5238.

Vacher, H., J.-W. Yang, O. Cerda, A. Autillo-Touati, B. Dargent and J. S. Trimmer (2011). "Cdk-mediated phosphorylation of the Kvβ2 auxiliary subunit regulates Kv1 channel axonal targeting." The Journal of Cell Biology **192**(5): 813-824.

van den Heuvel, S. and E. Harlow (1993). "Distinct roles for cyclin-dependent kinases in cell cycle control." Science **262**(5142): 2050-2054.

van Heemst, D. (2010). "Insulin, IGF-1 and longevity." Aging Dis **1**(2): 147-157.

Van Wart, A., J. S. Trimmer and G. Matthews (2007). "Polarized distribution of ion channels within microdomains of the axon initial segment." The Journal of Comparative Neurology **500**(2): 339-352.

Verstegen, A. M. J., E. Tagliatti, G. Lignani, A. Marte, T. Stolero, M. Atias, A. Corradi, F. Valtorta, D. Gitler, F. Onofri, A. Fassio and F. Benfenati (2014). "Phosphorylation of Synapsin I by Cyclin-Dependent Kinase-5 Sets the Ratio between the Resting and Recycling Pools of Synaptic Vesicles at Hippocampal Synapses." Journal of Neuroscience **34**(21): 7266-7280.

Walker, G. A. and G. J. Lithgow (2003). "Lifespan extension in C. elegans by a molecular chaperone dependent upon insulin-like signals." Aging Cell **2**(2): 131-139.

Wang, H.-S., Z. Pan, W. Shi, B. S. Brown, R. S. Wymore, I. S. Cohen, J. E. Dixon and D. McKinnon (1998). "KCNQ2 and KCNQ3 potassium channel subunits: molecular correlates of the M-channel." Science **282**(5395): 1890-1893.

Wang, K. and D. J. Klionsky (2011). "Mitochondria removal by autophagy." Autophagy **7**(3): 297-300.

Wang, Q., D. M. Walsh, M. J. Rowan, D. J. Selkoe and R. Anwyl (2004). "Block of long-term potentiation by naturally secreted and synthetic amyloid beta-peptide in hippocampal slices is mediated via activation of the kinases c-Jun N-terminal kinase, cyclin-dependent kinase 5, and p38 mitogen-activated protein kinase as well as metabotropic glutamate receptor type 5." J Neurosci **24**(13): 3370-3378.

Wang, X., B. Su, H. g. Lee, X. Li, G. Perry, M. A. Smith and X. Zhu (2009). "Impaired Balance of Mitochondrial Fission and Fusion in Alzheimer's Disease." Journal of Neuroscience **29**(28): 9090-9103.

Wang, X., M. H. Yan, H. Fujioka, J. Liu, A. Wilson-Delfosse, S. G. Chen, G. Perry, G. Casadesus and X. Zhu (2012). "LRRK2 regulates mitochondrial dynamics and function through direct interaction with DLP1." Human Molecular Genetics **21**(9): 1931-1944.

Wang, X., W. Wang, L. Li, G. Perry, H.-g. Lee and X. Zhu (2014). "Oxidative stress and mitochondrial dysfunction in Alzheimer's disease." Biochimica et Biophysica Acta (BBA) - Molecular Basis of Disease **1842**(8): 1240-1247.

Watson, M. R., R. D. Lagow, K. Xu, B. Zhang and N. M. Bonini (2008). "A Drosophila Model for Amyotrophic Lateral Sclerosis Reveals Motor Neuron Damage by Human SOD1." Journal of Biological Chemistry **283**(36): 24972-24981.

Wei, F.-Y., K. Tomizawa, T. Ohshima, A. Asada, T. Saito, C. Nguyen, J. A. Bibb, K. Ishiguro, A. B. Kulkarni, H. C. Pant, K. Mikoshiba, H. Matsui and S.-i. Hisanaga (2005). "Control of cyclin-dependent kinase 5 (Cdk5) activity by glutamatergic regulation of p35 stability: Glutamatergic regulation of Cdk5-p35 activity." Journal of Neurochemistry **93**(2): 502-512.

Wen, Y., E. Planel, M. Herman, H. Y. Figueroa, L. Wang, L. Liu, L. F. Lau, W. H. Yu and K. E. Duff (2008). "Interplay between Cyclin-Dependent Kinase 5 and Glycogen Synthase Kinase 3 Mediated by Neuregulin Signaling Leads to Differential Effects on Tau Phosphorylation and Amyloid Precursor Protein Processing." Journal of Neuroscience **28**(10): 2624-2632.

Williamson, T. L. and D. W. Cleveland (1999). "Slowing of axonal transport is a very early event in the toxicity of ALS–linked SOD1 mutants to motor neurons." Nature neuroscience **2**(1): 50-56.

Winckler, B., P. Forscher and I. Mellman (1999). "A diffusion barrier maintains distribution of membrane proteins in polarized neurons." Nature **397**(6721): 698-701.

Winklhofer, K. F. and C. Haass (2010). "Mitochondrial dysfunction in Parkinson's disease." Biochimica et Biophysica Acta (BBA) - Molecular Basis of Disease **1802**(1): 29-44.

Winslow, A. R., C.-W. Chen, S. Corrochano, A. Acevedo-Arozena, D. E. Gordon, A. A. Peden, M. Lichtenberg, F. M. Menzies, B. Ravikumar, S. Imarisio, S. Brown, C. J. O'Kane and D. C. Rubinsztein (2010). "α-Synuclein impairs macroautophagy: implications for Parkinson's disease." The Journal of Cell Biology **190**(6): 1023-1037.

Wong, A. S., R. H. Lee, A. Y. Cheung, P. K. Yeung, S. K. Chung, Z. H. Cheung and N. Y. Ip (2011). "Cdk5-mediated phosphorylation of endophilin B1 is required for induced autophagy in models of Parkinson's disease." Nat Cell Biol **13**(5): 568-579.

Woodhouse, A., T. C. Dickson, A. K. West, C. A. McLean and J. C. Vickers (2006). "No difference in expression of apoptosis-related proteins and apoptotic morphology in control, pathologically aged and Alzheimer's disease cases." Neurobiology of Disease **22**(2): 323-333.

Wullner, U., J. Kornhuber, M. Weller, J. B. Schulz, P. A. Loschmann, P. Riederer and T. Klockgether (1999). "Cell death and apoptosis regulating proteins in Parkinson's disease-- a cautionary note." Acta Neuropathol **97**(4): 408-412.

Xiao, C. and R. M. Robertson (2016). "Timing of Locomotor Recovery from Anoxia Modulated by the white Gene in Drosophila." Genetics **203**(2): 787-797.

Xiong, Y., H. Zhang and D. Beach (1992). "D type cyclins associate with multiple protein kinases and the DNA replication and repair factor PCNA." Cell **71**(3): 505-514.

Yamada, T., P. L. McGeer and E. G. McGeer (1992). "Lewy bodies in Parkinson's disease are recognized by antibodies to complement proteins." Acta Neuropathol **84**(1): 100-104.

Yamada, T., W. Fischle, T. Sugiyama, C. D. Allis and S. I. S. Grewal (2005). "The Nucleation and Maintenance of Heterochromatin by a Histone Deacetylase in Fission Yeast." Molecular Cell **20**(2): 173-185.

Yan, L. J. and R. S. Sohal (1998). "Mitochondrial adenine nucleotide translocase is modified oxidatively during aging." Proc Natl Acad Sci U S A **95**(22): 12896-12901.

Yang, W. and S. Hekimi (2010). "A mitochondrial superoxide signal triggers increased longevity in Caenorhabditis elegans." PLoS Biol **8**(12): e1000556.

Yang, Y., Y. Ogawa, K. L. Hedstrom and M. N. Rasband (2007). "βIV spectrin is recruited to axon initial segments and nodes of Ranvier by ankyrinG." The Journal of Cell Biology **176**(4): 509-519.

Ye, Q., I. Callebaut, A. Pezhman, J.-C. Courvalin and H. J. Worman (1997). "Domain-specific interactions of human HP1-type chromodomain proteins and inner nuclear membrane protein LBR." Journal of Biological Chemistry **272**(23): 14983-14989.

Yoon, Byung C., H. Jung, A. Dwivedy, Catherine M. O'Hare, Krishna H. Zivraj and Christine E. Holt (2012). "Local Translation of Extranuclear Lamin B Promotes Axon Maintenance." Cell **148**(4): 752-764.

Yoshimura, T. and M. N. Rasband (2014). "Axon initial segments: diverse and dynamic neuronal compartments." Curr Opin Neurobiol **27**: 96-102.

Zhang, B., P. Tu, F. Abtahian, J. Q. Trojanowski and V. M. Lee (1997). "Neurofilaments and orthograde transport are reduced in ventral root axons of transgenic mice that express human SOD1 with a G93A mutation." J Cell Biol **139**(5): 1307-1315.

Zhang, G., J. Li, S. Purkayastha, Y. Tang, H. Zhang, Y. Yin, B. Li, G. Liu and D. Cai (2013). "Hypothalamic programming of systemic ageing involving IKK-beta, NF-kappaB and GnRH." Nature **497**(7448): 211-216.

Zhang, P., P. C. Yu, A. H. Tsang, Y. Chen, A. K. Fu, W. Y. Fu, K. K. Chung and N. Y. Ip (2010). "S-nitrosylation of cyclin-dependent kinase 5 (cdk5) regulates its kinase activity and dendrite growth during neuronal development." J Neurosci **30**(43): 14366-14370.

Zhang, S., L. Edelmann, J. Liu, J. E. Crandall and M. A. Morabito (2008). "Cdk5 Regulates the Phosphorylation of Tyrosine 1472 NR2B and the Surface Expression of NMDA Receptors." Journal of Neuroscience **28**(2): 415-424.

Zhang, X., F. Bertaso, J. W. Yoo, K. Baumgartel, S. M. Clancy, V. Lee, C. Cienfuegos, C. Wilmot, J. Avis, T. Hunyh, C. Daguia, C. Schmedt, J. Noebels and T. Jegla (2010). "Deletion of the potassium channel Kv12.2 causes hippocampal hyperexcitability and epilepsy." Nat Neurosci **13**(9): 1056-1058.

Zhang, X., J. Q. Davis, S. Carpenter and V. Bennett (1998). "Structural requirements for association of neurofascin with ankyrin." J Biol Chem **273**(46): 30785-30794.

Zhang, Y., Y. Ikeno, W. Qi, A. Chaudhuri, Y. Li, A. Bokov, S. R. Thorpe, J. W. Baynes, C. Epstein, A. Richardson and H. Van Remmen (2009). "Mice deficient in both Mn superoxide dismutase and glutathione peroxidase-1 have increased oxidative damage and a greater incidence of pathology but no reduction in longevity." J Gerontol A Biol Sci Med Sci **64**(12): 1212-1220.

Zhao, W., D. R. Beers, J. S. Henkel, W. Zhang, M. Urushitani, J.-P. Julien and S. H. Appel (2010). "Extracellular mutant SOD1 induces microglial-mediated motoneuron injury." Glia **58**(2): 231-243.

Zheng, Y.-L., B.-S. Li, J. Kanungo, S. Kesavapany, N. Amin, P. Grant and H. C. Pant (2007). "Cdk5 Modulation of mitogen-activated protein kinase signaling regulates neuronal survival." Molecular biology of the cell **18**(2): 404-413.

Zou, S., S. Meadows, L. Sharp, L. Y. Jan and Y. N. Jan (2000). "Genome-wide study of aging and oxidative stress response in Drosophila melanogaster." <u>Proceedings of the National Academy of Sciences</u> **97**(25): 13726-13731.

Zukerberg, L. R., G. N. Patrick, M. Nikolic, S. Humbert, C. L. Wu, L. M. Lanier, F. B. Gertler, M. Vidal, R. A. Van Etten and L. H. Tsai (2000). "Cables links Cdk5 and c-Abl and facilitates Cdk5 tyrosine phosphorylation, kinase upregulation, and neurite outgrowth." <u>Neuron</u> **26**(3): 633-646.

Joshua Spurrier

2827 West Queen Lane | Philadelphia, PA 19129 | josh.spurrier2@gmail.com | cell: (301) 788-3439

Education

Ph.D.   **Johns Hopkins University – National Institutes of Health**………….….………August 2017
Graduate Partnership Program
Cellular, molecular, developmental biology, and biophysics
Baltimore, MD and Bethesda, MD

B.S.   **Drexel University**, Magna Cum Laude……..……………………………………..June 2010
Biological Sciences with mathematics minor
Philadelphia, PA

Awards   NIH Graduate Student Research Award……………………………………………………2016
Dean's List at Drexel University ………………………………………………..2005-2010
Anthony J. Drexel Academic Scholarship recipient ………………………………….2005-2010
Stephen Phillips Memorial Scholarship recipient…………………...….…………….2005-2010

Research   **National Institutes of Health**, Bethesda, MD……...…………….….…...................2011-Present
Experience   Pre-doctoral fellow, Laboratory of Edward Giniger, Ph.D.
Dissertation Title: *Investigating the mechanisms of p35-associated neurodegeneration and its effects on aging.*
- Established that Cdk5/p35 kinase dysfunction causes neurodegeneration in *Drosophila*
- Utilized RNA expression profile to develop metric for physiological age of flies
- Demonstrated that Cdk5/p35 kinase dysfunction accelerates aging both physiologically and at the gene expression level

National Institutes of Health, Bethesda, MD..……………...…………………..2010-2011
Post-baccalaureate IRTA
- Examined effects of human HIV-1 Nef on human leukocyte chemokine receptor expression levels by fluorescence staining
- Quantified chemokine receptor internalization with FACS following Nef expression
- Investigated mechanism of Nef-induced receptor internalization

Merck and Co, Inc., West Point, PA……………………………………………………2009
Merck Co-op
- Dissected adult mice and rats and isolated RNA from various tissues
- Used immunofluorescence staining to screen tissue samples for liponanoparticle RNA-delivery vehicles biodistribution
- Quantified RNA levels to test efficacy of liponanoparticle delivery
- Analyzed data and prepared presentations for meetings with senior scientists

TetraLogic Pharmaceuticals, Malvern, PA……...…………………………………….2008
Research Assistant
- Generated recombinant adenovirus to express fluorescent target genes
- Tested efficacy of IAP antagonists in cell culture system
- Discussed findings with senior scientists in weekly meetings

LifeSensors Inc., Malvern, PA……...………………………..……………………………2007

Scientist
- Tested fusion-tag for enhanced protein expression and purification in insect cells
- Verified functional activity of expressed proteins following their isolation
- Reported results in weekly meetings with fellow scientists

National Institutes of Health, Frederick, MD…………………………....…2004-2005, 2006

Cancer Research Training Awardee
- Extracted DNA from mouse embryos and adult tissue, and performed bisulfite sequencing
- Analyzed DNA methylation in treated male mice and untreated offspring to research mechanism for transgenerational inheritance
- Summarized and presented data to a collaboration of senior scientists

Lab Skills	- Mouse/fly handling	- Mouse/fly dissections	- Cell culture
	- PCR/qPCR	- RNA/DNA/protein extraction	- Cloning
	- FACS	- Western/Northern/Southern blots	- Tissue staining
	- Confocal microscopy	- Immunofluorescence staining	- Genetics

Certifications and Training
- Mouse Workshop: Hands On Animal Techniques (April 22, 2016)
- 3D Image Analysis (Imaris, ImageJ, Zen) (December 21, 2012)
- Agilent GeneSpring (September 3, 2014)
- Partek Genomics Suite (May 14, 2015)
- Data Analytics with MATLAB (May 9, 2015)
- Database for Annotation, Visualization and Integrated Discovery (DAVID) (April 16, 2014)
- Scientists Teaching Science (June 19, 2014)
- Summer Research Mentor Training (June 27, 2014)

Professional Activities

National Institutes of Health, Bethesda, MD…………………….…….…...………...…2016
- Advised and mentored a summer student to enhance laboratory skills and encourage critical thinking

National Institutes of Health, Bethesda, MD……………...………………...…2015-2017
- Judged posters at the yearly NIH Post-bac Poster Day to develop young trainees' presentation skills, critical thinking and scientific understanding

Gwynn Park High School, Brandywine, MD…....……………………………….2013-2016
- Judged projects at the yearly Science fair to teach students about the scientific method and encourage continued interest in STEM fields

Johns Hopkins University, Baltimore, MD...……...…………………………...…2011-2012
- Served as a teaching assistant for Biochemistry lab to ensure successful completion of experiments and assist grading reports and exams

Academic Talks	Investigating the mechanism of Cdk5-associated neurodegeneration and its effects on aging. (April 10, 2015). Drosophila Neuroscience Colloquium, NIH, Bethesda, MD.
	Investigating the mechanisms of neurodegeneration in Drosophila Cdk5/p35 kinase mutants. (August 21, 2014). Graduate Student Seminar Series, NIH, Bethesda, MD.
Poster Presentations	**Spurrier J**, Shukla A, and Giniger E. Cdk5 dysfunction increases the intrinsic rate of aging. CSHL's Mechanisms of Aging Conference, Cold Spring Harbor, NY, 2016.
	Spurrier J, Shukla A, Trunova-Smith, V, and Giniger E. Investigating the role of the axon initial segment in neurodegeneration. Howard Nash Poster Day, NIH, Bethesda, MD, 2016.
	Spurrier J, Shukla A, Trunova-Smith, V, and Giniger E. Investigating the role of the axon initial segment in neurodegeneration. Axons: From Cell Biology to Pathology Keystone Symposia, Sante Fe, NM, 2016.
	Spurrier J, Shukla A, Trunova-Smith, V, and Giniger E. Investigating the role of the axon initial segment in neurodegeneration. Graduate Student Symposium, NIH, Bethesda, MD, 2016.
	Spurrier J, McLinden K, and Giniger E. Cdk5 loss of function leads to accelerated aging. Howard Nash Poster Day, NIH, Bethesda, MD, 2015.
	Spurrier J, McLinden K, and Giniger E. Cdk5 loss of function leads to accelerated aging. Drosophila Research Conference, Chicago, IL, 2015.
	Spurrier J, McLinden K, and Giniger E. Microarray Analysis of Drosophila Cdk5/p35 kinase mutants. Graduate Student Symposium, NIH, Bethesda, MD, 2015.
	Spurrier J, McLinden K, and Giniger E. Microarray Analysis of Drosophila Cdk5/p35 kinase mutants. Johns Hopkins University CMDB Graduate Student Retreat, Fairfield, PA, 2014.
	Spurrier J, McLinden K, and Giniger E. Investigating initiation of Cdk5-associated neurodegeneration. Drosophila Research Conference, San Diego, CA, 2014.
	Spurrier J, McLinden K, and Giniger E. Development of a neurodegeneration assay in Drosophila Cdk5/p35 kinase mutants. Graduate Student Symposium, NIH, Bethesda, MD, 2014.

Spurrier J, McLinden K, and Giniger E. Characterizing the targets of *Drosophila* Cdk5/p35 kinase and their role in neurodegeneration. Graduate Student Symposium, NIH, Bethesda, MD, 2013.

Publications   **Spurrier J**, Shukla A, Johnson K, McLinden K, Kuzina I, Gu J, and Giniger E. Altered activity of Cdk5/p35 kinase causes neurodegeneration in part by accelerating the rate of aging. (submitted 7/2017)

Trunova S, Prithviraj R, **Spurrier J**, Kuzina I, Gu J, and Giniger E. 2015: Cdk5 regulates developmental remodeling of mushroom body neurons in Drosophila. *Developmental Dynamics* 244(12): 1550-63.

Chandrasekaran P, Moore V, Buckley M, **Spurrier J**, Kehrl J, and Venkatesan S. 2014: HIV-1 Nef down-modulates C-C and C-X-C chemokine receptors via ubiquitin and ubiquitin-independent mechanism. *PLoS One* 9(1): e86998.

Shiao, YH, Leighty, RM, Wang, C, Ge, X, Crawford, EB, **Spurrier, JM**, McCann, SD, Fields, JR, Fornwald, L, Riffle, L, Driver, C, Quinones, OA, Wilson, RE, Kasprzak, KS, Travlos, GS, Alvord, WG, and Anderson, LM. 2012: Molecular and organismal changes in offspring of male mice treated with chemical stressors. *Environmental and Molecular Mutagenesis* 53(5): 392-407.

Abou-Kheir W, Hynes PG, Martin P, Yin JJ, Liu Y-N, Seng V, Lake R, **Spurrier J**, and Kelly K. 2011: Self-Renewing *Pten-/-TP53-/-* Protospheres Produce Metastatic Adenocarcinoma Cell Lines with Multipotent Progenitor Activity. *PLoS ONE* 6(10): e26112.

Shiao, Y-H, Leighty, RM, Wang, C, Ge, X, Crawford, EB, **Spurrier, JM**, McCann, SD, Fields, JR, Fornwald, L, Riffle, L, Driver, C, Quiñones, OA, Wilson, RE, Kasprzak, KS, Travlos, GS, Alvord, WG, and Anderson. LM. 2011: Ontogeny-driven rDNA rearrangement, methylation, and transcription, and paternal influence. *PLoS ONE* 6(7): e22266.

Liu, L, **Spurrier, JM**, Butt, TR, and Strickler, JE. 2008: Enhanced protein expression in the baculovirus/insect cell system using engineered SUMO fusions. *Protein Expression and Purification* 62(1): 21-28.